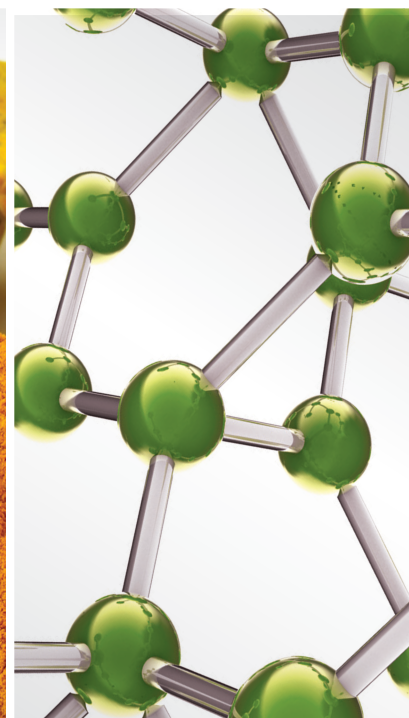# Mechanistic Roles of Plant Secondary Metabolites in Oxidative Stress-Linked Diseases

Lead Guest Editor: Saheed Sabiu
Guest Editors: Stephen Amoo and Taofik Sunmonu

Mechanistic Roles of Plant Secondary Metabolites in Oxidative Stress-Linked Diseases

Mechanistic Roles of Plant Secondary Metabolites in Oxidative Stress-Linked Diseases

Lead Guest Editor: Saheed Sabiu
Guest Editors: Stephen Amoo and Taofik Sunmonu

Arthur De Sá Ferreira (iD), Brazil
Nunziatina De Tommasi (iD), Italy
Marinella De leo (iD), Italy
Gourav Dey (iD), India
Dinesh Dhamecha, USA
Claudia Di Giacomo (iD), Italy
Antonella Di Sotto (iD), Italy
Mario Dioguardi, Italy
Jeng-Ren Duann (iD), USA
Thomas Efferth (iD), Germany
Abir El-Alfy, USA
Mohamed Ahmed El-Esawi (iD), Egypt
Mohd Ramli Elvy Suhana, Malaysia
Talha Bin Emran, Japan
Roger Engel (iD), Australia
Karim Ennouri (iD), Tunisia
Giuseppe Esposito (iD), Italy
Tahereh Eteraf-Oskouei, Iran
Robson Xavier Faria (iD), Brazil
Mohammad Fattahi (iD), Iran
Keturah R. Faurot (iD), USA
Piergiorgio Fedeli (iD), Italy
Laura Ferraro (iD), Italy
Antonella Fioravanti (iD), Italy
Carmen Formisano (iD), Italy
Hua-Lin Fu (iD), China
Liz G Müller (iD), Brazil
Gabino Garrido (iD), Chile
Safoora Gharibzadeh, Iran
Muhammad N. Ghayur (iD), USA
Angelica Gomes (iD), Brazil
Elena González-Burgos, Spain
Susana Gorzalczany (iD), Argentina
Jiangyong Gu (iD), China
Maruti Ram Gudavalli (iD), USA
Jian-You Guo (iD), China
Shanshan Guo, China
Narcís Gusi (iD), Spain
Svein Haavik, Norway
Fernando Hallwass, Brazil
Gajin Han (iD), Republic of Korea
Ihsan Ul Haq, Pakistan
Hicham Harhar (iD), Morocco
Mohammad Hashem Hashempur (iD), Iran
Muhammad Ali Hashmi (iD), Pakistan

Waseem Hassan (iD), Pakistan
Sandrina A. Heleno (iD), Portugal
Pablo Herrero (iD), Spain
Soon S. Hong (iD), Republic of Korea
Md. Akil Hossain (iD), Republic of Korea
Muhammad Jahangir Hossen (iD), Bangladesh
Shih-Min Hsia (iD), Taiwan
Changmin Hu (iD), China
Tao Hu (iD), China
Weicheng Hu (iD), China
Wen-Long Hu, Taiwan
Xiao-Yang (Mio) Hu, United Kingdom
Sheng-Teng Huang (iD), Taiwan
Ciara Hughes (iD), Ireland
Attila Hunyadi (iD), Hungary
Liaqat Hussain (iD), Pakistan
Maria-Carmen Iglesias-Osma (iD), Spain
Amjad Iqbal (iD), Pakistan
Chie Ishikawa (iD), Japan
Angelo A. Izzo, Italy
Satveer Jagwani (iD), USA
Rana Jamous (iD), Palestinian Authority
Muhammad Saeed Jan (iD), Pakistan
G. K. Jayaprakasha, USA
Kyu Shik Jeong, Republic of Korea
Leopold Jirovetz (iD), Austria
Jeeyoun Jung (iD), Republic of Korea
Nurkhalida Kamal (iD), Saint Vincent and the
Grenadines
Atsushi Kameyama (iD), Japan
Kyungsu Kang, Republic of Korea
Wenyi Kang (iD), China
Shao-Hsuan Kao (iD), Taiwan
Nasiara Karim (iD), Pakistan
Morimasa Kato (iD), Japan
Kumar Katragunta (iD), USA
Deborah A. Kennedy (iD), Canada
Washim Khan, USA
Bonglee Kim (iD), Republic of Korea
Dong Hyun Kim (iD), Republic of Korea
Junghyun Kim (iD), Republic of Korea
Kyungho Kim, Republic of Korea
Yun Jin Kim (iD), Malaysia
Yoshiyuki Kimura (iD), Japan

Nebojša Kladar, Serbia
Mi Mi Ko, Republic of Korea
Toshiaki Kogure, Japan
Malcolm Koo, Taiwan
Yu-Hsiang Kuan, Taiwan
Robert Kubina, Poland
Chan-Yen Kuo, Taiwan
Kuang C. Lai, Taiwan
King Hei Stanley Lam, Hong Kong
Fanuel Lampiao, Malawi
Ilaria Lampronti, Italy
Mario Ledda, Italy
Harry Lee, China
Jeong-Sang Lee, Republic of Korea
Ju Ah Lee, Republic of Korea
Kyu Pil Lee, Republic of Korea
Namhun Lee, Republic of Korea
Sang Yeoup Lee, Republic of Korea
Ankita Leekha, USA
Christian Lehmann, Canada
George B. Lenon, Australia
Marco Leonti, Italy
Hua Li, China
Min Li, China
Xing Li, China
Xuqi Li, China
Yi-Rong Li, Taiwan
Vuanghao Lim, Malaysia
Bi-Fong Lin, Taiwan
Ho Lin, Taiwan
Shuibin Lin, China
Kuo-Tong Liou, Taiwan
I-Min Liu, Taiwan
Suhuan Liu, China
Xiaosong Liu, Australia
Yujun Liu, China
Emilio Lizarraga, Argentina
Monica Loizzo, Italy
Nguyen Phuoc Long, Republic of Korea
Zaira López, Mexico
Chunhua Lu, China
Ângelo Luís, Portugal
Anderson Luiz-Ferreira, Brazil
Ivan Luzardo Luzardo-Ocampo, Mexico

Michel Mansur Machado, Brazil
Filippo Maggi, Italy
Juraj Majtan, Slovakia
Toshiaki Makino, Japan
Nicola Malafronte, Italy
Giuseppe Malfa, Italy
Francesca Mancianti, Italy
Carmen Mannucci, Italy
Juan M. Manzaneque, Spain
Fatima Martel, Portugal
Carlos H. G. Martins, Brazil
Maulidiani Maulidiani, Malaysia
Andrea Maxia, Italy
Avijit Mazumder, India
Isac Medeiros, Brazil
Ahmed Mediani, Malaysia
Lewis Mehl-Madrona, USA
Ayikoé Guy Mensah-Nyagan, France
Oliver Micke, Germany
Maria G. Miguel, Portugal
Luigi Milella, Italy
Roberto Miniero, Italy
Letteria Minutoli, Italy
Prashant Modi, India
Daniel Kam-Wah Mok, Hong Kong
Changjong Moon, Republic of Korea
Albert Moraska, USA
Mark Moss, United Kingdom
Yoshiharu Motoo, Japan
Yoshiki Mukudai, Japan
Sakthivel Muniyan, USA
Saima Muzammil, Pakistan
Benoit Banga N'guessan, Ghana
Massimo Nabissi, Italy
Siddavaram Nagini, India
Takao Namiki, Japan
Srinivas Nammi, Australia
Krishnadas Nandakumar, India
Vitaly Napadow, USA
Edoardo Napoli, Italy
Jorddy Neves Cruz, Brazil
Marcello Nicoletti, Italy
Eliud Nyaga Mwaniki Njagi, Kenya
Cristina Nogueira, Brazil

Sakineh Kazemi Noureini (iD), Iran
Rômulo Dias Novaes, Brazil
Martin Offenbaecher (iD), Germany
Oluwafemi Adeleke Ojo (iD), Nigeria
Olufunmiso Olusola Olajuyigbe (iD), Nigeria
Luís Flávio Oliveira, Brazil
Mozaniel Oliveira (iD), Brazil
Atolani Olubunmi (iD), Nigeria
Abimbola Peter Oluyori (iD), Nigeria
Timothy Omara, Austria
Chiagoziem Anariochi Otuechere (iD), Nigeria
Sokcheon Pak (iD), Australia
Antônio Palumbo Jr, Brazil
Zongfu Pan (iD), China
Siyaram Pandey (iD), Canada
Niranjan Parajuli (iD), Nepal
Gunhyuk Park (iD), Republic of Korea
Wansu Park (iD), Republic of Korea
Rodolfo Parreira (iD), Brazil
Mohammad Mahdi Parvizi (iD), Iran
Luiz Felipe Passero (iD), Brazil
Mitesh Patel, India
Claudia Helena Pellizzon (iD), Brazil
Cheng Peng, Australia
Weijun Peng (iD), China
Sonia Piacente, Italy
Andrea Pieroni (iD), Italy
Haifa Qiao (iD), USA
Cláudia Quintino Rocha (iD), Brazil
DANIELA RUSSO (iD), Italy
Muralidharan Arumugam Ramachandran,
Singapore
Manzoor Rather (iD), India
Miguel Rebollo-Hernanz (iD), Spain
Gauhar Rehman, Pakistan
Daniela Rigano (iD), Italy
José L. Rios, Spain
Francisca Rius Diaz, Spain
Eliana Rodrigues (iD), Brazil
Maan Bahadur Rokaya (iD), Czech Republic
Mariangela Rondanelli (iD), Italy
Antonietta Rossi (iD), Italy
Mi Heon Ryu (iD), Republic of Korea
Bashar Saad (iD), Palestinian Authority
Sabiu Saheed, South Africa

Mohamed Z.M. Salem (iD), Egypt
Avni Sali, Australia
Andreas Sandner-Kiesling, Austria
Manel Santafe (iD), Spain
José Roberto Santin (iD), Brazil
Tadaaki Satou (iD), Japan
Roland Schoop, Switzerland
Sindy Seara-Paz, Spain
Veronique Seidel (iD), United Kingdom
Vijayakumar Sekar (iD), China
Terry Selfe (iD), USA
Arham Shabbir (iD), Pakistan
Suzana Shahar, Malaysia
Wen-Bin Shang (iD), China
Xiaofei Shang (iD), China
Ali Sharif (iD), Pakistan
Karen J. Sherman (iD), USA
San-Jun Shi (iD), China
Insop Shim (iD), Republic of Korea
Maria Im Hee Shin, China
Yukihiro Shoyama, Japan
Morry Silberstein (iD), Australia
Samuel Martins Silvestre (iD), Portugal
Preet Amol Singh, India
Rajeev K Singla (iD), China
Kuttulebbai N. S. Sirajudeen (iD), Malaysia
Slim Smaoui (iD), Tunisia
Eun Jung Sohn (iD), Republic of Korea
Maxim A. Solovchuk (iD), Taiwan
Young-Jin Son (iD), Republic of Korea
Chengwu Song (iD), China
Vanessa Steenkamp (iD), South Africa
Annarita Stringaro (iD), Italy
Keiichiro Sugimoto (iD), Japan
Valeria Sulsen (iD), Argentina
Zewei Sun (iD), China
Sharifah S. Syed Alwi (iD), United Kingdom
Orazio Taglialatela-Scafati (iD), Italy
Takashi Takeda (iD), Japan
Gianluca Tamagno (iD), Ireland
Hongxun Tao, China
Jun-Yan Tao (iD), China
Lay Kek Teh (iD), Malaysia
Norman Temple (iD), Canada

Kamani H. Tennekoon, Sri Lanka
Seong Lin Teoh, Malaysia
Menaka Thounaojam, USA
Jinhui Tian, China
Zipora Tietel, Israel
Loren Toussaint, USA
Riaz Ullah, Saudi Arabia
Philip F. Uzor, Nigeria
Luca Vanella, Italy
Antonio Vassallo, Italy
Cristian Vergallo, Italy
Miguel Vilas-Boas, Portugal
Aristo Vojdani, USA
Yun WANG, China
QIBIAO WU, Macau
Abraham Wall-Medrano, Mexico
Chong-Zhi Wang, USA
Guang-Jun Wang, China
Jinan Wang, China
Qi-Rui Wang, China
Ru-Feng Wang, China
Shu-Ming Wang, USA
Ting-Yu Wang, China
Xue-Rui Wang, China
Youhua Wang, China
Kenji Watanabe, Japan
Jintanaporn Wattanathorn, Thailand
Silvia Wein, Germany
Katarzyna Winska, Poland
Sok Kuan Wong, Malaysia
Christopher Worsnop, Australia
Jih-Huah Wu, Taiwan
Sijin Wu, China
Xian Wu, USA
Zuoqi Xiao, China
Rafael M. Ximenes, Brazil
Guoqiang Xing, USA
JiaTuo Xu, China
Mei Xue, China
Yong-Bo Xue, China
Haruki Yamada, Japan
Nobuo Yamaguchi, Japan
Junqing Yang, China
Longfei Yang, China

Mingxiao Yang, Hong Kong
Qin Yang, China
Wei-Hsiung Yang, USA
Swee Keong Yeap, Malaysia
Albert S. Yeung, USA
Ebrahim M. Yimer, Ethiopia
Yoke Keong Yong, Malaysia
Fadia S. Youssef, Egypt
Zhilong Yu, Canada
RONGJIE ZHAO, China
Sultan Zahiruddin, USA
Armando Zarrelli, Italy
Xiaobin Zeng, China
Y Zeng, China
Fangbo Zhang, China
Jianliang Zhang, China
Jiu-Liang Zhang, China
Mingbo Zhang, China
Jing Zhao, China
Zhangfeng Zhong, Macau
Guoqi Zhu, China
Yan Zhu, USA
Suzanna M. Zick, USA
Stephane Zingue, Cameroon

Contents

Research Article

Botanical from *Piper capense* Fruit Can Help to Combat the Melanoma as Demonstrated by *In Vitro* and *In Vivo* Studies

Brice E. N. Wamba,[1,2] Paramita Ghosh,[1] Armelle T. Mbaveng ⓘ,[2] Sayantan Bhattacharya,[1] Mitra Debarpan,[1] Saha Depanwita,[1] Mustafi Mitra Saunak,[3] Victor Kuete ⓘ,[2] and Nabendu Murmu ⓘ[1]

[1]*Department of Signal Transduction and Biogenic Amines, Chittaranjan National Cancer Institute, 37, S.P. Mukherjee Road, Kolkata 700026, India*
[2]*Department of Biochemistry, Faculty of Science, University of Dschang, Dschang, Cameroon*
[3]*Department of Pathology, Chittaranjan National Cancer Institute, 37, S. P. Mukherjee Road, Kolkata 700026, India*

Correspondence should be addressed to Victor Kuete; kuetevictor@yahoo.fr and Nabendu Murmu; nabendu.murmu@cnci.org.in

Piper capense belongs to Piperaceae family and has long been used as a traditional medicine to treat various diseases in several parts of Africa. The present study aims to investigate the effect of *Piper capense* fruit extract (PCFE) alone and in combination with dacarbazine on metastatic melanoma cell line B16-F10 and *in vivo* in C57BL/6J mice. Cytotoxic effects of PCFE alone and in association with dacarbazine on B16-F10 cells were studied by 3-(4, 5-dimethylthiazol-2-yl)-2, 5-diphenyl tetrazolium bromide (MTT) assay and colony formation assay. Wound healing assay, immunofluorescence staining, and western blot analysis were performed to evaluate the individual and combined effect of PCFE and dacarbazine on epithelial-mesenchymal transition (EMT). For *in vivo* studies, C57BL/6J mice were subcutaneously injected with B16-F10 cells (5×10^5 cells/mL), and the effect of PCFE and dacarbazine was studied on tumor development. The alteration of EMT was evaluated by targeting E-cadherin, vimentin, and CD133 in PCFE alone and in combination with dacarbazine-treated tumor tissues by western blot analysis. Phytochemical screening of PCFE reveals the presence of certain secondary metabolites. Our results showed that PCFE alone and in association with dacarbazine has a good activity in preventing B16-F10 melanoma cell progression and clonogenicity. This extract also regulated EMT. *In vivo* results showed that PCFE (100 mg/kg body weight) reduced tumor size in C57BL/6J mice along with the decrease in the expression of vasculogenic mimicry (VM) tubes as well as an improvement in the qualitative and quantitative expression of markers involved in EMT. Our study suggests that PCFE may be useful for managing the growth and metastasis of melanoma.

1. Introduction

Cancer is increasingly recognized as a critical public health problem worldwide, specifically in some parts of Africa where people are poor and do not have the financial means to obtain adequate treatment even though the survival rates are lower compared to other countries [1].

The latest World Health Organization (WHO) global data show 18.1 million new cases and 9.6 million cancer deaths in 2018 [2]. It is recognized as the leading and the second leading cause of death, respectively, in economically

developed and developing countries [3]. WHO Bulletin in 2018 reports 15769 cases of cancer detected against 10533 cases of deaths or more than half of the incidence in Cameroon [2]. There are more than a hundred different cancers depending on the organ affected. Malignant melanoma is the most aggressive form of skin cancer. About 96480 new cases of melanoma have been diagnosed (57220 in men and 39260 in women) and 7230 cases of death (4740 in men and 2490 in women) from this disease in the United States in 2019 according to the work of Siegel et al. [4]. Melanomas which are not of epithelial origin develop from

neural crest-derived pigmented melanocytes [5]. In Africa and more particularly in Cameroon, its incidence in 2018 has been estimated at 148 cases against 89 cases of death [2].

These growing burdens in developing countries are caused by not only etiological factors [6] but also risk factors such as genetics, population growth and ageing, urbanisation, and the adoption of new lifestyles (smoking, alcoholism, and lack of physical exercise). This has led to a rapid increase in incidence, environmental pollution, lack of preventive measures, delay in diagnosis, and a deficit of health workers trained in oncology. If adequate measures are not taken quickly, cancer mortality will continue to increase at the same rate as incidence [7, 8]. The scientific community, in its quest to find ways and means to reduce the morbidity and mortality rate associated with this disease, has set up several treatment strategies. These strategies include chemotherapy, radiotherapy, and surgery which are the most important and have given rise to the hope of eradicating this disease, though it was later on discovered that cancer cells were capable of developing resistant mechanisms to overcome the lethal action of conventional drugs (chemotherapy) given that it is the most widely used treatment method.

Cancer can be subdivided into several types according to the causal agent and the affected organ. Melanoma is particularly common among Caucasians, especially Northern and North-Western Europeans, living in sunny climates. There are higher rates in Oceania, North America, Europe, Southern Africa, and Latin America. This geographic pattern reflects the primary cause, ultraviolet light (UV) exposure in conjunction with the amount of skin pigmentation in the population. A crucial conundrum that goes hand in hand with tumor aggressiveness and poor prognosis of patients is drug resistance. Many tumors, especially melanoma, have the tendency to show resistance against various chemotherapeutic drugs that make the treatment difficult at best [9]. Although the general mode of action for drug resistance is thought to be achieved by the ATP-binding cassette (ABC) transporter system [10] present in the cancer stem cell (CSC) population, the molecular signalling is different in melanoma. Dacarbazine, a potent alkylating agent, is considered the gold standard for melanoma treatment. But the response rate of the drug is only 15–20% [11], and the possible mechanism of evasion is mediated by the upregulation of interleukin-8 (IL-8) and vascular endothelial growth factor (VEGF) expressions, two major proteins that regulate angiogenesis, drug resistance, and tumor cell growth by an autocrine mechanism [12–14].

Besides being the most widely used chemotherapeutic agent for eliminating malignant melanoma, the response rate and duration of dacarbazine treatment are disappointing due to the resistant property of the cells and it is still uncertain whether combination therapies are superior to the single-agent dacarbazine [15, 16] in various randomized phase III studies. In 2018 in Africa, melanoma of skin cancer caused 6629 new cases and 4143 deaths [2].

Cancer cells have developed resistance to existing conventional drugs over time, but also signs of toxicity have been observed; for example, doxorubicin, a widely used chemodrug, causes renal and cardiac toxicity [17–20], and 5-fluorouracil, a common chemotherapeutic agent, is known to cause myelotoxicity and cardiotoxicity [21, 22]. All of these justify the urgency in the search for naturally occurring anticancer drugs with fewer side effects and designed to overcome the resistance problem. Several studies have already been carried out with plant extracts in relation to melanoma cell line B16-F10; for example, Pandey [23], showed the *in vivo* antitumor potential of extracts from the different parts of *Bauhinia variegata* Linn. Rajasekar et al. [24] showed the anticancerous effect of *Lithospermum erythrorhizon* extract *in vitro* and *in vivo*. Uscanga-Palomeque et al. [25] showed the inhibitory effect of *Cuphea aequipetala* extracts on melanomas *in vitro* and *in vivo*. In coherence with these findings, a keen interest in a Cameroonian pharmacopoeia plant called *Piper capense* from the Piperaceae family was taken into consideration due to its therapeutic virtues, most especially in the treatment of several illnesses like cancer when used in the form of formulation [26, 27]. *Piper capense* L. is traditionally used in Cameroon to treat cancers [28]; the aerial part of *Piper capense* L. is traditionally used in the Comoro Islands for diarrhoea and cough [29], with their traditional use in South Africa for the treatment of wounds, vaginal discharge, infertility, sore throat, and tongue sores. Both the aerial part and the plant roots when boiled are also used against malaria in Kenya [30]. Nevertheless, its *in vitro* cytotoxic activity on several types of cancer cell lines, notably methanolic extract against CCRF-CEM leukemia cell lines (inhibitory concentration 50% (IC_{50}): 6.95 μg/mL), HL60 (IC_{50}: 8.16 μg/mL), HL60AR (IC_{50}: 11.22 μg/mL), and CEM/ADR5000 (IC_{50}: 6.56 μg/mL), breast adenocarcinoma cell lines MDA-MB231 (IC_{50}: 4.17 μg/mL) and MDA-MB231/BCRP (IC_{50}: 19.45 μg/mL), colon carcinoma cell lines HCT116 p53+/+ (IC_{50}: 4.64 μg/mL) and HCT116 p53−/− (IC_{50}: 4.62 μg/mL), glioblastoma cell lines U87MG (IC_{50}: 13.48 μg/mL) and U87MG.ΔEGFR (IC_{50}: 7.44 μg/mL), has been demonstrated [28, 31]. The activities of *P. capense* MeOH and aqueous extracts against *Mycobacterium tuberculosis* and *C. albicans* with minimal inhibitory concentrations (MICs) of 512 μg/mL and 0.56 μg/mL, respectively [32, 33], have been demonstrated.

Despite all these studies and the results found in the literature, no report on *Piper capense* extract on melanoma cell lines has been documented *in vitro* as well as *in vivo*. Hence, this work aims to evaluate the *in vitro* and *in vivo* anticancer effects of the methanol extract of PCFE alone and in combination with dacarbazine on B16-F10 murine melanoma.

2. Material and Methods

2.1. Collection and Identification of Plant Material. The fruits of *Piper capense* Linn (Piperaceae) were purchased from the Dschang City main market, in the Menoua Division of the West Region of Cameroon. The plant was subsequently identified and authenticated at the National Herbarium of Cameroon (NHC) by Mr. Fulbert Tadjouteu, Yaoundé, where a sample was deposited and registered under reference number 6018/SRF-Cam.

2.2. Preparation of the PCFE.

2.2. Preparation of the PCFE. The plant was cleaned and ground and the powder obtained was macerated in methanol in the proportions 1 : 3 (m/v) for 48 hours at room temperature followed by filtration using Whatman No.1 paper. The filtrate obtained was concentrated using a rotary evaporator under reduced pressure (BÜCHI R-200) at 40°C where the crude extract was obtained. The extract was thereafter lyophilized and stored at −20°C for future use.

2.3. Chemicals, Antibodies, and Cell Line. 3-(4,5-Dimethylthiazol-2-yl)-2, 5-diphenyl tetrazolium bromide (MTT) (Merck) has been used for the revelation of viable cells, Dimethylsulfoxide (DMSO) (Merck) was used to dissolve the formazan crystals formed, Dulbecco's modified Eagle medium (DMEM) and high glucose culture medium supplemented with fetal bovine serum (FBS) (Gibco) were used for the cultivation and maintenance of the B16-F10 cell line, and penicillin/streptomycin (Invitrogen) was used for the preparation of culture media; 4', 6-diamino-2-phenylindole (DAPI) (LB097-10MG) was purchased from HIMEDIA Laboratories (Mumbai, India) and used as a nuclear counterstain; dacarbazine was purchased from Celon Laboratories (Telangana State, India) and used as reference chemotherapeutic drug.

The aqueous solution of dacarbazine was freshly prepared and exposed to sunlight at least one hour before any experiment to activate the chemotherapeutic drug.

Antibodies vimentin (mouse IgG1; NBP2-32910) and CD133 (rabbit IgG; NB120-16518) were purchased from Novus Biologicals (10730 E. Briarwood Avenue Centennial, CO 80112); E-cadherin (rabbit IgG; sc-7870), β-actin (rabbit IgG; sc-47778), and CD31 (mouse IgG) (sc-1506) were purchased from Santa Cruz Biotechnology (Bergheimer Str. 89–2, 69115 Heidelberg, Germany, Europe). All secondary antibodies (anti-mouse IgG-HRP: sc-2031, anti-rabbit IgG-HRP: sc-2004, and anti-mouse IgGk BP-PE: sc-516141) were purchased from Santa Cruz Biotechnology (Bergheimer Str. 89–2, 69115 Heidelberg, Germany, Europe). For periodic acid-Schiff staining (PAS), periodic acid was purchased from Merck (Massachusetts, USA); Schiff's reagent and hematoxylin were purchased from SRL (India).

2.4. Cell Culture. The cell line B16-F10 murine melanoma was obtained from the National Centre for Cell Science (NCCS), Pune, India. It was cultured and maintained in Dulbecco's modified Eagle medium (DMEM) and a high glucose culture medium supplemented with 10% fetal bovine serum (FBS) and 1% penicillin/streptomycin in an incubator at 37°C in an atmosphere containing 5% CO_2. All experiments were carried out after three passages.

2.5. Phytochemical Screening of Piper capense. The main classes of secondary metabolites, alkaloids (Mayer's tests), sterols (Salkowski's test), polyphenols (ferric chloride test), tannins (gelatin test), saponins (foam test), flavonoids (aluminum chloride test), triterpenes (Liebermann–Burchard's test), and anthraquinones

(Borntrager's test), have been investigated following the phytochemical methods as described in [34, 35].

2.6. In Vitro Evaluation

2.6.1. MTT Assay. The assay was carried out following the experimental protocol described in [36]. Briefly, 100 μL of culture medium at a density of 1×10^4 cells per well in a 96-well plate was exposed to 100 μL increasing concentrations of PCFE (10–1000 μg/mL) for 24 hours. 10 μL of 5 mg/mL MTT (3-(4, 5-dimethylthiazol-2-yl)-2, 5diphenyltetrazolium bromide) was added to each well and incubated for 2 hours at 37°C. After incubation, 100 μL DMSO was added to each well and the absorbance was measured at 570 nm using a microtitre plate reader (Tecan Infinite M200). Results were expressed as a percentage of viable cells as compared to 100% representing control cells. The IC_{50} value was calculated using nonlinear regression (curve fit) followed by log (inhibition) vs. response equation in GraphPad Prism software. The amount of drug was plotted on the X-axis as the log of drug concentration and OD was plotted on the Y-axis.

2.6.2. Clonogenic Assay. B16-F10 cells were seeded at a very low number (500 cells in 2 mL/well) in six-well plates. After 24 h, they were treated with the optimum concentration of PCFE (100 μg/mL) alone and in combination with dacarbazine at 1000 μg/mL [37] and incubated for 72 hours. The colonies were fixed with methanol and stained with Harry's hematoxylin. The number of colonies defined as >50 cells/colony was counted under the bright field of a light microscope (Leica DM1000, Germany) at 200x magnification [38].

2.6.3. Wound Healing Assay. The wound healing assay was performed in a 6-well plate following the experimental protocol described in [39]. 2 mL of B16-F10 cells was cultured in DMEM without serum to minimize cellular proliferation. Wounds were generated by scratching the 90% confluent cell monolayer with a sterile 200 μl pipette tip. The unattached cells were washed away with PBS, and cells were treated with PCFE (100 μg/mL) alone and in combination with dacarbazine (1000 μg/mL) diluted in DMEM. Images of the wounds were acquired every 24 h under a phase-contrast microscope. The scratch area was measured using Wound Healing Tool in Image J software and relative scratch closure was calculated as the average length of the relative scratch gap based on the change in the scratch area at time zero.

2.6.4. Immunofluorescence Staining (IFS). For immunofluorescence analysis, 2 mL of B16-F10 cells in DMEM culture media was seeded on coverslips in six-well plates and cultured overnight. Cells were treated with PCFE (100 μg/mL) alone and in combination with dacarbazine (1000 μg/mL) for 24 h. The coverslips were fixed with methanol and incubated for 1 hour with 1 : 400 dilution of primary antibody against vimentin, E-cadherin, and CD133 followed by incubation with goat anti-mouse IgG-FITC (green) and goat anti-mouse IgG-PE (red) at 1 : 300 dilutions [40]. Coverslips were

mounted with glycerol, and images were captured with a fluorescence microscope (Leica DM4000 B, Germany).

2.6.5. Western Blot Analysis. Briefly, 2 mL of B16-F10 cells was seeded in six-well plates and treated with individual and combination doses of PCFE (100 μg/mL) and dacarbazine for 24 hours. After incubation, treated cells were lysed in cold western blot lysis buffer (15 mM Tris, 2 mM EDTA, 50 mM 2-mercaptoethanol, 20% glycerol, 0.1% Triton X-100, 1 mM PMSF, 1 mM sodium fluoride, 1 mM sodium orthovanadate, 1 μg/mL aprotinin, 1 μg/mL leupeptin, and 1 μg/mL pepstatin) for 5 minutes at room temperature. Cell lysates were sonicated and centrifuged at 13500 rpm for 15 minutes. Protein samples (50 μg per lane) were thereafter resolved on a 10% sodium dodecyl sulfate-polyacrylamide gel (SDS-PAGE), blotted onto nitrocellulose membranes, blocked in TBS-T (0.1% Triton in 1xTBS), and probed with primary antibodies (E-cadherin, vimentin, CD133, and actin) overnight at 4°C. The membranes were incubated with the appropriate horseradish peroxidase-conjugated secondary antibodies. The immunoreactive protein bands were developed by an enhanced chemiluminescence kit (BioVision ECL Western Blot Substrate) and the immunoreactive bands were analyzed by using Image Lab software (Bio-Rad, GS 800) [41].

2.7. In Vivo Evaluation

2.7.1. Experimental Animals. The male mice of strain C57BL/6J (aged 4-5 weeks; weight 22–25 g) were reared in the Animal House Department of the Chittaranjan National Cancer Institute in appropriate conditions with an alternating light-dark cycle of 12 hours and controlled temperature (22 ± 2°C). They were fed with a standard mouse diet and received water and feed ad libitum. The mice were acclimatized for seven days before being divided into different subgroups according to well-defined criteria before the onset of each experiment. The distribution of the mice was based on their body weight and tumor size as well. The animals were treated according to the recommendations of the Institutional Animal Ethics Committee (IAEC) of the Chittaranjan National Cancer Institute, Kolkata, just as the protocols used in this study were approved by this committee (Project no. IAEC-1774/NM-14/2019/9; 25.06.2019).

2.7.2. Evaluation of the Effect of PCFE and Dacarbazine on Tumor Development in Mice. To check the effect of PCFE on solid melanoma tumor tissue, B16-F10 cells were administered in C57BL/6J mice. Five- to six-week-old C57BL/6J mice were subcutaneously injected with 2.5×10^4 B16-F10 cells (in 200 μL of PBS) into the right dorsolateral flanks. Treatment with the PCFE began once the tumors were visible and reached an average volume of 50 to 70 mm³. Animals were separated into six different groups (5 mice per group) receiving PCFE 50, 100, 150, 200, and 250 mg/kg body weight (b.w.), respectively, and control group. The choice of doses ≤250 mg/kg was made on the basis of the results of the acute and subchronic toxicity studies of PCFA

carried out by Wamba and collaborators which highlighted in their work the nontoxic effects of PCFE at a dose of 250 mg/kg b.w./day and the toxic effects of PCFE at high doses [42]. After 15 days of intraperitoneal treatment, tumor size was determined and animals were sacrificed by cervical dislocation [43]. Tumors were collected for further analysis.

2.7.3. Combination Treatment. In order to check the effect of dacarbazine alone and in combination with PCFE in solid melanoma tumor, the experiment was designed in 5 groups. The first group was treated with dacarbazine at 80 mg/kg body weight [37]; second, third, and fourth groups were treated with different doses of PCFE 100, 150, and 200 mg/kg b.w., respectively, along with dacarbazine, and the fifth group was considered as a control. The treatment was carried out over a period of seven days; on the 8th day, all animals were sacrificed. After determining the size of the tumor for each treatment group, the tumor tissues of the different groups were treated specifically for further experiments.

2.7.4. CD31 Immunohistochemistry with PAS Staining for Identification of VM Tubes. Formalin-fixed paraffin-embedded (FFPE) sections (5 μm) were kept in xylene for 20 minutes at 55°C and later dipped and deparaffinised in xylene for 10 min (3 changes). The tissue sections were rehydrated with various grades of alcohol. For CD31 expression, an immunochemistry study was performed according to the standard protocol as mentioned in the immunoperoxidase secondary detection system (DAB 150, Merck Millipore). After staining with DAB, the tissues were incubated with a freshly prepared periodic acid solution (5 mg/mL) for 15 min at room temperature [44]. The slides were treated with Schiff base for 20–30 min in dark and counterstained with Harris hematoxylin. Pink stained VM tubes in the sections were photographed using a bright-field microscope (Leica DM1000, Germany).

2.7.5. Qualitative and Quantitative Estimation of the Markers that Play a Key Role in the VM. A qualitative analysis was made with the aid of immunofluorescence staining following the experimental protocol previously described [40]. The tissues were rehydrated with different grades of alcohol, blocked with a blocking buffer solution (1% bovine fetal serum (FBS), and incubated separately with primary antibodies anti-E-cadherin and anti-vimentin, followed by treatment with secondary antibodies marked PE and FITC. 4′, 6-Diamino-2-phenylindole (DAPI) (1 mg/mL; 1 : 10000) was used for nuclear staining. After mounting the slides, images were captured using a Leica BM 4000B fluorescence microscope (Germany). The alteration of EMT was evaluated by targeting E-cadherin, vimentin, and CD133 in PCFE alone and in combination with dacarbazine-treated tumor tissues. The mice melanoma tissues were homogenized and lysed (UP200S) in a western blot lysis buffer and centrifuged at 13500 rpm for 15 minutes (Thermo Scientific Biofuge Stratos). The lysate thus obtained was separated on SDS-PAGE and probed with desired primary and secondary antibodies.

2.7.6. CD31 Immunohistochemistry with PAS Staining for Identification of Microvessel Density. To evaluate microvessel density for angiogenic activity in PCFE and dacarbazine-treated tumor tissues, CD31 immunohistochemistry with PAS staining was performed according to the standard protocol previously described [45]. The diameters of the microvessel were measured and their numbers were estimated after skeletonization of the endothelium in three different fields using ImageJ software.

2.8. Statistical Analysis. Statistical analyses were performed with GraphPad Prism 5 software. Representative data from three independent experiments are shown as mean value ± SEM. One-way analysis of variance (ANOVA) followed by post hoc Tukey's test was used to determine the significance of the difference between mean values relative to the control. The p value was calculated to determine significant differences (p value <0.05).

3. Results

3.1. Qualitative Phytochemical Composition of PCFE. The results of the phytochemical screening reported in Table 1 revealed the presence of alkaloids, polyphenols, saponins, tannins, and sterols in the plant extract while secondary metabolites such as anthraquinones, flavonoids, and triterpenes were absent in the plant extract.

3.2. PCFE Inhibits the Proliferation of B16-F10 Melanoma Cell Line

3.2.1. MTT Assay. To investigate the role of PCFE and dacarbazine on B16-F10 melanoma cells, MTT assay was performed. B16-F10 cells were treated with increasing concentrations of PCFE (10 to 1000 mg/mL) for 24 hours and subjected to MTT assay. The result showed a decrease in the viability of B16-F10 cells as compared to the control (Figure 1(a)). The IC_{50} value of treated B16-F10 cells was calculated to be 47.38 μg/mL (Figure 1(b)).

3.2.2. Colony Formation Assay. To further confirm the cytotoxicity of PCFE on melanoma cells, colony formation assay was performed. Cells were treated with single and combined doses of PCFE and dacarbazine for 24 hours. Result revealed that PCFE alone and in combination with dacarbazine significantly ($p < 0.0001$; F ratio = 244.3; $R^2 = 0.989$) decreased the number of colonies in B16-F10 cells up to 35% and 12%, respectively (Figures 1(c) and 1(d)).

3.3. PCFE Inhibits EMT in B16-F10 Melanoma Cells

3.3.1. Wound Healing Assay. Wound healing assay showed that PCFE (100 μg/mL) and dacarbazine (1000 μg/mL) decreased the invasion and migration of the B16-F10 melanoma cells. However, PCFE treatment and combination treatment inhibit wound healing after 48 hours (Figure 2).

TABLE 1: Phytochemical composition of PCFE.

Chemical classes	*Piper capense* extract
Extractive yield (%)	12.80
Alkaloids	+
Anthraquinones	−
Flavonoids	−
Polyphenols	+
Saponins	+
Tannins	+
Sterols	+
Triterpenes	−

(+): present; (−): absent; yield is obtained by the ratio of the mass of the extract to the methanol obtained to the mass of the plant powder.

3.3.2. Immunofluorescence Staining. In order to evaluate the effect of PCFE and dacarbazine on EMT of B16-F10 cells, immunofluorescence assay was performed. Fluorescence intensity was quantified and represented as a percentage of intensity. The results revealed that PCFE at a concentration of 100 μg/mL downregulates the expression of the vimentin and upregulates E-cadherin protein expression in B16-F10 cells. However, treatment with dacarbazine (1000 mg/mL) showed strong immunopositive expressions of vimentin and no detectable E-cadherin expression in B16-F10 cells. Conversely, in the combination treatment (PCFE 100 μg/mL and dacarbazine 1000 μg/mL), detectable expressions of E-cadherin and moderate immunopositive expression of vimentin were observed (Figure 3(a)).

3.3.3. Western Blot Analysis. Western blot analysis was performed to evaluate the expression of E-cadherin, vimentin, and CD133. The results obtained showed a significant decrease in the expression of the vimentin ($p < 0.0001$; F ratio = 51.86; $R^2 = 0.9511$) and CD133 ($p < 0.0001$; F ratio = 33.74; $R^2 = 0.9268$) proteins compared to the control (Figure 3(b)). However, the expression of vimentin with dacarbazine treatment was not statistically significant with the control (calculated by Tukey's multiple comparison test) (Figure 3(c)). But we observed significant downregulation with PCFE alone at a concentration of 100 μg/mL and in association with dacarbazine. Conversely, we observed a significant increase in the expression of E-cadherin protein ($p < 0.0001$; F ratio = 102.4; $R^2 = 0.9746$) at different treatment concentrations compared to the progressive control as described progressively with effective upregulation at the treatment dose corresponding to the association between PCFE and dacarbazine. PCFE extract alone or in association with dacarbazine used in this work results in a downregulation of vimentin and CD133 proteins and an upregulation of the E-cadherin protein compared to the control (Figures 3(b) and 3(c)).

3.4. Antitumoral Activity of PCFE and Dacarbazine on B16-F10 Melanoma in Mice

3.4.1. PCFE Reduces Tumor Size in B16-F10 Melanoma Mice. An increase in tumor size was observed in animals treated with dacarbazine ($4.0 \times 4.3 \, cm^2$) compared to control

(a)

(b)

(c)

(d)
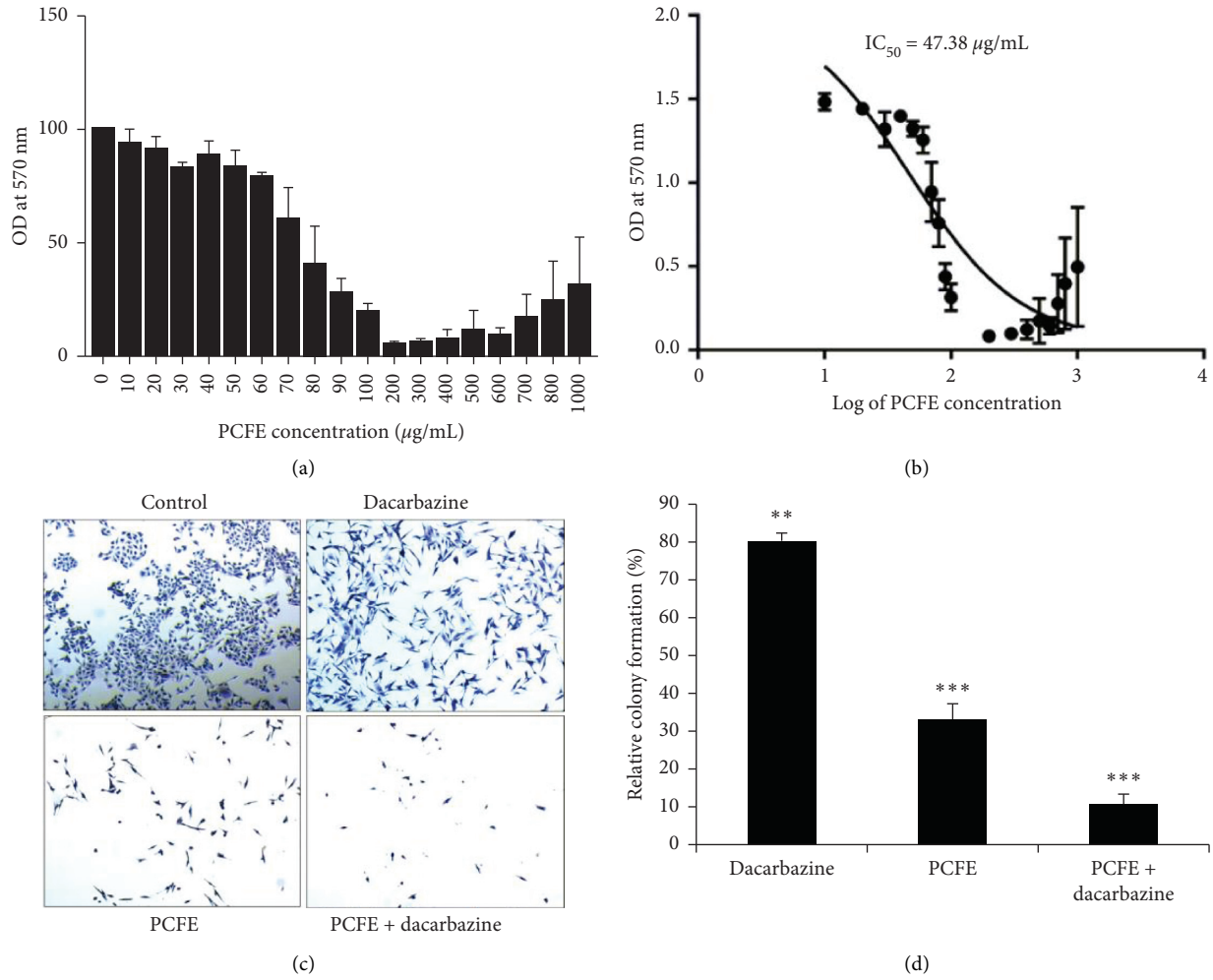
FIGURE 1: Cytotoxic effect of PCFE in B16-F10 cells. The percentage viability of PCFE-treated B16-F10 cells was calculated as OD of the drug-treated sample/OD of the nontreated sample $\times$ 100 (a). IC_{50} of melanoma cells treated with increasing concentration of PCFE was calculated as 47.38 μg/ml (b). PCFE alone and in combination with dacarbazine significantly induced inhibition of colony formation and development of B16-F10 cells *in vitro* (c, d). Statistical significance of each treatment group with untreated control is analyzed by one-way ANOVA test ($p_{\text{ANOVA}} < 0.0001$) followed by post hoc Tukey's test. Data are represented as mean $\pm$ SD of triplicate determinations from their independent experiments with $^*p$ value <0.05, $^{**}p$ value <0.01, and $^{***}p$ value <0.0001 versus untreated control and among each group.
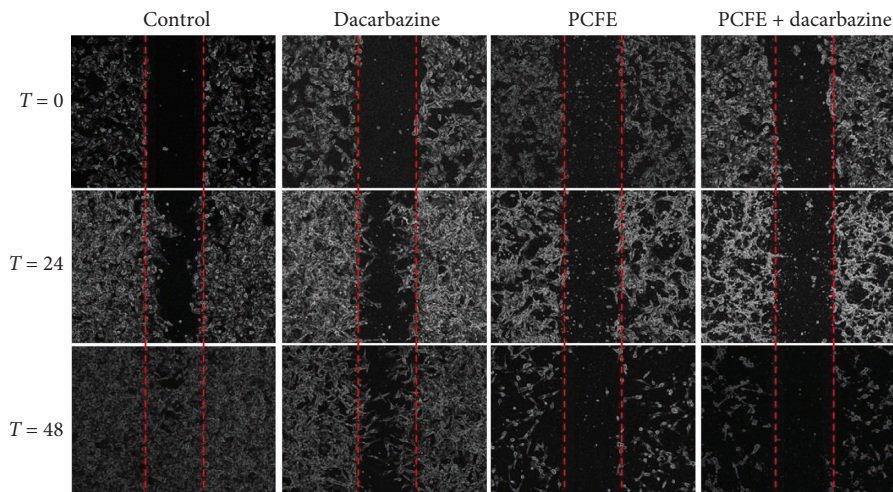
FIGURE 2: Antimigratory effect of PCFE on B16-F10. PCFE alone and in combination with dacarbazine prevents cell migration as compared to the control.

(a)

(b)

(c)
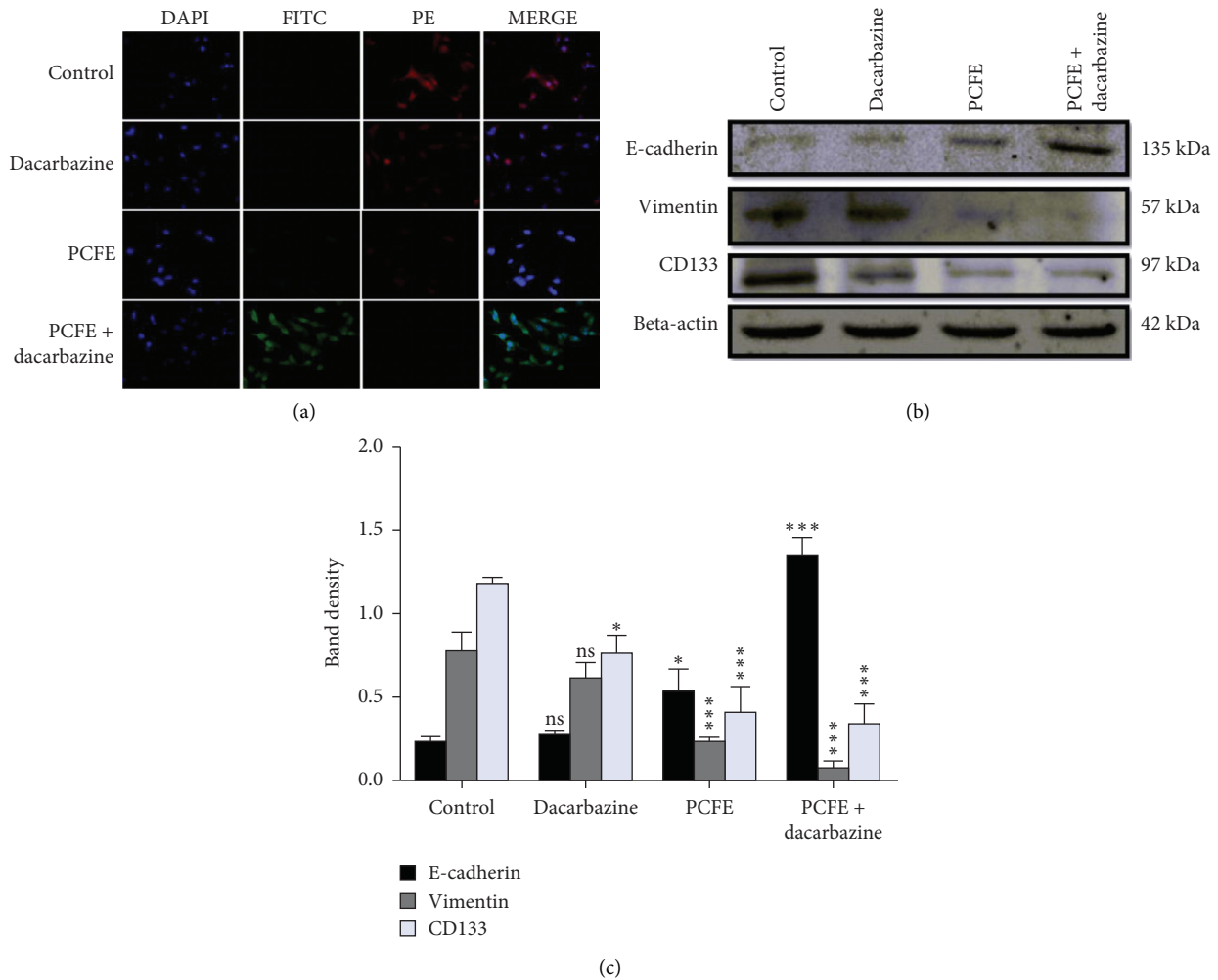
FIGURE 3: PCFE treatment modulates the expression of EMT markers *in vitro*. PCFE alone and in combination with dacarbazine upregulates the expression of FITC-tagged (green) E-cadherin and downregulates PE-tagged (red) vimentin of B16-F10 cells as compared to the untreated control (a). Western blot analysis and densitometric plot also showed significant upregulation of E-cadherin and downregulation of vimentin as well as CD133 (b, c). Statistical significance of each treatment group with untreated control is analyzed by one-way ANOVA test ($p_{ANOVA} < 0.0001$) followed by post hoc Tukey's test. Data are represented as mean $\pm$ SD of triplicate determinations from their independent experiments; ns: not significant, $^*p$ value <0.05, $^{**}p$ value <0.01, and $^{***}p$ value <0.0001 versus untreated control and among each group.

animals (3.3×3.1 cm^2). In contrast, there was a remarkable decrease in tumor size in animals treated with different doses of PCFE: 50 mg/kg (2.4×2.6 cm^2), 100 mg/kg (0.8×1.0 cm^2), 150 mg/kg (1.0×1.1 cm^2), 200 mg/kg (1.6×1.7 cm^2), and 250 mg/kg (2.4×2.5 cm^2). PCFE at different concentrations in combination with dacarbazine at 80 mg/kg showed remarkable inhibition in tumor size: dacarbazine + 100 mg/kg dose (1.1×1.3 cm^2), dacarbazine + 150 mg/kg dose (1.9×1.8 cm^2), and dacarbazine + 200 mg/kg dose (2.8×2.5 cm^2). PCFE at the dose of 100 mg/kg b.w. showed maximum antitumor effect alone in melanoma mice as well as in combination with dacarbazine at 80 mg/kg b.w (Figures 4(a) and 4(b)).

3.4.2. PCFE Inhibits the Formation and/or Development of Vasculogenic Mimicry.
CD31-PAS immunohistochemistry results of dacarbazine-treated tumor tissue isolated from

mice melanoma showed enormous VM tubes. However, different doses of PCFE alone and in combination with dacarbazine treatment showed inhibition of vasculogenic mimicry tubes (CD31 negative/PAS positive). 100 mg/kg b.w. doses of PCFE alone and in the presence of dacarbazine showed a significant decrease in the tumor size and therefore a decrease in the number of tubes at different doses of treatment (Figures 5(a) and 5(b)).

3.4.3. Qualitative and Quantitative Effect of PCFE and Dacarbazine on the Expression of the Markers that Play a Key Role in the VM and EMT.
The immunofluorescence carried out on the corresponding tissue sections, each at a precise dose, made it possible to demonstrate the effect of different doses of PCFE alone and in association with dacarbazine on protein expression. These proteins are involved in the heart of

(a)

(b)
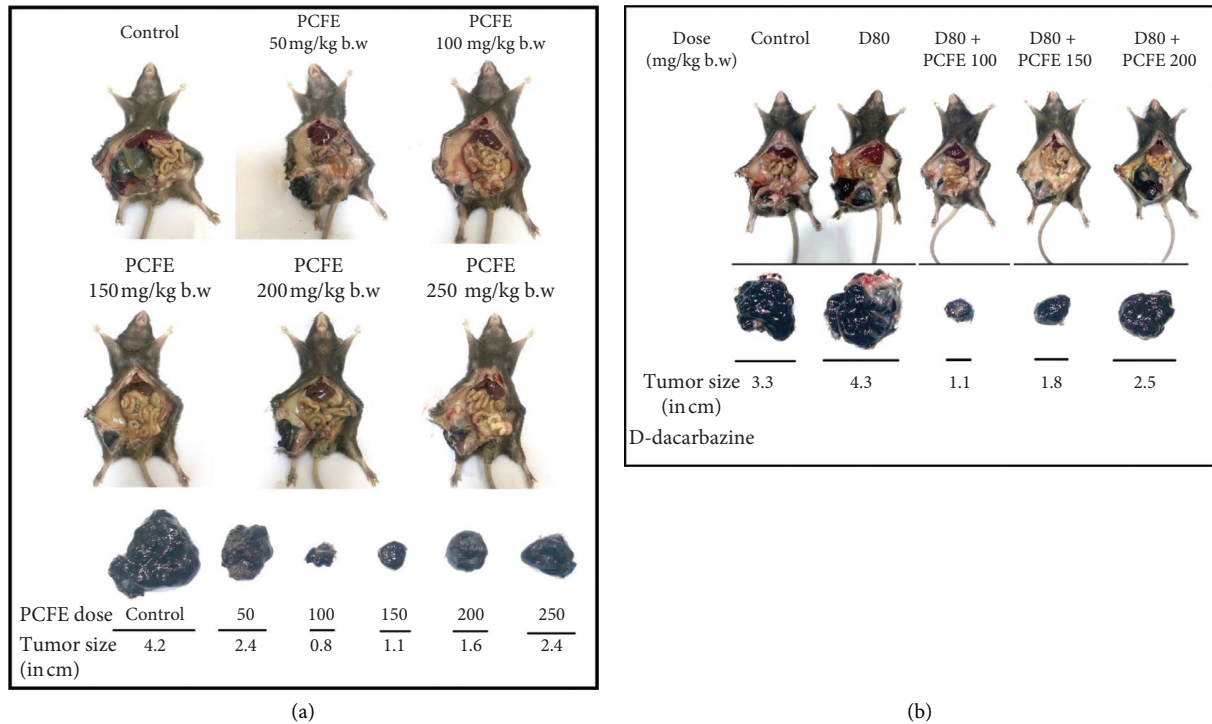
FIGURE 4: PCFE alone and in combination with dacarbazine causes a decrease in tumor size of B16-F10 melanoma mice. The treatment of melanoma mice with various doses of PCFE alone (a) and in combination with dacarbazine (b). PCFE alone at 100 mg/kg b.w. and in combination with dacarbazine showed a maximum decrease in tumor size as compared to the untreated control and other treatment regimes.

EMT, especially in the inhibition of the expression of vimentin (progressive reduction of the red color) and activation of the expression of E-cadherin (progressive increase in green color), dose dependently in groups of animals treated with PCFE compared to the control group (infected and untreated group). 100 mg/kg dose of PCFE was found to be the dose with the best ability to regulate the expression of these proteins both when administered individually and in combination with dacarbazine (Figure 6(a)). Similar results were obtained from western blot analysis of mice melanoma tumor lysates treated with different doses of PCFE which showed significant downregulation of CD133 ($p < 0.0001$; F ratio = 70.74; $R^2 = 0.963$) and vimentin ($p < 0.0001$; F ratio = 152; $R^2 = 0.982$) and upregulation of E-cadherin expression ($p < 0.0001$; F ratio = 158.1; $R^2 = 0.983$) (Figures 6(b) and 6(c)). However, a better regulation was observed in terms of expression at the dose of 100 mg/kg individually and in combination with dacarbazine (Figure 6(d)).

3.4.4. Effect of PCFE and Dacarbazine on Microvessel Density. This test was performed in order to evaluate the effect of different doses of PCFE on the antigenic vessels present in the tumors collected from different groups of animals. The treatment of animals with the PCFE resulted in a progressive and significant decrease in the number and diameter of the different antiangiogenic vessels in different groups of animals tested and those treated more intensely treated with the 100 mg/kg dose (Figures 7 and 8).

4. Discussion

According to the International Agency for Research on Cancer (IARC) in 2018, the global cancer burden was estimated at 18.1 million for new cases against 9.6 million cancer deaths. Both metastatic and nonmetastatic melanomas have over time developed resistance to conventional anticancer drugs, which are nowadays classified as a public health hazard with reference to their relatively high mortality rate. There is therefore an urgent need to find new effective, low-toxicity substances, and given that phytochemicals are a poorly explored field makes it an unexplored gold mine for researchers. *Piper capense* is a food plant used in Cameroon and other countries in the world in the preparation of dishes and also for its therapeutic virtues [46, 47]. This plant species found in the natural flora of Cameroon has already been the subject of several *in vitro* studies on its anticancer activities on several cancer cell lines [28, 48]. Nevertheless, no reports in the literature have so far shown activities of this plant on melanoma both *in vitro* and *in vivo*, hence the essence of this work.

Several classes of secondary metabolites in plants are known to have cytotoxic and antitumor activities, including alkaloids, polyphenols, saponins, tannins, and sterols [49, 50]. The presence of alkaloids, polyphenols, saponins, tannins, and sterols in the methanol extract of *Piper capense* may justify its anticancer activities *in vitro* and *in vivo* observed in this work. The phytochemical screening results obtained in this study corroborate those of Fankam et al. [51].
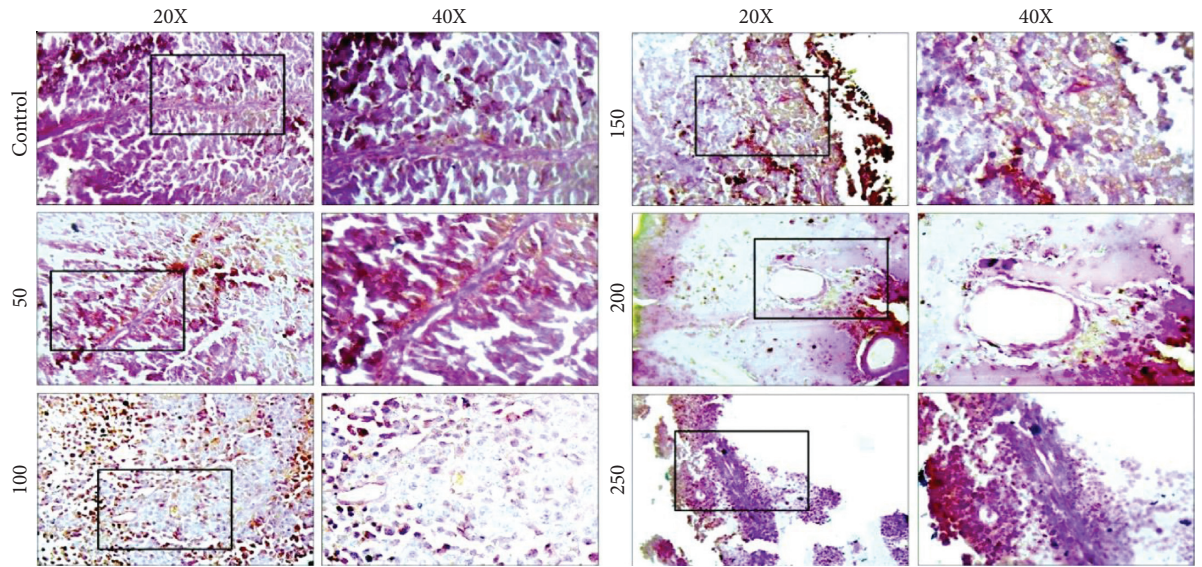
(a)
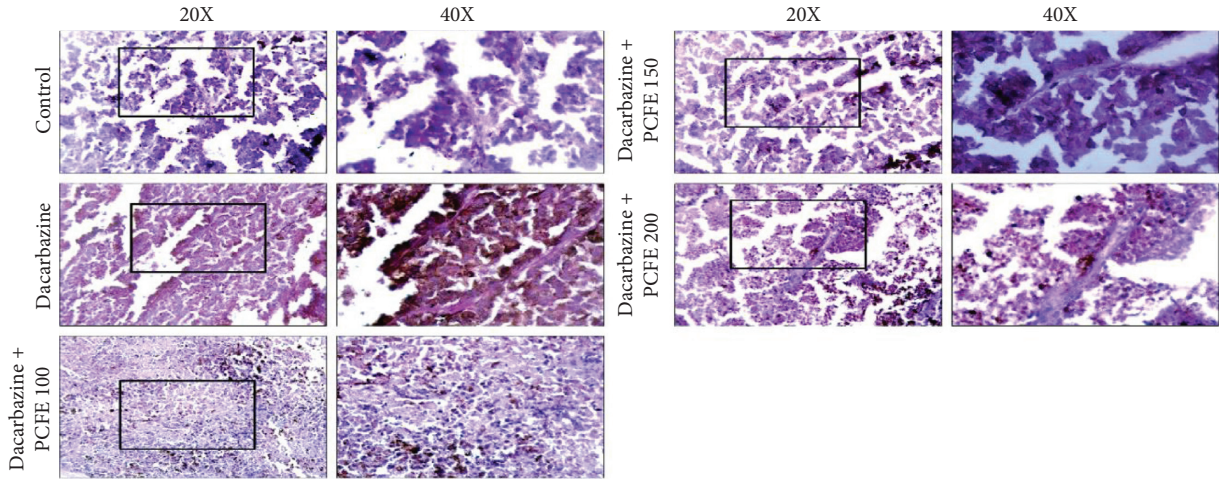
(b)

Figure 5: Effect of PCFE on the development of vasculogenic mimicry. CD31-PAS immunohistochemistry result showed PCFE alone (a) and in association with dacarbazine (b) inhibits the formation and development of vasculogenic mimicry in B16-F10 melanoma mice.
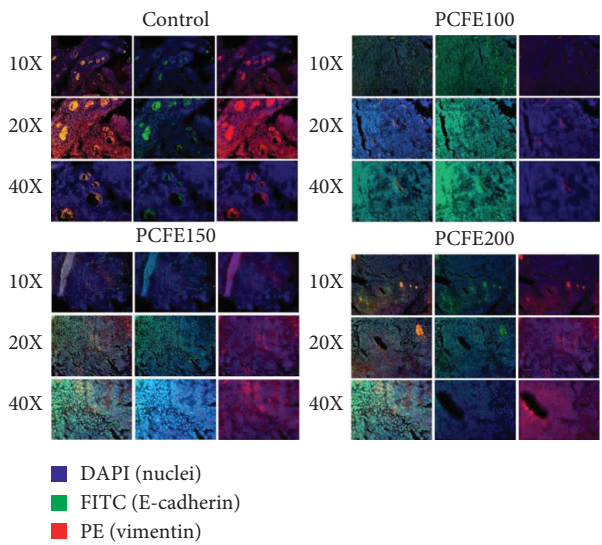
(a)
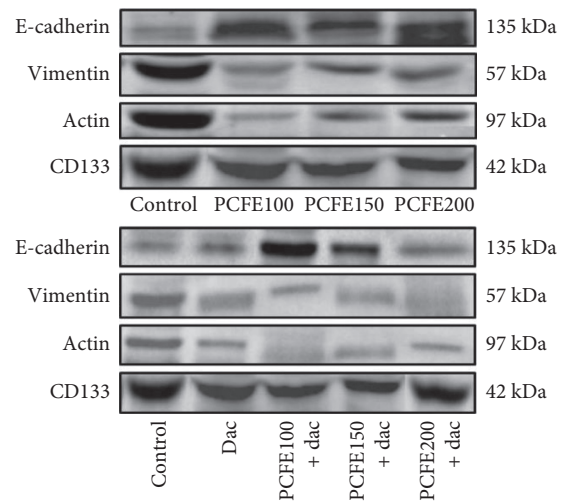
(b)

Figure 6: Continued.

(c)

(d)
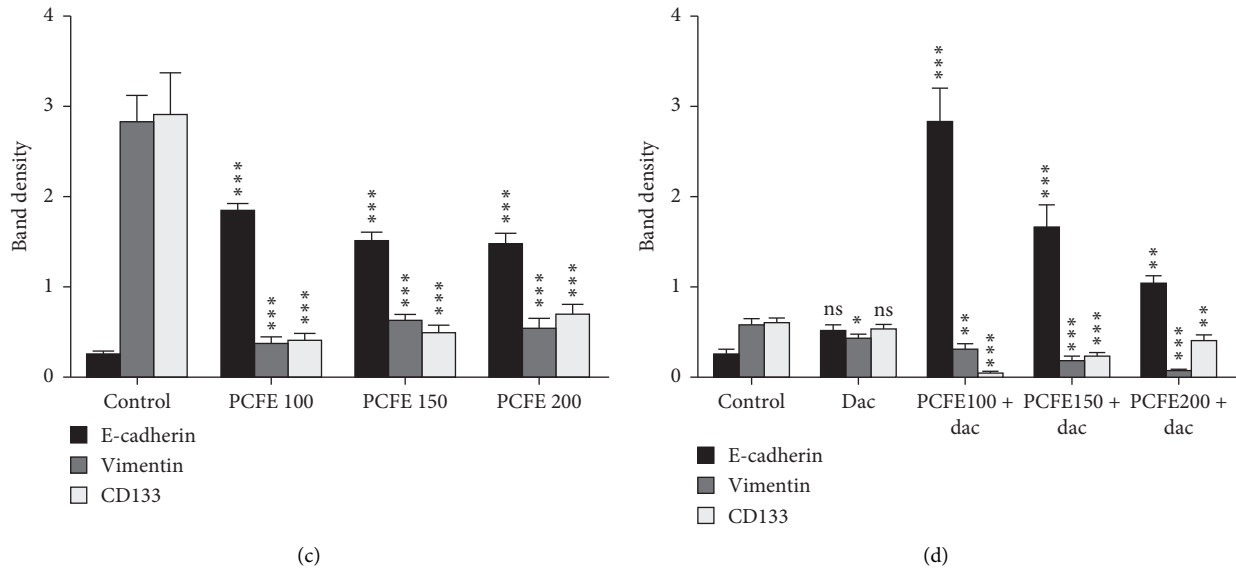
FIGURE 6: Qualitative and quantitative effect of PCFE on the expression of the markers that play a key role in the VM and EMT. Immunofluorescence study with various individual treatments of PCFE and in combination with dacarbazine in mice melanoma tumor sample showed an increase in the expression of E-cadherin and decrease in vimentin (a). Western blot analysis (b) and its densitometry plot (c, d) also showed significant upregulation of E-cadherin and downregulation of vimentin and CD133 in tumor tissue lysate of mice melanoma. Statistical significance of each treatment group with untreated control is analyzed by one-way ANOVA test ($p_{ANOVA} < 0.0001$) followed by post hoc Tukey's test. Data are represented as mean ± SD of triplicate determinations from their independent experiments with *p value <0.05, **p value <0.01, and ***p value <0.0001 versus untreated control and among each group.


(a)
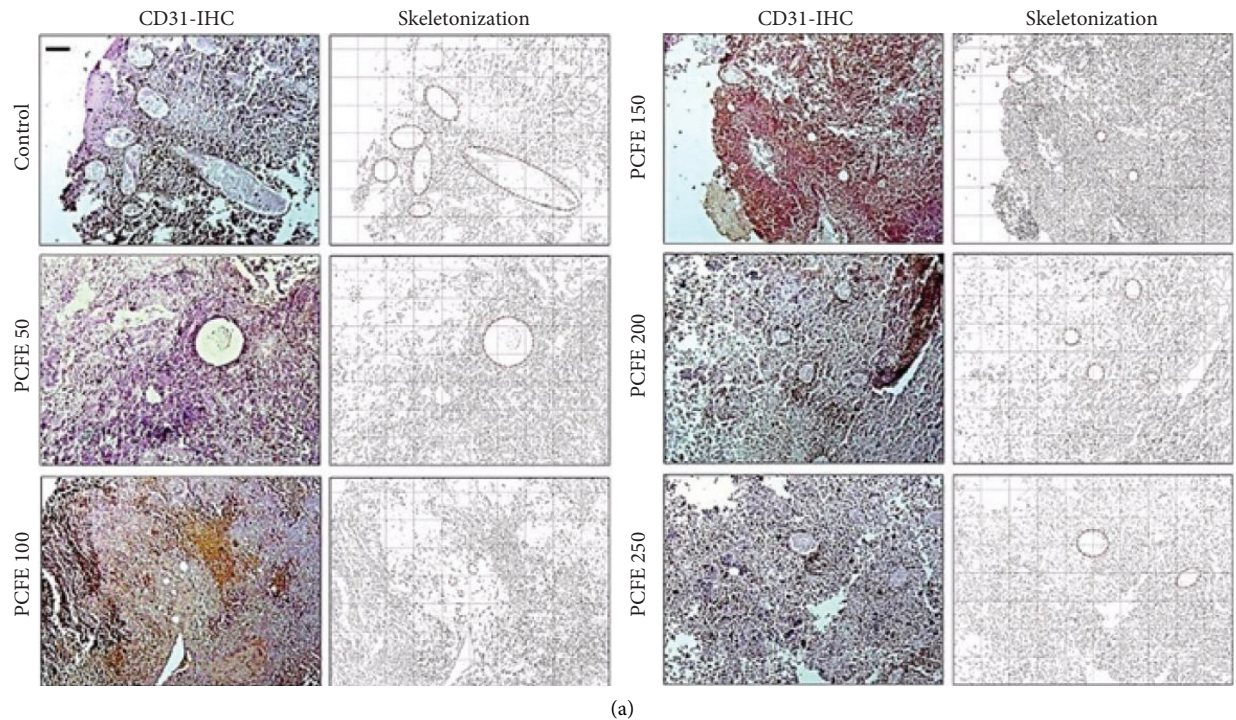
FIGURE 7: Continued.
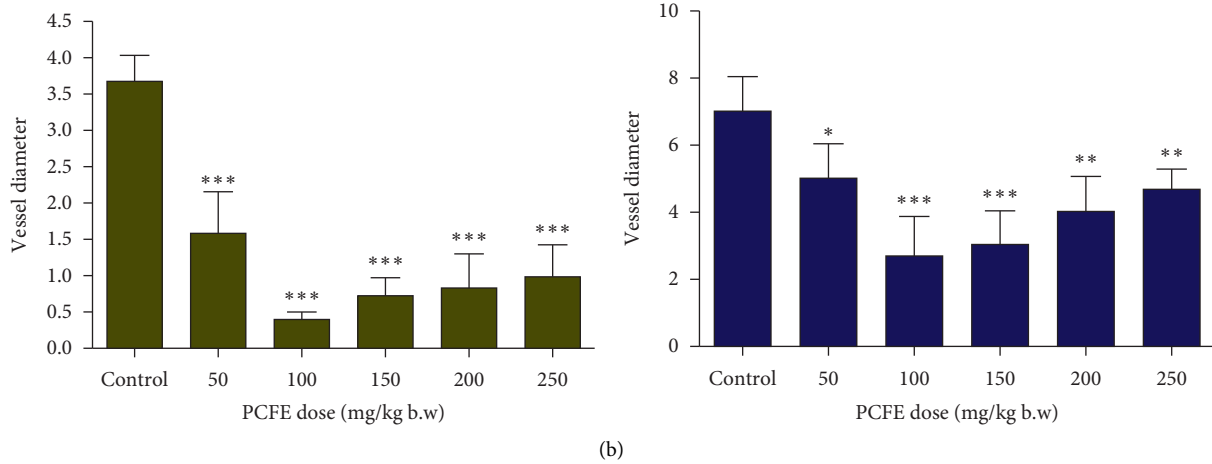
Figure 7: Effect of PCFE on microvessel density. PCFE alone at different doses effectively reduces microvessel size and density in B16-F10 melanoma mice.
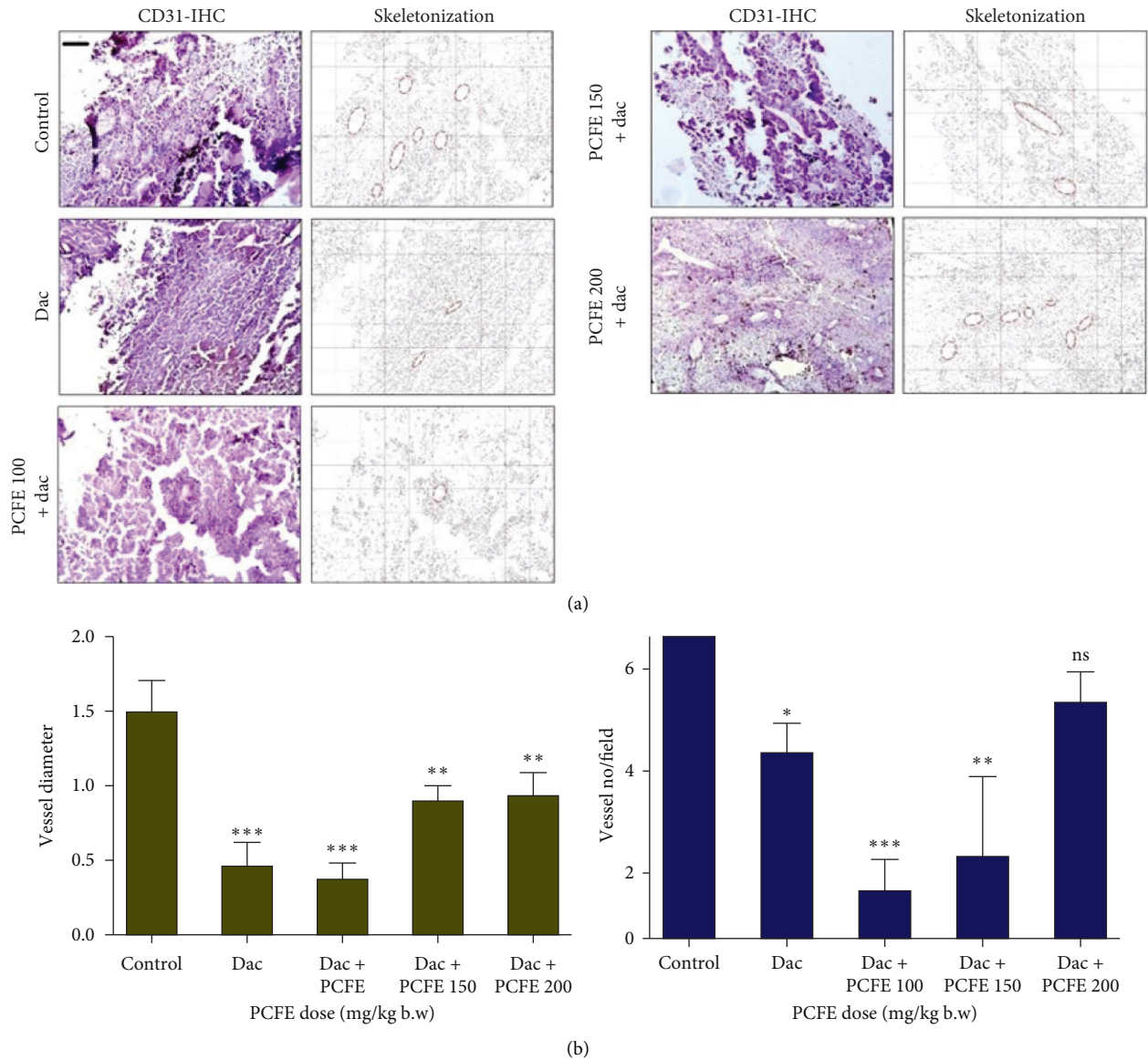
Figure 8: Effect of PCFE in association with dacarbazine on microvessel density. PCFE at different doses in combination with dacarbazine effectively reduces microvessel size and density in B16-F10 melanoma mice.

Research on new drugs focuses on substances targeting a specific metabolic pathway or acting on a molecular target with a key role in the survival of cancer stem cells (CSCs), especially those with the ability to restore the expression of proteins involved in EMT. Epithelial-mesenchymal transition is a cellular process in which cells lose their epithelial characteristics and acquire mesenchymal characteristics. EMT has been associated with various tumor functions, including tumor initiation, malignant progression, tumor tenacity, tumor cell migration, metastasis, and treatment resistance [52, 53] and is often defined by downregulation of the epithelial marker E-cadherin and upregulation of the mesenchymal markers vimentin and CD133 [54].

The results obtained in this work show the ability of PCFE to induce a cytotoxic effect on B16-F10 cells and the ability of PCFE alone and in combination with dacarbazine to prevent and/or inhibit colony formation and also for the inhibition of wound healing of B16-F10 melanoma cells and to the reversal of markers involved in EMT by modification of their expression *in vitro*. All these activities could be attributed to the presence of various secondary metabolites with proven anticancer activity in this plant extract [55]. Many works have demonstrated the antiproliferative effect of secondary metabolites such as alkaloids, phenolic compounds, and triterpenes [28, 56, 57]. PCFE alone and in combination with dacarbazine-induced shrinkage of tumor size in animals by inhibiting the development of VM tubes and microvessel density. It also restored the expression of proteins involved in EMT (downregulation of CD133 and vimentin markers and upregulation of E-cadherin) both *in vitro* and *in vivo*. These activities could be due to the presence of the secondary metabolites endowed with anticancer activity in the extract. These results corroborate those of other previous works that have shown that spices possess cytotoxic activities either by induction of apoptosis or by cell cycle arrest at a specific phase [28, 58] and action on EMT markers *in vitro* and *in vivo* [59–61].

The work done by Woguen et al. [48] on the evaluation of the phytochemical composition of essential oil of fruits of *P. capense* by GC-MS revealed the presence of two major compounds (β-pinene and (E)-caryophyllene) with good cytotoxic activities. β-Pinene and *(E)*-caryophyllene are compounds belonging to the class of phenolics and terpenoids, respectively; the latter were identified in PCFE. Phenolics and terpenoids are classes of secondary metabolites with antiproliferative and antitumor activities [48, 56]. The presence of these classes of metabolites in PCFE may account for the *in vitro* and *in vivo* anticancer activities observed in this study.

Some compounds like piperine found in alkaloids having anticancer activities *in vitro* and *in vivo* as documented in the literature are also found in plants belonging to the genus *Piper* and the species *Piper nigrum*, *Piper longum*, and *Piper capense* [61–63]. In view of the above, the similarities between the results with the methanol extract of *Piper capense* obtained in this study and those with piperine obtained in other studies lead us to suggest that alkaloids (one group of secondary metabolite highlighted in PCFE) could also be responsible for the activities observed in this study. The

results of this study showed the capacity of PCFE to inhibit the formation and development of VM tubes which are indeed neoformed vessels which play a role in supplying the cancerous cells with nutrients at the level of the primary tumor [64]. The inhibition of the development of these VM tubes by PCFE accompanied by the restoration of the expression of proteins involved in EMT could justify the decrease in the size of the tumor because it lacks a supply route. Also, the antiangiogenic activities of this plant extract were observed in this study as shown previously [65]. These aforementioned activities demonstrate and sufficiently justify the antiproliferative activity of PCFE and could be due to the possible presence of alkaloids in this plant.

The work of Greenshields et al. [66] demonstrates the ability of piperine to inhibit the growth of triple breast cancer xenografts in immune-deficient mice corroborating the results of this study which was carried out on moles of mice of C57BL/6J strains with melanomas. Makhov et al. [67] showed a remarkable effect of the association of an anticancer agent (docetaxel) with piperine through the improvement of the antitumor activity in the xenograft model of human castration-resistant prostate cancer. This is consistent with the results obtained in our study given that a remarkable improvement in the activity of dacarbazine (conventional chemotherapeutic drug of melanoma) administered in association with the PCFE was noted both *in vitro* and *in vivo*. A justification for this activity could be due to the possible presence of one or many active compounds that can be found in the different groups of secondary metabolite that we have highlighted in PCFA.

5. Conclusion

In conclusion, this study, which is the first of its kind to evaluate the anticancer activity of the methanol extract of *Piper capense* fruit against melanoma *in vitro* and *in vivo*, clearly demonstrates the ability of PCFE to inhibit cell proliferation alone and in combination with dacarbazine *in vitro*, to induce the shrinkage of the melanoma tumor size in mice by modification of expression of the markers involved in EMT through downregulation of CD133 and vimentin markers and up-regulation of the E-cadherin marker *in vivo* in melanoma models with the best effect at 100 mg/kg b.w. These results coupled with those in the literature indicate that the *Piper capense* plant is a very good candidate plant for the formulation of phytomedicines in the treatment of melanoma. One of the limitations of this study is the characterization of the phytochemical constituents and mostly the bioactive as well as potentially toxic constituents of the tested methanol extract. However, this work is ongoing and constitutes the aim of our further investigations.

Abbreviations

PCFE: *Piper capense* fruit extract
MTT: 3-(4, 5-Dimethylthiazol-2-yl)-2, 5-diphenyl tetrazolium bromide
EMT: Epithelial-to-mesenchymal transition
DAB: 3′3-Diaminobenzidine

DMEM: Dulbecco's modified Eagle medium
FBS: Fetal bovine serum
VM: Vasculogenic mimicry
MIC: Minimal inhibitory concentration
ABC: ATP-binding cassette
CSC: Cancer stem cell
IC_{50}: Inhibitory concentration 50%
WHO: World Health Organization.

Data Availability

All data generated or analyzed during this study are included in this published article.

Ethical Approval

All the experimentation was carried out in strict accordance with the established guidelines on the use of experimental animals (Project no. IAEC-1774/NM-14/2019/9; 25.06.2019).

Conflicts of Interest

VK is an Associate Editor in *Evidence-Based Complementary and Alternative Medicine*; all the other authors declare that there are no conflicts of interest.

Authors' Contributions

BENW, PG, VK, and NM conceptualized the study, formulated the hypothesis, and designed the study. DS, DM, and ATM gave valuable inputs in designing the experiments. BENW, PG, DM, and DS interpreted the data. BENW, VK, and NM wrote the manuscript. ATM, VK, and NM supervised the entire project. BENW, PG, DM, DS, SMM, ATM, VK, and NM read and approved the final version of the manuscript.

Acknowledgments

References

[1] D. A. Vorobiof and R. Abratt, "The cancer burden in Africa," *South African Medical Journal = Suid-Afrikaanse Tydskrif Vir Geneeskunde*, vol. 97, no. 10, pp. 937–939, 2007.

[2] International Agency for Research on Cancer (IARC), *Latest Global Cancer Data: Cancer Burden Rises to 18.1 Million New Cases and 9.6 Million Cancer Deaths in 2018*, Press Release, London, UK, 2020.

[3] A. L. Torre, F. Bray, L. R. Siegel, J. Ferlay, J. Lortet-Tieulent, and A. Jemal, "Global cancer statistics," *A Cancer Journal for Clinicians*, vol. 65, pp. 87–108, 2012.

[4] R. L. Siegel, K. D. Miller, and A. Jemal, "Cancer statistics, 2019," *CA: A Cancer Journal for Clinicians*, vol. 69, no. 1, pp. 7–34, 2019.

[5] P. Prasad, A. Vasas, J. Hohmann, A. Bishayee, and D. Sinha, "Cirsiliol suppressed epithelial to mesenchymal transition in B16F10 malignant melanoma cells through alteration of the PI3K/akt/NF-κB signaling pathway," *International Journal of Molecular Sciences*, vol. 20, no. 3, p. 608, 2019.

[6] P. Aubry and B.-A. Gaüzère, "Les cancers dans les pays en développement actualités," 2016.

[7] A. Jemal, F. Bray, M. M. Center, J. Ferlay, E. Ward, and D. Forman, "Global cancer statistics," *CA: A Cancer Journal for Clinicians*, vol. 61, no. 2, pp. 69–90, 2011.

[8] ALIAM (Alliance des Ligues francophones Africaines et Méditerranéens), "Les cancers en Afrique Francophone," *Ligue Nationale Contre le Cancer (France)*, vol. 13, pp. 1–36, 2017.

[9] M. Zigler, G. J. Villares, D. C. Lev, V. O. Melnikova, and M. Bar-Eli, "Tumor immunotherapy in melanoma," *American Journal of Clinical Dermatology*, vol. 9, no. 5, pp. 307–311, 2008.

[10] M. Dean, T. Fojo, and S. Bates, "Tumour stem cells and drug resistance," *Nature Reviews Cancer*, vol. 5, no. 4, pp. 275–284, 2005.

[11] D. C. Lev, A. Onn, V. O. Melinkova et al., "Exposure of melanoma cells to dacarbazine results in enhanced tumor growth and metastasis *in vivo*," *Journal of Clinical Oncology*, vol. 22, no. 11, pp. 2092–2100, 2004.

[12] D. C. Lev, M. Ruiz, L. Mills, E. C. McGary, J. E. Price, and M. Bar-Eli, "Dacarbazine causes transcriptional up-regulation of interleukin 8 and vascular endothelial growth factor in melanoma cells: a possible escape mechanism from chemotherapy," *Cancer Cell*, vol. 8, pp. 299–309, 2005.

[13] O. Casanovas, D. J. Hicklin, G. Bergers, and D. Hanahan, "Drug resistance by evasion of antiangiogenic targeting of VEGF signaling in late-stage pancreatic islet tumors," *Cancer Cell*, vol. 8, no. 4, pp. 299–309, 2005.

[14] G. H. Goren, R. Halaban, and G. Neufeld, "Human melanoma cells but not normal melanocytes express vascular endothelial growth factor receptors," *Biochemical and Biophysical Research Communications*, vol. 190, pp. 702–708, 2005.

[15] M. R. Middleton, J. J. Grob, N. Aaronson et al., "Randomized phase III study of temozolomide versus dacarbazine in the treatment of patients with advanced metastatic malignant melanoma," *Journal of Clinical Oncology*, vol. 18, no. 1, p. 158, 2000.

[16] M. R. Middleton, P. Lorigan, J. Owen et al., "Randomized phase III study comparing dacarbazine, BCNU, cisplatin and tamoxifen with dacarbazine and interferon in advanced melanoma," *British Journal of Cancer*, vol. 82, pp. 1158–1162, 2010.

[17] A. Avilés, N. Arévila, J. C. Díaz Maqueo, M. J. Nambo, R. Garcia, and M. J. Nambo, "Late cardiac toxicity of doxorubicin, epirubicin, and mitoxantrone therapy for Hodgkin's disease in adults," *Leukemia & Lymphoma*, vol. 11, no. 3-4, pp. 275–279, 1993.

[18] E. Leo, R. Arletti, F. Forni, and R. Cameroni, "General and cardiac toxicity of doxorubicin-loaded gelatin nanoparticles," *Farmaco*, vol. 52, pp. 385–388, 1997.

[19] S. Kilickap, E. Akgul, S. Aksoy, K. Aytemir, and I. Barista, "Doxorubicin-induced second degree and complete atrioventricular block," *Europace*, vol. 7, no. 3, pp. 227–230, 2005.

[20] L. Manil, P. Couvreur, and P. Mahieu, "Acute renal toxicity of doxorubicin (adriamycin)-loaded cyanoacrylate nanoparticles," *Pharmaceutical Research*, vol. 12, no. 1, pp. 85–87, 1995.

[21] J. S. Macdonald, "Toxicity of 5-fluorouracil," *Oncology*, vol. 13, pp. 33-34, 1999.

[22] G. Rexroth and V. Scotland, "Cardiac toxicity of 5-fluorouracil," *Medizinische Klinik*, vol. 89, pp. 680–688, 1994.

[23] S. Pandey, "*In Vivo* antitumor potential of extracts from different parts of *Bauhinia variegata* linn. Against B16-F10 melanoma tumour model in C57BL/6 mice," *Applied Cancer Research*, vol. 37, p. 33, 2017.

[24] S. Rajasekar, D. J. Park, C. Park et al., "In vitro and in vivo anticancer effects of Lithospermum erythrorhizon extract on B16F10 murine melanoma," *Journal of Ethnopharmacology*, vol. 144, no. 2, pp. 335–345, 2012.

[25] A. C. Uscanga-Palomeque, P. Zapata-Benavides, S. Saavedra-Alonso et al., "Inhibitory effect of *Cuphea aequipetala* extracts on murine B16-F10 melanoma *in vitro* and *in vivo*," *BioMed Research International*, vol. 11, 2019.

[26] Y. W. Xin, W. D. Qi, and C. Y. Han, "Traditional chinese medicine for treating respiratory cancer," 2009.

[27] T. C. Chen, "Observation of the medicine made by oneself in treating with 97 cases with gastric diseases," *Practice of Medical Technology*, vol. 15, pp. 593-594, 2008.

[28] V. Kuete, L. P. Sandjo, B. Wiench, and T. Efferth, "Cytotoxicity and modes of action of four Cameroonian dietary spices ethno-medically used to treat Cancers: echinops giganteus, Xylopia aethiopica, Imperata cylindrica and Piper capense," *Journal of Ethnopharmacology*, vol. 149, no. 1, pp. 245–253, 2013.

[29] A. M. Kaou, V. Mahiou-Leddet, S. Hutter et al., "Antimalarial activity of crude extracts from nine African medicinal plants," *Journal of Ethnopharmacology*, vol. 116, no. 1, pp. 74–83, 2008.

[30] A. Koch, P. Tamez, J. Pezzuto, and D. Soejarto, "Evaluation of plants used for antimalarial treatment by the Maasai of Kenya," *Journal of Ethnopharmacology*, vol. 101, no. 1-3, pp. 95–99, 2005.

[31] V. Kuete, B. Krusche, M. Youns et al., "Cytotoxicity of some Cameroonian spices and selected medicinal plant extracts," *Journal of Ethnopharmacology*, vol. 134, no. 3, pp. 803–812, 2011.

[32] E. M. Tekwu, T. Askun, V. Kuete et al., "Antibacterial activity of selected Cameroonian dietary spices ethno-medically used against strains of *Mycobacterium tuberculosis*," *Journal of Ethnopharmacology*, vol. 142, no. 2, pp. 374–382, 2012.

[33] V. Steenkamp, A. C. Fernandes, and C. E. J. Van Rensburg, "Screening of Venda medicinal plants for antifungal activity against Candida albicans," *South African Journal of Botany*, vol. 73, no. 2, pp. 256–258, 2007.

[34] J. B. Harbone, *Phytochemical Methods: A Guide to Modern Techniques of Plant Analysis*, Chapman & Hall, London, UK, 1973.

[35] H. M. P. Poumale, R. Hamm, Y. Zang, Y. Shiono, and V. Kuete, "Coumarins and related compounds from the medicinal plants of Africa," in *Medicinal Plant Research in Africa: Pharmacology and Chemistry*, V. Kuete, Ed., vol. 1, pp. 261–300, Elsevier, Oxford, UK, 2013.

[36] T. Mossmann, "Rapid colorimetric assay for cellular growth and survival: application to proliferation and cytotoxicity assays," *Journal of Immunological Methods*, vol. 65, pp. 55–63, 1983.

[37] S. Bhattacharyya, D. Mitra, S. Ray et al., "Reversing effect of Lupeol on vasculogenic mimicry in murine melanoma progression," *Microvascular Research*, vol. 121, pp. 52–62, 2019.

[38] N. A. P. Franken, H. M. Rodermond, J. Stap, J. Haveman, and C. Van Bree, "Clonogenic assay of cells *in vitro*," *Nature Protocols*, vol. 1, no. 5, p. 2315, 2006.

[39] C.-C. Liang, A. Y. Park, and J.-L. Guan, "*In vitro* scratch assay: a convenient and inexpensive method for analysis of cell migration *in vitro*," *Nature Protocols*, vol. 2, no. 2, p. 329, 2007.

[40] C. Wählby, F. Erlandsson, E. Bengtsson, and A. Zetterberg, "Sequential immunofluorescence staining and image analysis for detection of large numbers of antigens in individual cell nucleifluorescence staining and image analysis for detection of large numbers of antigens in individual cell nuclei," *Cytometry*, vol. 47, no. 1, pp. 32–41, 2002.

[41] F. A. Bhat, G. Sharmila, S. Balakrishnan et al., "Quercetin reverses EGF-induced epithelial to mesenchymal transition and invasiveness in prostate cancer (PC-3) cell line via EGFR/PI3K/Akt pathway," *The Journal of Nutritional Biochemistry*, vol. 25, no. 11, pp. 1132–1139, 2014.

[42] B. E. N. Wamba, A. T. Mbaveng, G. M. Tazoho, and V. Kuete, "Botanical from the medicinal spice, *Piper capense* is safe as demonstrated by oral acute and subchronic toxicity investigations," *Heliyon*, vol. 6, 2020.

[43] Vertebrate Animal Research, "AVMA guidelines for the euthanasia of animals: 2013 edition," 2013.

[44] M. J. C. Hendrix, E. A. Seftor, R. E. B. Seftor et al., "Regulation of uveal melanoma interconverted phenotype by hepatocyte growth factor/scatter factor (HGF/SF)," *American Journal of Pathology*, vol. 152, no. 4, pp. 855–863, 1998.

[45] N. C. Munshi and C. Wilson, "Increased bone marrow microvessel density in newly diagnosed multiple myeloma carries a poor prognosis," *Seminars in Oncology*, vol. 28, no. 6, pp. 565–569, 2001.

[46] N. Ahmad, H. Fazal, B. H. Abbasi, S. Farooq, M. Ali, and M. A. Khan, "Biological role of *Piper nigrum* L. (Black pepper): a review," *Asian Pacific Journal of Tropical Biomedicine*, vol. 2, pp. 1945–1953, 2012.

[47] I. A. Oyemitan, "Chapter 27- african medicinal spices of genus *Piper capense*," in *Medicinal Spices and Vegetables from Africa*, pp. 581–597, Elsevier Inc: Academic Press, London, UK, 2017.

[48] V. Woguem, F. Maggic, H. P. D. Fogang et al., "Antioxidant, antiproliferative and antimicrobial activities of the volatile oil from the wild pepper *Piper capense* used in Cameroon as a culinary spice," *Natural Product Communications*, vol. 8, pp. 1791–1796, 2013.

[49] A. Kinghorn, "Plant secondary metabolites as potential anticancer agents and cancer chemopreventives," *Molecules*, vol. 5, no. 12, pp. 285–288, 2000.

[50] R. B. Birudu and M. J. Naik, "Anticancer properties of secondary metabolites of medicinal plants in carcinoma," *British Biomedical Bulletin*, vol. 2, pp. 662–668, 2014.

[51] A. G. Fankam, V. Kuete, K. I. Voukeng, J.-R. Kuiaté, and J.-M. Pages, "Antibacterial activities of selected Cameroonian spices and their synergistic effects with antibiotics against multidrug-resistant phenotypes," *BMC Complementary and Alternative Medicine*, vol. 11, p. 104, 2011.

[52] M. A. Nieto, R. Y.-J. Huang, R. A. Jackson, and J. P. Thiery, "EMT: 2016," *Cell*, vol. 166, no. 1, pp. 21–45, 2016.

[53] B. D. Craene and G. Berx, "Regulatory networks defining EMT during cancer initiation and progression," *Nature Reviews Cancer*, vol. 13, no. 2, pp. 97–110, 2013.

[54] A. Puisieux, T. Brabletz, and J. Caramel, "Oncogenic roles of EMT-inducing transcription factors," *Nature Cell Biology*, vol. 16, no. 6, pp. 488–494, 2014.

[55] V. Kuete, O. Karaosmanoglu, and H. Sivas, "Chapter 10-anticancer activities of african medicinal spices and

vegetables," in *Medicinal Spices and Vegetables from Africa*, pp. 271–297, Academic Press, London, UK, 2017.

[56] Y.-L. Chen, S.-Z. Lin, J.-Y. Chang et al., "*In vitro* and *in vivo* studies of a novel potential anticancer agent of iso-chaihulactone on human lung cancer A549 cells," *Biochemical Pharmacology*, vol. 72, no. 3, pp. 308–319, 2006.

[57] A. T. Mbaveng, F. Damen, İ. Çelik, P. Tane, V. Kuete, and T. Efferth, "Cytotoxicity of the crude extract and constituents of the bark of *Fagara tessmannii* towards multi-factorial drug resistant cancer cells," *Journal of Ethnopharmacology*, vol. 235, pp. 28–37, 2019.

[58] V. Kuete, L. P. Sandjo, A. T. Mbaveng, M. Zeino, and T. Efferth, "Cytotoxicity of compounds from Xylopia aethiopica towards multi-factorial drug-resistant cancer cells," *Phytomedicine*, vol. 22, no. 14, pp. 1247–1254, 2015.

[59] A. M. D'Alessandro, A. Mancini, A. R. Lizzi et al., "Crocus sativus stigma extract and its major constituent crocin possess significant antiproliferative properties against human prostate cancer," *Nutrition and Cancer*, vol. 65, pp. 930–942, 2013.

[60] H. Jikihara, G. Qi, K. Nozoe et al., "Aged garlic extract inhibits 1,2-dimethylhydrazine-induced colon tumor development by suppressing cell proliferation," *Oncology Reports*, vol. 33, no. 3, pp. 1131–1140, 2015.

[61] J. Zheng, Y. Zhou, Y. Li, D.-P. Xu, S. Li, and H.-B. Li, "Spices for prevention and treatment of cancers," *Nutrients*, vol. 8, no. 8, p. 495, 2016.

[62] M. Pedersen, B. Metzler, G. Stafford, J. Van Staden, A. Jäger, and H. Rasmussen, "Amides from piper capense with CNS activity-a preliminary sar analysis," *Molecules*, vol. 14, no. 9, pp. 3833–3843, 2009.

[63] P. Umadevi, K. Deepti, and D. V. R. Venugopal, "Synthesis, anticancer and antibacterial activities of piperine analogs," *Medicinal Chemistry Research*, vol. 22, no. 11, pp. 5466–5471, 2013.

[64] L. Qiao, N. Liang, J. Zhang et al., "Advanced research on vasculogenic mimicry in cancer," *Journal of Cellular and Molecular Medicin*, vol. 19, no. 2, pp. 315–326, 2015.

[65] R. Folberg, M. J. C. Hendrix, and A. J. Maniotis, "Vasculo-genic mimicry and tumor angiogenesis," *American Journal of Pathology*, vol. 156, pp. 61–381, 2000.

[66] A. L. Greenshields, C. D. Doucette, K. M. Sutton et al., "Piperine inhibits the growth and motility of triple-negative breast cancer cells," *Cancer Letters*, vol. 357, no. 1, pp. 129–140, 2015.

[67] P. Makhov, K. Golovine, D. Canter et al., "Co-administration of piperine and docetaxel results in improved anti-tumor efficacy via inhibition of CYP3A4 activity," *The Prostate*, vol. 72, no. 6, pp. 661–667, 2012.

Research Article

Therapeutic and Preventive Effects of *Olea europaea* Extract on Indomethacin-Induced Small Intestinal Injury Model in Rats

Fatemeh Sadat Mahdavi [iD],[1] **Parham Mardi** [iD],[1] **Seyed Saeed Mahdavi** [iD],[2] **Mohammad Kamalinejad** [iD],[3] **Seyed Ali Hashemi** [iD],[4] **Zohreh Khodaii** [iD],[5] **and Mahboobeh Mehrabani-Natanzi** [iD][6]

[1]*Student Research Committee, Alborz University of Medical Sciences, Karaj, Iran*
[2]*Faculty of Medicine, University of Debrecen, Debrecen, Hungary*
[3]*Department of Pharmacognosy, School of Pharmacy, Shahid Beheshti University of Medical Sciences, Tehran, Iran*
[4]*Pathology Department, Faculty of Medicine, Alborz University of Medical Sciences, Karaj, Iran*
[5]*Dietary Supplements and Probiotic Research Center, Alborz University of Medical Sciences, Karaj, Iran*
[6]*Evidence-Based Phytotherapy and Complementary Medicine Research Center, Alborz University of Medical Sciences, Karaj, Iran*

Correspondence should be addressed to Zohreh Khodaii; zkhodaii@yahoo.com and Mahboobeh Mehrabani-Natanzi; mmehrabani95@gmail.com

Background. *Olea europaea* (known as olive fruit) has anti-inflammatory and antioxidant activities and many potential health benefits including gastric inflammation reduction has been shown previously. This study aimed to investigate the preventive and therapeutic effects of *O. europaea* extract on the early histological changes in indomethacin-induced small intestinal injury model with the plasma D-lactate concentration being measured as a tool for determination of intestinal permeability. *Methods.* In this experimental study, two separate protective and therapeutic protocols were designed. In both experiments, male Wistar rats were randomly divided into 4 groups and either pretreated with 0, 100, 200, or 400 mg/kg/day of *O. europaea* extract or received the treatment after administration of indomethacin. Their small intestines were examined to compare the histological changes. The intestinal injury severity was evaluated according to the presence of eosinophils, plasma cell infiltration, edema, congestion, and hyperplasia of the crypt using a histological scoring system. Also, measured were the presence of neutrophils, decreased villus length-to-crypt depth ratio, and destructed villus architecture. The plasma concentration of D-lactate was measured as well. *Results.* The therapeutic use of *O. europaea* decreased the eosinophil, edema, congestion, and crypt hyperplasia scores compared to the control group. Although no significant difference was seen between groups of the preventive experiment in plasma cell infiltration score, villus length-to-crypt depth ratio, neutrophil infiltration, and percentage of destructed villus architecture, treatment with *O. europaea* caused a reduction in edema, eosinophil, congestion, and crypt hyperplasia score. In both experiments, no significant difference was seen between groups for villus length-to-crypt depth ratio, neutrophil infiltration, and percentage of destructed villus architecture. Plasma D-lactate concentration was decreased in all *O. europaea*-treated groups compared to the control group in the therapeutic and preventive experiments ($p < 0.01$, one-way ANOVA followed by the Dunnett test). *Conclusion.* *O. europaea* extract can be used to decrease some side effects of indomethacin on intestinal tissue and enhances the gastrointestinal function. *O. europaea* extract could be considered as a potential herbal supplement in the treatment of intestinal morphological injuries.

1. Background

Nonsteroidal anti-inflammatory drugs (NSAIDs) are a group of anti-inflammatory drugs used to decrease pain and to treat immunological and rheumatological disorders [1, 2]. Peptic ulcer disease and intestinal inflammation are well-recognized complications of NSAID use [3, 4]. Indomethacin is an NSAID drug commonly used to reduce fever, pain, and stiffness and to treat gout and arthritis. Indomethacin prevents the synthesis of prostaglandins that prevent inflammation of the intestine and also disrupts blood circulation in the submucosa, causing dysregulation in mucosal cell growth that leads to hyperplasia [5, 6].

Structural and functional changes of intestinal mucosa can cause barrier dysfunction, which may lead to an increase in the permeability of the intestine [7]. Among all NSAIDs, indomethacin induces highest permeability changes. Increased intestinal permeability causes the passage of lipopolysaccharide and bacterial toxins into the bloodstream and, therefore, becomes a factor for several local and systemic inflammations [8, 9].

Antirheumatic, anti-inflammatory, antipyretic, vasodilatory, hypotensive, diuretic, and hypoglycemic effects of the olive fruit (*Olea europaea* L.) have been studied and described. These effects are attributed to monounsaturated fatty acids, aliphatic and triterpene alcohols, sterols, hydrocarbons, and several antioxidants that are present in this fruit. Potential health benefits of *O. europaea* against chronic diseases can be explained by its antioxidant activity and prevention of the harmful effects of free radicals. The antioxidant capacity of *O. europaea* is mainly due to oleuropein [10–12]. Prior studies have shown that *O. europaea* could reduce stomach inflammation caused by indomethacin [13, 14]. This study aims to investigate the preventive and therapeutic effects of *O. europaea* extract on the first histological changes in indomethacin-induced small intestinal injury models, and the plasma D-lactate concentration is measured as a tool for determination of intestinal permeability.

2. Methods

2.1. Plant Collection and Preparation of Extract. Green olive fruits (*Olea europaea*), collected at the end of the summer, were obtained from the Rudbar region, Gilan, Iran, and the fruits were scientifically authenticated by qualified field botanist (Prof. Maryam Ahvazi) at Medicinal Plants Research Center, Institute of Medicinal Plants, ACECR, Karaj, Iran. The voucher samples were deposited in the Herbarium and Raw Drug Repository (Alborz University of Medical Sciences). After cleaning the olive fruits, they were dried by exposure to air at room temperature and away from direct sunlight. The fruits were crushed and extracted with 80% ethanol (4 times per day, 20 cc solvent each time, for 25 days) in a percolator [15]. After extraction, the solvents were evaporated by a rotatory evaporator. The ethanol extract was stored in closed and dark containers at −20°C until used in the experiment.

2.2. Animals. In this experimental study, a total of 54 male Sprague-Dawley rats weighing 200–250 g at six weeks were obtained from Royan Research Institute (Tehran, Iran). The rats were kept in the animal facility at the Alborz University of Medical Sciences for one-week before starting experimentation at a temperature of $22 \pm 2°C$ with a relative humidity of 50% and a 12 : 12-hour light-dark cycle. Additionally, they had free access to a standard diet and water. The study was carried out following the institutional and international guidelines after approval by the Ethical Committee of Alborz University of Medical Sciences (Abzums.Rec.1397.024).

3. Experimental Protocol

3.1. Therapeutic Experimental Design

3.1.1. Induction of Small Intestinal Injury. A total of 30 male Sprague-Dawley rats were used to evaluate the curative effect of the *O. europaea* extract on indomethacin-induced small intestinal injury model. Indomethacin was administrated in 27 rats to induce histological injury to the small intestine. Three rats were administered by oral gavage with distilled water for three days as a healthy control group. Twenty-seven male Wistar rats were orally administered indomethacin 15 mg/kg q 12 hours for three days [16] (Sigma-Aldrich, 17378-5G, Germany). On day 4, randomly, 3 of the affected rats (3-day control group) and the healthy control group were euthanized, and their small intestines were removed. The small intestinal injury was investigated and compared.

3.1.2. Administration of the O. europaea Extract. After inducing injury with indomethacin, the remaining rats were randomly divided into four groups (6 rats each). From day 4, animals in the 10-day control group received no extract medication, but they were given an oral gavage of distilled water (0.5 cc) daily for seven days. Each of the other three treatment groups received either 100, 200, or 400 mg/kg of *O. europaea* extract daily from day 4 to day 10 [17].

After ten days, all rats were humanely dissected, blood samples were collected from the rat heart and collected into vacuum tubes which contained sodium citrate as anticoagulant, and the small intestine was immediately removed for histological studies.

3.2. Preventive Experimental Design. For evaluating the preventive effect of *O. europaea* extract, a separate group of 24 male Sprague-Dawley rats were used, and they were randomly divided into four groups. The rats were initially pretreated orally with distilled water (0.5 cc) in the prevention control group, and either 100, 200, or 400 mg/kg of *O. europaea* extract daily in the three prevention groups for four days. On day 5, indomethacin 15 mg/kg q 12 hours started to be administrated plus either distilled water (0.5 cc) in the prevention control group, or plus 100, 200, or 400 mg/ kg of *O. europaea* extract in the prevention groups for three

days. After seven days, all rats were euthanized, and blood and intestinal tissue samples were collected.

Both therapeutic and preventive experimental protocols are summarized in Figure 1.

4. Histological Studies

At the end of the experiment, the rats were euthanized by intraperitoneal injection of sodium pentobarbitone (concentration of 60 mg/ml) at a dose of 180 mg/kg. Thereafter, the confirmation of euthanasia was made by absence of the tail pinch reflex. After gathering the blood samples, rats were sacrificed by cervical dislocation. The abdomen was opened, and the small intestine excised. Histological observations were carried out on jejunal segments from rats of each group. Jejunum segments were immediately injected with 10% formalin and left in the same fixative solution for 30 minutes. Then, the sections were dissected along the anti-mesenteric border and cleaned of fecal content. Eventually, they were fixed in a 10% formalin for 24 hours. Four sections were randomly chosen from each of the jejunum segments. Hematoxylin and eosin (H&E) staining was performed in routinely processed paraffin-embedded sections. Histological alterations were observed by two independent pathologists without previous knowledge of samples' study group origin [16, 18].

The histological sections were evaluated using standard light microscopy, and the intestinal injury severity was evaluated by assessing the presence of eosinophils, plasma cell infiltration, neutrophils, edema, congestion, hyperplasia of the crypt, decreased villus length-to-crypt depth ratio, and destructed villus architecture (Figure 2).

The numbers of eosinophils in four different microscopic fields (40×) were counted, and the mean number was reported. Then, it was categorized according to eosinophil level into mild (0 to 10 eosinophils), moderate (11 to 20 eosinophils), or severe (more than 20 eosinophils). The severity of plasma cell infiltration in the lamina propria, edema, and congestion was reported in three grades of mild, moderate, and severe as well.

Hyperplasia of the crypt is defined as observing more than one mitosis in a single crypt. Reporting hyperplasia in up to 25% of the crypts visible in a low power microscopic field is classified as mild, 25% to 50% as moderate, and more than 50% as severe crypt hyperplasia. The presence of neutrophils was being investigated, and even a single cell considered important enough to be reported.

For villus length-to-crypt depth ratio measurement, three villi and three intestinal crypts per slide were studied, and only those regions of the intestinal sections presenting proper morphology were used. Histomorphometry measurements were carried out under low microscopic power. The height of each villus was defined as the length from top of the villus to the crypt transition, and the crypt depth as the length from the villus-crypt junction to the crypt base. Normal or destructed villus architectures were reported according to the pathologists' subjective opinion. In case of a difference of opinion between the two pathologists, a third opinion from another expert was requested.

5. D-Lactate Measurement

Heart blood samples were collected just after the rats were euthanized, for serum D-lactate level assessment. The plasma from systemic blood samples was obtained and subjected to deproteination and neutralization processes by acid/base precipitation using perchloric acid and potassium hydroxide. The protein-free plasma was then assayed for D(-)-lactate concentration (mmol/L) by the enzymatic-spectrophotometric method with minor modifications [19].

6. Statistical Analysis

Using SPSS 22.0 software (SPSS Inc., Chicago, IL, USA), D-lactate levels were compared within groups by one-way ANOVA followed by the Dunnett test. One-way ANOVA and chi-square are used to evaluate the difference between groups in terms of the crypt-to-villus ratio and architecture disturbance, respectively. The Mann–Whitney U test was used for plasma cell infiltration, edema, eosinophil, congestion, and hyperplasia. A p value of <0.05 was considered to be statistically significant, and all data were expressed as mean ± standard deviation (SD) in each group.

7. Results

To ensure the induction of indomethacin-induced intestinal injury in rats, the plasma cell infiltration score was compared between the healthy group and the three-day control groups. The plasma cell infiltration score was significantly lower in the healthy group compared to the three-day control or ten-day control group (Figure 3).

The therapeutic effects of *O. europaea* against indomethacin-induced intestinal injury were evaluated. *O. europaea*, at a dose of 100 mg/kg, decreased the eosinophil, edema, and crypt hyperplasia scores compared to the control group. 200 mg/kg of *O. europaea* caused a reduction in eosinophil, hyperplasia, plasma cell infiltration, and congestion scores. Eosinophil, crypt hyperplasia, and plasma cell infiltration scores were eliminated in the 400 mg/kg dose group in comparison with the control group ($p < 0.05$, Mann–Whitney). No significant difference in groups was seen between villus length-to-crypt depth ratio, neutrophil infiltration, and percentage of destructed villus architecture ($p > 0.05$, one-way ANOVA, and chi-square, respectively).

To assess the preventive effects of *O. europaea* against indomethacin-induced intestinal injury, *O. europaea* was administered by oral gavage for four days before oral administration of indomethacin. Intestinal biopsy revealed lower edema and eosinophil score in all prevention groups compared to the control group. Also, *O. europaea*, at a dose of 200 mg/kg, decreased congestion and crypt hyperplasia score ($p < 0.05$, Mann–Whitney). No significant difference was seen between groups for plasma cell infiltration score, villus length-to-crypt depth ratio, neutrophil infiltration,
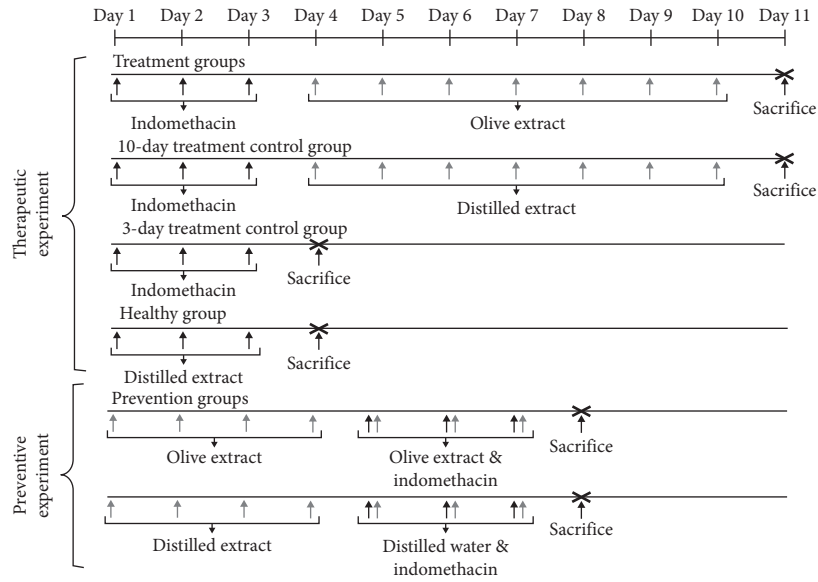
FIGURE 1: Therapeutic and preventive experimental designs.

(a)

(b)

(c)

(d)
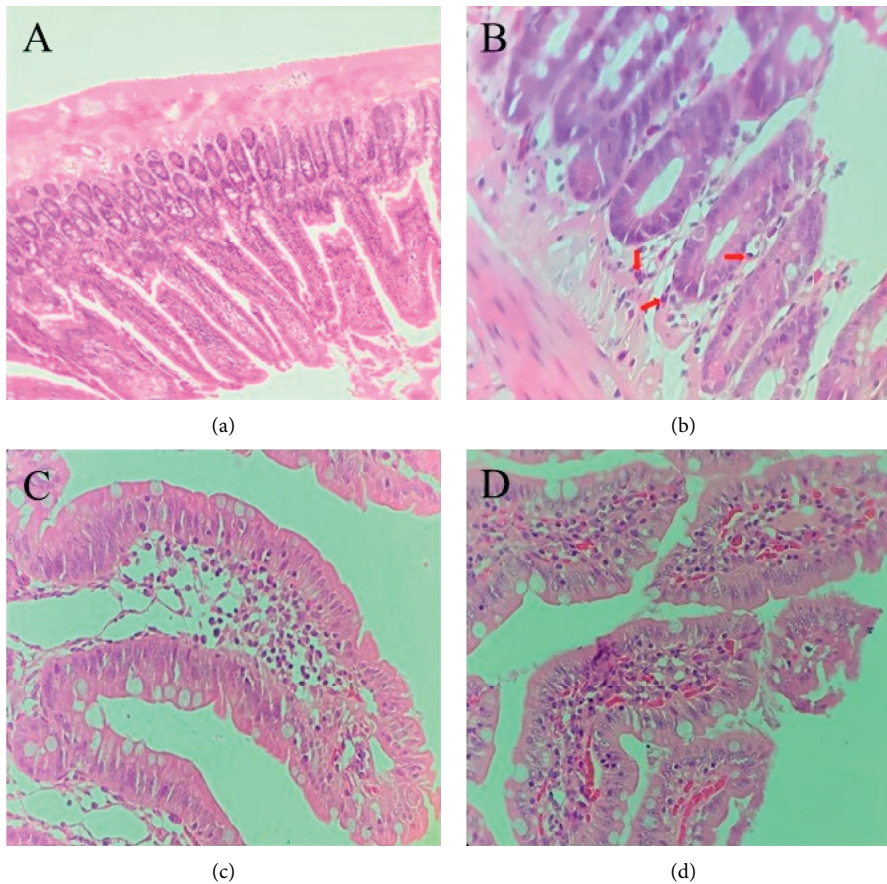
FIGURE 2: Histological alterations in the small intestine. Images show the H&E-stained sections from jejunum. (a) Normal intestinal wall structure without histological abnormalities in rats of the healthy group (magnification ×10). (b) Arrows show eosinophils in the epithelium of the intestine in rats of the control group (magnification ×40). (c) A grade 3 villus edema and (d) a grade 3 congestion, observed in rats of the control group (magnification ×40).
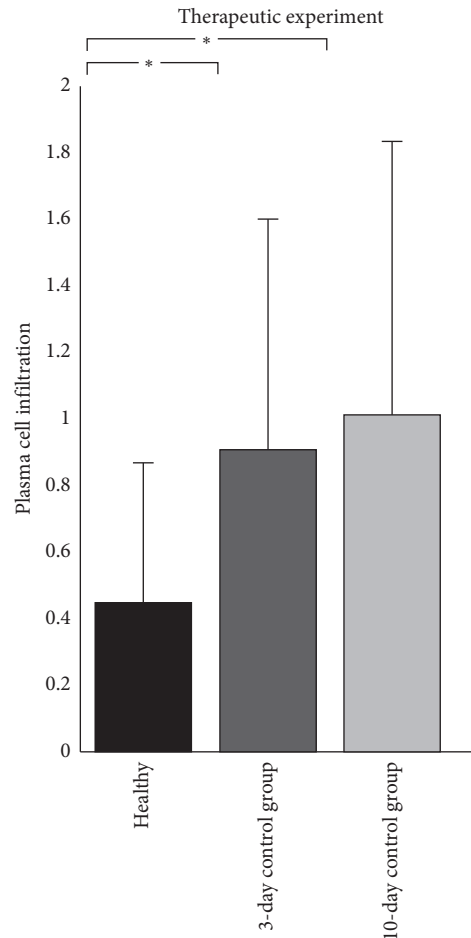
FIGURE 3: Plasma cell infiltration scores were compared to ensure the induction of indomethacin-induced small intestinal injury in rats. Data are expressed as mean ± standard deviation. The plasma cell infiltration score was significantly lower in the healthy group compared to the three-day control or ten-day control group ($^*p$ value <0.05).

and percentage of destructed villus architecture ($p > 0.05$, Mann–Whitney, one-way ANOVA, and chi-square, respectively) (Figure 4).

Histological studies were followed by plasma D-lactate concentration analysis in both preventive and therapeutic experiments. In the therapeutic experiment, the D-lactate concentration was decreased in all *O. europaea*-treated groups in comparison with the control group ($p < 0.05$, one-way ANOVA followed by the Dunnett test). Also, in the preventive experiment, D-lactate concentration was significantly lower in all *O. europaea*-treated groups compared to the control group ($p < 0.05$, one-way ANOVA followed by the Dunnett test) (Figure 5).

8. Discussion

NSAIDs often cause mucosal lesions in the small intestine in humans [20]. Researchers are diverting attention from using aminosalicylates and glucocorticoids for the treatment of NSAID-induced intestinal inflammation to new therapeutic strategies such as using antioxidants [21–25]. NSAID-induced lipid peroxidation and oxidative stress cause ulcers in the gastrointestinal mucosa [26]. Some

reports have indicated that oral administration of NSAIDs cause gastrointestinal oxidative injury through increased lactate dehydrogenase (LDH) leakage, mucosal lipid peroxidation (MDA), DNA damage, and decreased gastric mucus secretion in vivo. Thus, upregulation of antioxidant enzymes, such as glutathione peroxidase (GPx), glutathione reductase (GR), superoxide dismutase (SOD), and heme oxygenase-1 (HO-1), might be a major mechanism of action against oxidative stress-associated gastrointestinal ulcers [27–29].

Several studies have investigated the phenolic composition of the olive fruit. The phenolic compounds present in *Olea europaea* L., especially the oleuropein, are associated with antioxidant, antihypertensive, hypoglycemic, hypocholesterolemia, and cardioprotective activity [30, 31]. Oleuropein is a potent antioxidant with anti-inflammatory properties [32]. Prevention of free radical formation by oleuropein may be due to its ability to chelate metal ions, such as copper (Cu) and iron (Fe), which catalyze free radical generation reactions, as well as its ability to inhibit several inflammatory enzymes, such as lipoxygenases [33, 34].

Prior studies demonstrate that *O. europaea* L. extract has protective function in certain diseases [35, 36]. This study
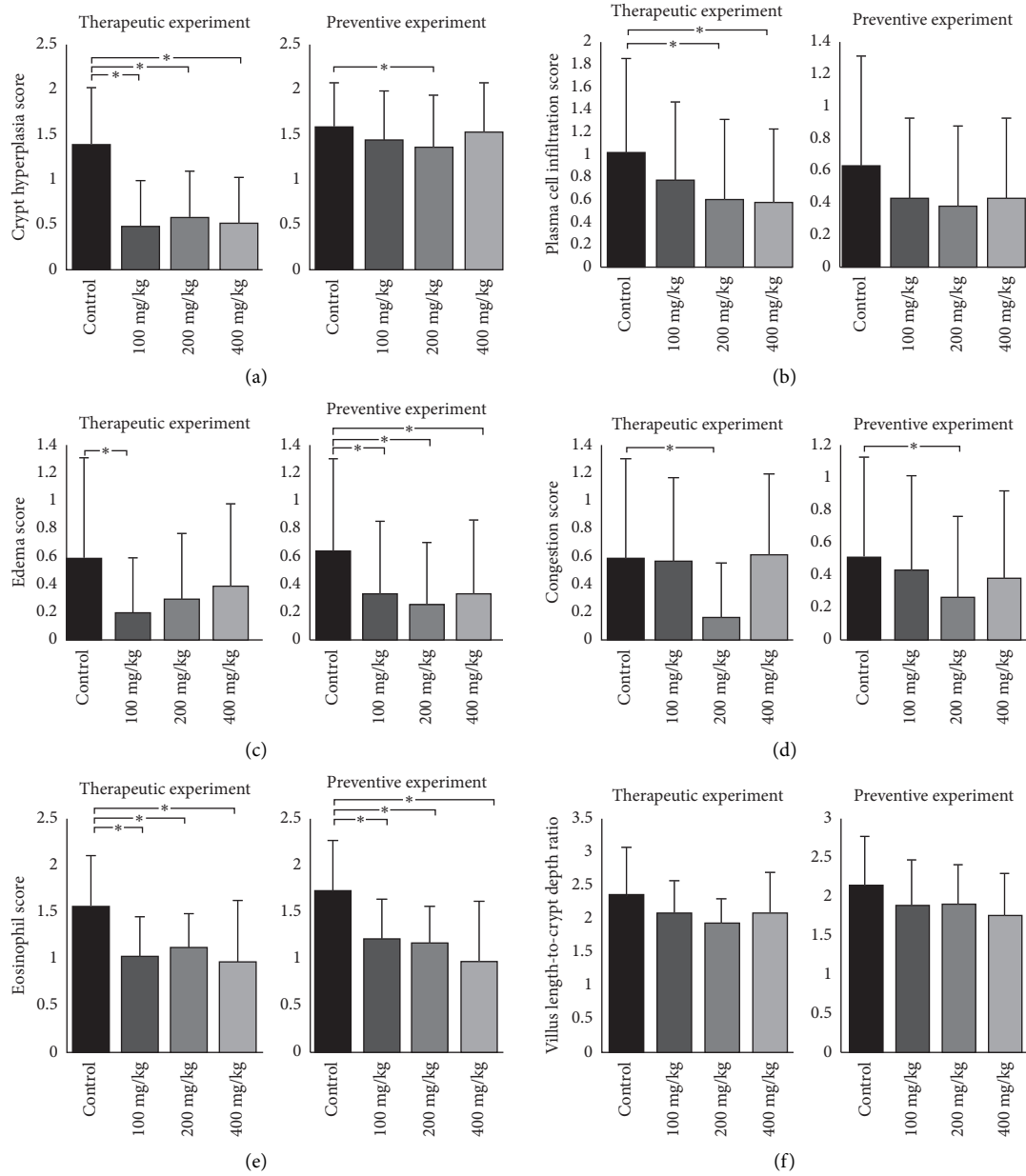
FIGURE 4: Continued.

(g)

(h)
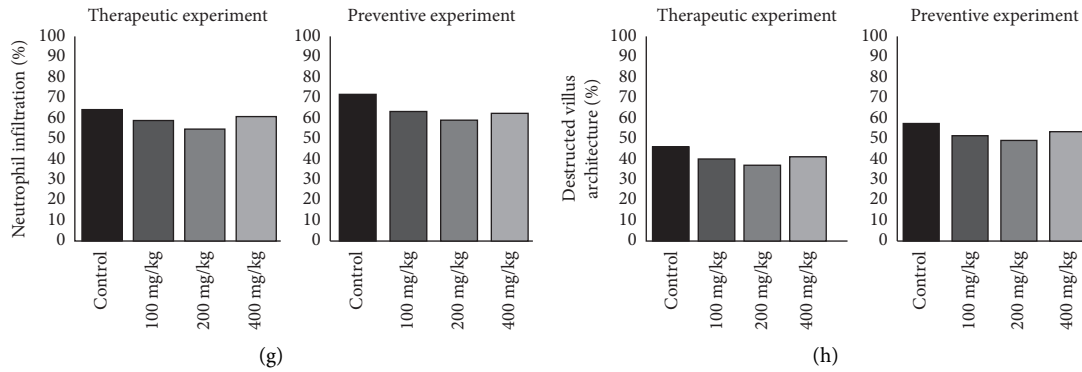
Figure 4: Histological changes in the small intestine. (a) Crypt hyperplasia score was decreased in all doses of *O. europaea* compared to the control group in the therapeutic experiment. However, only *O. europaea* at a dosage of 200 mg/kg was effective in the preventive experiment. (b) Plasma cell infiltration scores were lower in the dosage of 200 and 400 mg/kg of *O. europaea* in the therapeutic experiment. Although, no significant difference in groups of preventive experiment was seen. (c) Edema score was decreased in the dosage of 100 mg/kg of *O. europaea* in the therapeutic experiment and all doses in the preventive experiment. (d) Congestion scores were lower in a dosage of 200 mg/kg of *O. europaea* in both experiments. (e) All groups treated with *O. europaea* in therapeutic and preventive experiments showed a significant reduction in eosinophil scores. (f) Villus length-to-crypt depth ratio was not changed between groups of both experiments. Data in sections A to F are expressed as mean ± standard deviation. (g) Presence of neutrophils is expressed as percent indicating the percentage of the study population that was found to show at least one neutrophil during our investigations. We did not find any statistically significant difference anywhere in our experiments. (h) Percentage of destructed villus architecture was not different between any of the study groups. *p value <0.05.
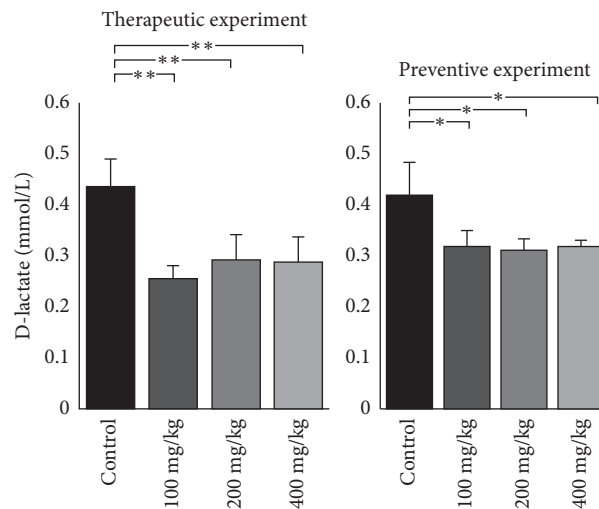
Figure 5: The D-lactate concentration (mmol/L) was decreased in all *O. europaea*-treated groups in comparison to the control group of the therapeutic experiment ($p < 0.01$). Also, in the preventive experiment, D-lactate concentration was significantly lower in all *O. europaea*-treated groups compared to the control group ($p < 0.05$). All data are expressed as mean ± standard deviation. *p value <0.05 and **p value<0.01.

evaluates the preventive and therapeutic effects of *O. europaea* L. fruits on indomethacin-induced intestinal injury using histopathological studies and D-lactate level assessment.

Preventive administration of *O. europaea* L. at dose 200 mg/kg/day decreased edema, congestion, crypt hyperplasia, and eosinophil score in the histological evaluation and D-lactate level compared to the control group.

Dan et al. showed that the eosinophil number in the histological study is not only attributed to the severity of inflammation but can be used as an index to assess the

treatment efficacy [37]. Crypt hyperplasia is characterized by an increased number of mitoses, due to the extension of the proliferative compartment from the crypt bases along the length of the crypt. Crypt hyperplasia is a valid and reliable measure of intestinal inflammation and its response to treatment effects of preclinical studies [38]. Our findings indicate that preventive administration of *O. europaea* in a dose of 200 mg/kg and therapeutic administration of the extract in all doses decrease crypt hyperplasia and eosinophil infiltration. Although a different eosinophil scoring system was used in our study, Ciobanu et al. have demonstrated that

rifaximin decreases infiltrated eosinophils number, concluding that it is also efficient in preventing degenerative intestinal lesions induced by indomethacin [39].

It has been proposed that the infiltration of the bowel mucosa by neutrophils is an essential stage in NSAIDs' injuries. Similar to Ciobanu et al.'s study [39], in our study, assessment of neutrophil infiltration was not different between any of our preventive, therapeutic groups compared to the control group, suggesting that other mechanisms may also be involved. Watanabe et al. reported that lipopolysaccharides (LPS)/toll-like receptor 4 (TLR 4)/MyD88-dependent signaling pathway on macrophages plays an essential role in the activation of an inflammatory cascade induced by NSAIDs. In addition, a bias might be present in our scoring system, which would explain the results [40, 41].

Indomethacin not only causes vasoconstriction but increases the risk of kidney problems, ischemic heart disease, and heart failure [42–44]. In our study, edema was significantly decreased in all our preventive experimental groups compared to the control group, and there was a discrepancy in our therapeutic experimental findings, in terms of the edema score. The results of our congestion scores were also inconclusive. The discrepancy in our findings may be attributed to preventable but irreversible cardiac effects of indomethacin. Despite this, edema and congestion appear to be unreliable indicators of indomethacin-induced small intestinal injury [45, 46].

Crypt-to-villus ratio and villus architecture took longer to change. These two indices were not altered in both of our experiments. Due to our short experiment duration, a more extended follow-up period may be required to detect any differences [45, 47, 48].

In our study, unlike the preventive experiment, the therapeutic experiment showed a significant decrease in plasma cell infiltration as a factor indicative of inflammation. We suggest that different immunological responses may justify the contrast between our therapeutic and preventive experiments [49, 50].

Intestinal permeability is an essential factor when assessing the effects of NSAIDs on intestinal integrity [51, 52]. D-lactate is closely related to the intestinal integrity and is attributed to specific conditions such as leaky gut and NSAIDs induced intestinal injury. Prior studies indicate that D-lactate could be used as a major diagnostic index [53]. Confirming histological findings, the D-lactate level was significantly lower in all our *O. europaea*-treated groups in both therapeutic and preventive studies.

9. Conclusion

Overall, we conclude that, although *O. europaea* significantly reduced inflammation and injury caused by indomethacin, its preventive effects were less evident than its therapeutic effects on the indomethacin-induced intestinal injury. Our study revealed that the best dose was determined to be 200 mg/kg for both experiments.

Data Availability

No data have been submitted to any open-access databases. All the data supporting the study are presented in the manuscript or available upon request.

Ethical Approval

The present study was confirmed by the Ethics Committee of Alborz University of Medical Sciences (Abzums.-Rec.1397.024) (15/7/2018).

Disclosure

FSM and PM are the first authors. All funding bodies did not participate in the design of the study, collection, analysis, and interpretation of data and in writing the manuscript.

Conflicts of Interest

The authors declare that they have no conflicts of interest regarding the publication of this paper.

Authors' Contributions

FSM and PM contributed equally, and they conducted the experiments, participated in preparing the manuscript, and conducted the statistical analysis. SSM supervised the experiments and edited the manuscript. SAH and MK conducted the experiments and revised the manuscript critically. MMN and ZK drafted the manuscript and revised it. All the authors read and approved the final version of the manuscript.

References

[1] A. Gupta and M. Bah, "NSAIDs in the treatment of postoperative pain," *Current Pain and Headache Reports*, vol. 20, no. 11, p. 62, 2016.

[2] S. Ramiro, "I12. NSAIDS, conventional synthetic dmards and biologics IN spa: THEIR role and impact ON disease outcomes," *Rheumatology*, vol. 56, no. suppl_2, 2017.

[3] Y. K. Shim and N. Kim, "Nonsteroidal anti-inflammatory drug and aspirin-induced peptic ulcer disease," *The Korean Journal of Gastroenterology*, vol. 67, no. 6, pp. 300–312, 2016.

[4] T. Fujiwara, K. Katakura, and H. Ohira, "Rheumatoid arthritis and gastrointestinal tract lesions (NSAID ulcers, amyloidosis)," in *Gastrointestinal and Hepatic Manifestations of*

Rheumatic Diseases, pp. 97–121, Springer, Berlin, Germany, 2019.

[5] W.-F. Fang, A. Broughton, and E. D. Jacobson, "Indomethacin-induced intestinal inflammation," *The American Journal of Digestive Diseases*, vol. 22, no. 9, pp. 749–760, 1977.

[6] S. Lucas, "The pharmacology of indomethacin," *Headache: The Journal of Head and Face Pain*, vol. 56, no. 2, pp. 436–446, 2016.

[7] R. M. Al-Sadi and T. Y. Ma, "IL-1β causes an increase in intestinal epithelial tight junction permeability," *The Journal of Immunology*, vol. 178, no. 7, pp. 4641–4649, 2007.

[8] I. Bjarnason, P. Smethurst, C. G. Fenn, C. E. Lee, I. S. Menzies, and A. J. Levi, "Misoprostol reduces indomethacin-induced changes in human small intestinal permeability," *Digestive Diseases and Sciences*, vol. 34, no. 3, pp. 407–411, 1989.

[9] J.-P. Ganda Mall, "Effects of dietary fibres on indomethacin-induced intestinal permeability in elderly: a randomised placebo controlled parallel clinical trial," *Nutrients*, vol. 12, no. 7, 2020.

[10] M. M. Özcan and B. Matthäus, "A review: benefit and bioactive properties of olive (Olea europaea L.) leaves," *European Food Research and Technology*, vol. 243, no. 1, pp. 89–99, 2017.

[11] J. Makowska-Wąs, "Identification of predominant phytochemical compounds and cytotoxic activity of wild olive leaves (Olea europaea L. ssp. sylvestris) harvested in south Portugal," *Chemistry & Biodiversity*, vol. 14, no. 3, Article ID e1600331, 2017.

[12] D. Ustuner, E. Colak, M. Dincer et al., "Posttreatment effects ofOlea EuropaeaL. Leaf extract on carbon tetrachloride-induced liver injury and oxidative stress in rats," *Journal of Medicinal Food*, vol. 21, no. 9, pp. 899–904, 2018.

[13] S. Al-Quraishy, M. S. Othman, M. A. Dkhil, and A. E. Abdel Moneim, "Olive (Olea europaea) leaf methanolic extract prevents HCl/ethanol-induced gastritis in rats by attenuating inflammation and augmenting antioxidant enzyme activities," *Biomedicine & Pharmacotherapy*, vol. 91, pp. 338–349, 2017.

[14] C. Song, Y. H. Hong, J. G. Park et al., "Suppression of Src and Syk in the NF-κB signaling pathway by Olea europaea methanol extract is leading to its anti-inflammatory effects," *Journal of Ethnopharmacology*, vol. 235, pp. 38–46, 2019.

[15] P. Najafizadeh, F Dehghani, M Panjeh Shahin, and S Hamzei Taj, "The effect of a hydro-alcoholic extract of olive fruit on reproductive argons in male sprague-dawley rat," *Iranian Journal of Reproductive Medicine*, vol. 11, no. 4, p. 293, 2013.

[16] D. S. Kwak, "The effect of DA-6034 on intestinal permeability in an indomethacin-induced small intestinal injury model," *Gut and Liver*, vol. 10, no. 3, pp. 406–411, 2016.

[17] P. Najafizadeh, "The effect of a hydro-alcoholic extract of olive fruit on reproductive argons in male sprague-dawley rat," *International Journal of Reproductive BioMedicine*, vol. 11, no. 4, pp. 293–300, 2013.

[18] S. Sabiu, T. Garuba, T. Sunmonu et al., "Indomethacin-induced gastric ulceration in rats: protective roles of Spondias mombin a nd Ficus exasperata," *Toxicology Reports*, vol. 2, pp. 261–267, 2015.

[19] R. B. Brandt, S. A. Siegel, M. G. Waters, and M. H. Bloch, "Spectrophotometric assay for d-(−)-lactate in plasma," *Analytical Biochemistry*, vol. 102, no. 1, pp. 39–46, 1980.

[20] D. A. Brodie, P. G. Cook, B. J. Bauer, and G. E. Dagle, "Indomethacin-induced intestinal lesions in the rat," *Toxicology and Applied Pharmacology*, vol. 17, no. 3, pp. 615–624, 1970.

[21] S. R. Bing, T. Kinouchi, K. Kataoka, T. Kuwahara, and Y. Ohnishi, "Protective effects of a culture supernatant ofLactobacillus acidophilusand antioxidants on ileal ulcer formation in rats treated with a nonsteroidal antiinflammatory drug," *Microbiology and Immunology*, vol. 42, no. 11, pp. 745–753, 1998.

[22] S. K. Das and C. Roy, "The protective role of Aegle marmelos on aspirin–induced gastro-duodenal ulceration in albino rat model: a possible involvement of antioxidants," *Saudi Journal of Gastroenterology: Official Journal of the Saudi Gastroenterology Association*, vol. 18, no. 3, p. 188, 2012.

[23] R. Anandan, P. G. V. Nair, and S. Mathew, "Anti-ulcerogenic effect of chitin and chitosan on mucosal antioxidant defence system in HCl-ethanol-induced ulcer in rats," *Journal of Pharmacy and Pharmacology*, vol. 56, no. 2, pp. 265–269, 2004.

[24] A. M. S. Gomaa, N. A. Abd El-Mottaleb, and H. A. Aamer, "Antioxidant and anti-inflammatory activities of alpha lipoic acid protect against indomethacin-induced gastric ulcer in rats," *Biomedicine & Pharmacotherapy*, vol. 101, pp. 188–194, 2018.

[25] S. Sabiu, T. Garuba, T. O. Sunmonu, A. O. Sulyman, and N. O. Ismail, "Indomethacin-induced gastric ulceration in rats: ameliorative roles ofSpondias mombinandFicus exasperata," *Pharmaceutical Biology*, vol. 54, no. 1, pp. 180–186, 2016.

[26] M. Gyenge, "Roles of pro-angiogenic and anti-angiogenic factors as well as matrix metalloproteinases in healing of NSAID-induced small intestinal ulcers in rats," *Life Sciences*, vol. 93, no. 12-14, pp. 441–447, 2013.

[27] T. Yoshikawa, Y. Naito, A. Kishi et al., "Role of active oxygen, lipid peroxidation, and antioxidants in the pathogenesis of gastric mucosal injury induced by indomethacin in rats," *Gut*, vol. 34, no. 6, pp. 732–737, 1993.

[28] J. Tanaka and Y. Yuda, "Lipid peroxidation in gastric mucosal lesions induced by indomethacin in rat," *Biological & Pharmaceutical Bulletin*, vol. 19, no. 5, pp. 716–720, 1996.

[29] M. Koc, H. Imik, and F. Odabasoglu, "Gastroprotective and anti-oxidative properties of ascorbic acid on indomethacin-induced gastric injuries in rats," *Biological Trace Element Research*, vol. 126, no. 1-3, pp. 222–236, 2008.

[30] O. Benavente-Garcıa, "Antioxidant activity of phenolics extracted from Olea europaea L. leaves," *Food Chemistry*, vol. 68, no. 4, pp. 457–462, 2000.

[31] O.-H. Lee and B.-Y. Lee, "Antioxidant and antimicrobial activities of individual and combined phenolics in Olea europaea leaf extract," *Bioresource Technology*, vol. 101, no. 10, pp. 3751–3754, 2010.

[32] S. H. Omar, "Oleuropein in olive and its pharmacological effects," *Scientia Pharmaceutica*, vol. 78, no. 2, pp. 133–154, 2010.

[33] I. Kruk, H. Y. Aboul-Enein, T. Michalska, K. Lichszteld, and A. Kładna, "Scavenging of reactive oxygen species by the plant phenols genistein and oleuropein," *Luminescence*, vol. 20, no. 2, pp. 81–89, 2005.

[34] J. Ruzzolini, S. Peppicelli, E. Andreucci et al., "Oleuropein, the main polyphenol of Olea europaea leaf extract, has an anti-cancer effect on human BRAF melanoma cells and potentiates the cytotoxicity of current chemotherapies," *Nutrients*, vol. 10, no. 12, p. 1950, 2018.

[35] S. Bulotta, "Beneficial effects of the olive oil phenolic components oleuropein and hydroxytyrosol: focus on protection against cardiovascular and metabolic diseases," *Journal of Translational Medicine*, vol. 12, no. 1, p. 219, 2014.

[36] S. H. Omar, "Cardioprotective and neuroprotective roles of oleuropein in olive," *Saudi Pharmaceutical Journal*, vol. 18, no. 3, pp. 111–121, 2010.

[37] D. Yi, "Establishment of a porcine model of indomethacin-induced intestinal injury," *Frontiers in Bioscience (Landmark Edition)*, vol. 23, pp. 2166–2176, 2018.

[38] P. J. Koelink, M. E. Wildenberg, L. W. Stitt et al., "Development of reliable, valid and responsive scoring systems for endoscopy and histology in animal models for inflammatory bowel disease," *Journal of Crohn's and Colitis*, vol. 12, no. 7, pp. 794–803, 2018.

[39] L. Ciobanu, M Taulescu, R Prundus et al., "Effects of rifaximin on indomethacin-induced intestinal damage in Guinea-pigs," *European Review for Medical and Pharmacological Sciences*, vol. 18, no. 3, pp. 344–351, 2014.

[40] S. Watanabe, Y. Kumazawa, and J. Inoue, "Liposomal lipopolysaccharide initiates TRIF-dependent signaling pathway independent of CD14," *PLoS One*, vol. 8, no. 4, Article ID e60078, 2013.

[41] K. Takeuchi, "Roles of COX inhibition in pathogenesis of NSAID-induced small intestinal damage," *Clinica Chimica Acta*, vol. 411, no. 7-8, pp. 459–466, 2010.

[42] P. McGettigan and D. Henry, "Cardiovascular risk with non-steroidal anti-inflammatory drugs: systematic review of population-based controlled observational studies," *PLoS Medicine*, vol. 8, no. 9, Article ID e1001098, 2011.

[43] P. L. Friedman, E. J. Brown, S. Gunther et al., "Coronary vasoconstrictor effect of indomethacin in patients with coronary-artery disease," *New England Journal of Medicine*, vol. 305, no. 20, pp. 1171–1175, 1981.

[44] A. J. M. Donker, L. Arisz, J. R. H. Brentjens, G. K. van der Hem, and H. J. G. Hollemans, "The effect of indomethacin on kidney function and plasma renin activity in man," *Nephron*, vol. 17, no. 4, pp. 288–296, 1976.

[45] A. Anthony, "Early histological features of small intestinal injury induced by indomethacin," *Alimentary Pharmacology & Therapeutics*, vol. 7, no. 1, pp. 29–40, 1993.

[46] F. D. Lee, "Drug-related pathological lesions of the intestinal tract," *Histopathology*, vol. 25, no. 4, pp. 303–308, 1994.

[47] Y. Wang, D. B. Gunasekara, M. I. Reed et al., "A micro-engineered collagen scaffold for generating a polarized crypt-villus architecture of human small intestinal epithelium," *Biomaterials*, vol. 128, pp. 44–55, 2017.

[48] A. Anthony, "Pre-ulcerative villous contraction and micro-vascular induced by indomethacin in the rat jejunum: a detailed morphological study," *Alimentary Pharmacology & Therapeutics*, vol. 9, no. 6, pp. 605–613, 1995.

[49] L. Zhang, K. Notohara, M. J. Levy, S. T. Chari, and T. C. Smyrk, "IgG4-positive plasma cell infiltration in the diagnosis of autoimmune pancreatitis," *Modern Pathology*, vol. 20, no. 1, pp. 23–28, 2007.

[50] Y. K. O. Teng, E. W. N. Levarht, R. E. M. Toes, T. W. J. Huizinga, and J. M. van Laar, "Residual inflammation after rituximab treatment is associated with sustained synovial plasma cell infiltration and enhanced B cell repopulation," *Annals of the Rheumatic Diseases*, vol. 68, no. 6, pp. 1011–1016, 2009.

[51] G. Sigthorsson, J. Tibble, J. Hayllar et al., "Intestinal permeability and inflammation in patients on NSAIDs," *Gut*, vol. 43, no. 4, pp. 506–511, 1998.

[52] I. Bjarnason and K. Takeuchi, "Intestinal permeability in the pathogenesis of NSAID-induced enteropathy," *Journal of Gastroenterology*, vol. 44, no. 19, pp. 23–29, 2009.

[53] Y.-M. Yao, Y. Yu, Y. Wu, L.-R. Lu, and Z.-Y. Sheng, "Plasma D (-)-lactate as a new marker for diagnosis of acute intestinal injury following ischemia-reperfusion," *World Journal of Gastroenterology*, vol. 3, no. 4, pp. 225–227, 1997.

Research Article

Cytotoxic Constituents of the Bark of *Hypericum roeperianum* towards Multidrug-Resistant Cancer Cells

Michel-Gael F. Guefack,[1] **Francois Damen,**[2] **Armelle T. Mbaveng** ⓘ **,**[1]
Simplice Beaudelaire Tankeo,[1] **Gabin T. M. Bitchagno,**[2] **İlhami Çelik,**[3]
James D. Simo Mpetga,[2] **and Victor Kuete** ⓘ [1]

[1]*Department of Biochemistry, Faculty of Science, University of Dschang, P.O. Box 67, Dschang, Cameroon*
[2]*Department of Chemistry, Faculty of Science, University of Dschang, P.O. Box 67, Dschang, Cameroon*
[3]*Department of Chemistry, Faculty of Science, Eskisehir Technical University, Eskisehir 26470, Turkey*

Correspondence should be addressed to Victor Kuete; kuetevictor@yahoo.fr

The global cancer burden remains a serious concern with the alarming incidence of one in eight men and one in eleven women dying in developing countries. This situation is aggravated by the multidrug resistance (MDR) of cancer cells that hampers chemotherapy. In this study, the cytotoxicity of the methanol extract (HRB), fractions (HRBa, HRBb, and HRBa1-5), and compounds from the bark of *Hypericum roeperianum* (HRB) was evaluated towards a panel of 9 cancer cell lines. The mode of action of the HRB and trichadonic acid (**1**) was also studied. Column chromatography was applied to isolate the constituents of HRB. The cytotoxicity of botanicals and phytochemicals was evaluated by the resazurin reduction assay (RRA). Caspase-Glo assay was used to evaluate the activity of caspases, and reactive oxygen species (ROS) (H_2DCFH-DA) were assessed by flow cytometry. Phytochemicals isolated from HRB were trichadonic acid (**1**), fridelan-3-one (**2**), 2-hydroxy-5-methoxyxanthone (**3**), norathyriol (**4**), 1,3,5,6-tetrahydroxyxanthone (**5**), betulinic acid (**6**), 3′-hydroxymethyl-2′-(4″-hydroxy-3″,5″-dimethoxyphenyl)-5′,6′:5,6-(6,8-dihydroxyxanthone)-1′,4′-dioxane (**7**), and 3′-hydroxymethyl-2′-(4″-hydroxy-3″,5″-dimethoxyphenyl)-5′,6′:5,6-(xanthone)-1′,4′-dioxane (**8**). Botanicals HRB, HRBa, HRBa2-4, HRBb, and doxorubicin displayed cytotoxic effects towards the 9 tested cancer cell lines. The recorded IC_{50} values ranged from 11.43 μg/mL (against the P-glycoprotein (gp)-overexpressing CEM/ADR5000 leukemia cells) to 26.75 μg/mL (against HCT116 (p53$^{+/+}$) colon adenocarcinoma cells) for the crude extract HRB. Compounds **1**, **5**, and doxorubicin displayed cytotoxic effects towards the 9 tested cancer cell lines with IC_{50} values varying from 14.44 μM (against CCRF-CEM leukemia cells) to 44.20 μM (against the resistant HCT116 (p53$^{-/-}$) cells) for **1** and from 38.46 μM (against CEM/ADR5000 cells) to 112.27 μM (against the resistant HCT116 (p53$^{-/-}$) cells) for **5**. HRB and compound **1** induced apoptosis in CCRF-CEM cells. The apoptotic process was mediated by enhanced ROS production for HRB or *via* caspases activation and enhanced ROS production for compound **1**. This study demonstrated that *Hypericum roeperianum* is a potential source of cytotoxic phytochemicals such as trichadonic acid and could be further exploited in cancer chemotherapy.

1. Introduction

Cancer continues to be a global threat, appearing as the second leading cause of death globally, with estimated 9.6 million deaths representing one in six deaths and with an estimated five-year prevalence of 43.8 million people [1]. Multidrug resistance (MDR) of cancer cells is a serious concern in chemotherapy. It is responsible for many therapeutic failures and high burdens globally, in patients suffering from cancer [2, 3]. Any modern protocol for new cytotoxic drug discovery today should integrate the ability of neoplastic cells to rapidly develop resistant phenotypes. Thus, resistant cell lines should be integrated into the cell panel used for the discovery of more efficient

substances. The present work has taken this into account and involves several models of MDR cancer cell lines such as the colon adenocarcinoma with p53 knockout phenotype, the leukemia cells with ATP-binding cassette (ABC)-transporter-overexpressing MDR-mediating-P-glycoprotein (P-gp; ABCB1/MDR1), the breast cancer bearing resistance protein (ABCG2/BCRP), and the transfectant glioblastoma multiforme harboring a mutation-activated EGFR gene (ΔEGFR). The effectiveness of natural products in the fight against cancer has been largely demonstrated [4]. Some clinically established cytotoxic drugs such as camptothecin, paclitaxel, vinblastine, or vincristine are naturally occurring compounds [4–6]. In addition, numerous botanicals and phytochemicals derived from African medicinal plants have been found active against MDR cancer cell lines [7, 8]. Some of such prominent phytochemicals include terpenoids: salvimulticanol and candesalvone B methyl ester [9], epunctanone [10], and ardisiacrispin B [11], phenolics: 2-acetyl-7-methoxynaphtho [2,3-b]furan-4,9-quinone [12], 6α-hydroxyphaseollidin [13], licoagrochalcone A [14], 7-dihydroxy-4′-methoxy-6,8-diprenylisoflavone, and 7,7″-di-O-methylchamaejasmin [15], and alkaloids: 1,3-dimethoxy-10-methylacridone [16], isotetrandrine [17], and ungeremine [18]. However, more hit compounds should be identified to increase our arsenal of cytotoxic compounds and to secure better the chances of later obtaining new clinically usable molecules. The present study was, therefore, designed to assess the cytotoxicity of botanicals and phytochemicals from the bark of *Hypericum roeperianum* Schimp. p. ex A. Rich (Guttiferae). The modes of action of compound **1**, such as its effects on cell cycle distribution and induction of apoptosis, on caspases activation, and on the production of reactive oxygen species (ROS), were also investigated. *Hypericum roeperianum* is a shrub or small tree growing in the tropical part of central, eastern, and southern tropical Africa, locally used alone or in association with various plants in the treatment of female sterility [19], as antiabortifacients [20] and as antifungal remedies [21]. Previous phytochemical investigations of this plant led to the isolation of a polyketide, 4-methoxy-3-(2-methylbut-3-en-2-yl)-6-phenyl-2H-pyran-2-one, xanthones: 1,5-dihydroxy-6-methoxyxanthone, 2-hydroxy-5-methoxyxanthone and 1,4,6,7-tetrahydroxyxanthone, and the xanthonolignoids: 8,10-dihydroxy-3-(4hydroxy-3,5-dimethoxyphenyl-2-(hydroxymethyl)-2, 3-dihydro-[1, 4]dioxino[2,3-c]xanthen-7-one and 8-hydroxy-10-methoxy-3-(4-hydroxy-3,5-dimethoxyphenyl-2-(hydroxymethyl)-2,3-dihydro-[1,4]dioxino[2,3-c]xanthen-7-one from the bark [22] and 10 other xanthones from the roots, namely, 5-O-methyl-2-deprenylrheediaxanthone B, 5-O-methylisojacareubin, 5-O-demethylpaxanthonin, roeperanone, 2-hydroxyxanthone, 5-hydroxy-2-methoxyxanthone, 1,5-dihydroxy-2-methoxyxanthone, 2-deprenyl rheediaxanthone B, isojacareubin, and calycinoxanthone D [23]. The cytotoxicity of botanicals from the bark of *Hypericum roeperianum* is being reported for the first time.

2. Material and Methods

2.1. Chemicals. Doxorubicin (98.0% purity) from Sigma-Aldrich (Munich, Germany) was obtained from the Johannes Gutenberg University Medical Center (Mainz, Germany). Geneticin >98% (used at 800 ng/mL and 400 μg/mL) in culture media to maintain the features of MDA-MB-231-*BCRP,* U87MG.Δ*EGFR,* and HCT116 (*p53$^{-/-}$*), respectively, was obtained from Sigma-Aldrich and stored at 72.18 mM. Hydrogen peroxide (H_2O_2) and valinomycin (at 1 mg/mL) were provided by Sigma-Aldrich (Taufkirchen, Germany).

2.2. Plant Material and Extraction. The bark of *Hypericum roeperianum* Schimp. p. ex A. Rich (Guttiferae) was collected in Bangang Wabane (South West Region of Cameroon) in October 2018. No permission was necessary for sample's collection. The identification of the plant was carried out by Dr. Tchiengue Barthelemy at the Cameroon National Herbarium (Yaoundé) where a voucher specimen was deposited under the number 24584/SRF/Cam. Dried barks of the plant (3.0 kg) were powdered and extracted with methanol (MeOH; 3 × 15 L) for 72 h at room temperature to afford a crude extract (HRB; 150.0 g) after filtration with Whatman paper no.1 and evaporation in vacuum, under reduced pressure. A portion of the resulting extract (140.0 g) was, then, exhausted in ethyl acetate to yield 65.0 g of the ethyl acetate extract (EtOAc) (HRBa) and the residue (HRBb; 75 g).

2.3. Fractionation and Purification of the Bark Extract of Hypericum roeperianum. Part of the ethyl acetate extract (EtOAc; 60.0 g) was submitted to silica gel flash chromatography using hexane-EtOAc and, then, EtOAc-MeOH mixtures of increasing polarities. Eighty fractions (frs) of 500 mL each were collected as follows: hexane 100% (sub-frs 1–3), hexane-EtOAc 90 : 10 (sub-frs 4–12), hexane-EtOAc 80 : 20 (sub-frs 13–18), hexane-EtOAc 70 : 30 (sub-frs 19–22), hexane-EtOAc 60 : 40 (sub-frs 23–27), hexane-EtOAc 50 : 50 (sub-frs 28–37), hexane-EtOAc 30 : 70(sub-frs 38–43), AcOEt 100% (sub-frs 44–52), EtOAc-MeOH 95 : 5 (sub-frs 53–57), EtOAc-MeOH 90 : 10 (sub-frs 58–62), EtOAc-MeOH 80 : 20 (sub-frs 63–69), and MeOH 100% (sub-frs 70–80). Based on their analytical thin-layer chromatography (TLC) profiles, these fractions were pooled into five fractions (frs) as follows: HRBa1 (Sub-frs 1–15, 8.0 g), HRBa2 (Sub-frs 16–25, 15.0 g), HRBa3 (Sub-frs 28–38, 9.5 g), HRBa4 (Sub-frs 39–68, 12.5 g), and HRBa5 (Sub-frs 69–80, 13.0 g).

Dry fraction HRBa2 (15.0 g) was dissolved in methanol affording a nonsoluble powder which was, then, filtered to give compound **1** (15 mg). The filtrate was subjected to silica gel column chromatography using hexane-AcOEt mixtures of increasing polarities as elution solvents. Sixty-five sub-frs of 150 mL each were collected as follows: Hex 100% (1–3), Hex-AcOEt 90:10 (Sub-frs 4–9), Hex-AcOEt 80 : 20 (Sub-frs 10–15), Hex-AcOEt 70 : 30 (Sub-frs 16–19), Hex-AcOEt 60 : 40 (Sub-frs 20–35), Hex-AcOEt 50 : 50 (Sub-frs 36–42), Hex-AcOEt 40 : 60 (Sub-frs 43–50), AcOEt 100% (Sub-frs 51–55), AcOEt-MeOH 90 : 10 (Sub-frs 56–60), and MeOH 100% (Sub-frs 61–65). Sub-frs 6–9 yielded compound **2**

(15.0 mg) as a white powder. Sub-frs EC23-29 yielded compound **3** (12.0 mg) as a yellow powder.

HRBa3 (9.5 g) was subjected to silica gel column chromatography using Hex-AcOEt mixtures of increasing polarities as elution solvents. Seventy-five sub-frs of 150 mL each were collected as follows: hexane 100% (sub-frs 1–4), Hex-AcOEt 90 : 10 (sub-frs 5–9), Hex-AcOEt 80 : 20 (sub-frs 9–16), Hex-AcOEt 70 : 30 (sub-frs 17–23), Hex-AcOEt 60 : 40 (sub-frs 24–35), Hex-AcOEt 50 : 50 (sub-frs 36–42), Hex-AcOEt 40 : 60 (sub-frs 43–47), AcOEt 100% (sub-frs 48–57), AcOEt-MeOH 90 : 10 (sub-frs 58–63), AcOEt-MeOH 80 : 20 (sub-frs 64–70), and MeOH 100% (sub-frs 71–75). Sub-frs 22–25 yielded compound **4** (18.0 mg) as a green-yellowish powder. Sub-frs 29–35 yielded compound **5** as a yellow powder (15.0 mg).

HRBa4 (12.5 g) was subjected to silica gel column chromatography using CH_2Cl_2-MeOH mixtures of increasing polarities as elution solvents. Fifty sub-frs of 150 mL each were collected as follows: CH_2Cl_2 100% (sub-frs 1–4), CH_2Cl_2-MeOH 95 : 5 (sub-frs 5–13), CH_2Cl_2-MeOH 90 : 10 (sub-frs 14–25), CH_2Cl_2-MeOH 85 : 15 (sub-frs 26–35), CH_2Cl_2-MeOH 80 : 20 (sub-frs 36–42), and MeOH 100% (subfrs 43–50). Sub-frs 6–11 yielded compound **6** (40.0 mg) as a white powder. Sub-frs 13–15 yielded compound **7** (12.0 mg) as a yellow powder. Sub-frs 19–23 yielded compound **8** (14.0 mg) as a yellow powder.

2.4. Cell Cultures.

Cell lines used in this work included drug-sensitive and drug-resistant phenotypes of earlier reported origin. They were all provided by Prof. Dr. Thomas Efferth from his cell lines collection; they have being used in cytotoxicity screening by our team for a decade [12–21]. These include two hematological cancer cell lines, namely, the drug-sensitive CCRF-CEM leukemia cell line and its multidrug-resistant P-gp-over-expressing subline CEM/ADR5000 cells [24–26] and nine carcinoma cell lines, namely, U87.MG glioblastoma cell line and its EGFR-transfected U87.MG$\Delta EGFR$ subline, HCT116 ($p53^{+/+}$) colon cancer cell line and its knockout clone HCT116 ($p53^{-/-}$), and MDA-MB-231-pcDNA3 breast cancer cell line and its *BCRP*-transfected multidrug-resistant MDA-MB-231-*BCRP* clone 23 cell line [27], as well as the normal AML12 hepatocytes, used to compare with HepG2 liver cancer cells [13].

2.5. Resazurin Reduction Assay (RRA) for Cell Growth Evaluation.

The RRA was applied to evaluate the cytotoxicity of botanicals, the isolated phytochemicals (**1–5, 7**, and **8**), and doxorubicin on the cell growth as reported earlier [18, 28]. Cells treated with various samples at different concentrations were incubated for 72 h in humidified 5% CO_2 atmosphere at 37°C. Cells were further coloured with resazurin and incubated for 1–2 h; the fluorescence was further measured with an Infinite M2000 Pro™ plate reader (Tecan, Crailsheim, Germany) at 544 nm as the excitation wavelength and 590 nm as the emission wavelength. The IC_{50} values represented the concentrations of the sample required to inhibit 50% of cell proliferation and were calculated from a calibration curve by linear regression using Microsoft Excel 2007 [29].

2.6. Flow Cytometric Evaluation of Cell Cycle Distribution and Apoptotic Cells.

Various concentrations of botanical HRB, phytochemical **1**, and doxorubicin or DMSO (solvent control) were used to treat CCRF-CEM cells (1×10^6 cells). Cells were further incubated for 24 h in humidified 5% CO_2 atmosphere at 37°C and analyzed using a BD Accury C6 Flow Cytometer (BD Biosciences, Heidelberg, Germany) by measuring the propidium iodide fluorescence of individual nucleus, as described earlier [10, 11]. Experiments were conducted thrice independently with three parallel measurements.

2.7. Assessment of Apoptosis by Annexin V/PI Staining.

The CCRF-CEM cells (1×10^6; 1 ml) were also treated with HRB, compound **1** and doxorubicin for 24 h (in humidified 5% CO_2 atmosphere at 37°C), and apoptosis was further assessed by flow cytometry using the flouresceinisothiocynate- (FITC-) conjugated annexin V/PI assay kit (eBioscience™ Annexin V; Invitogen, San Diego, USA), as previously published [10, 11]. Briefly, treated cells were centrifuged at 1200 rpm for 5 min, then washed twice with ice-cold PBS, resuspended in 500 μl binding buffer, and stained with 5 μl FITC-conjugated annexin V (10 mg/mL) and 10 μl PI (50 mg/ml). After 15 min incubation at room temperature (RT) in the dark, cells were analyzed using a BD Accury C6 Flow Cytometer (BD Biosciences). Cells stained with only annexin V were evaluated as being in early apoptosis. Cells stained with both annexin V and propidium iodide were evaluated as being in late apoptosis or in a necrotic stage.

2.8. Evaluation of Caspases Activities Using Caspase-Glo 3/7, Caspase-Glo 8, and Caspase-Glo 9.

Different concentrations of HRB and compound **1** were used to treat CCRF-CEM cells for 6 h. The activities of caspases were determined using Caspase-Glo 3/7, Caspase-Glo 8, and Caspase-Glo 9 Assay kits (Promega, Mannheim, Germany) by measuring the luminescence using an Infinite M2000 ProTM plate reader (Tecan), as reported previously [13].

2.9. Evaluation of Reactive Oxygen Species (ROS) Production.

Various concentrations of HRB and triterpenoid **1** were used to treat CCRF-CEM cells (1×10^6 cells); DMSO (solvent control); or hydrogen peroxide (H_2O_2; positive control). After 24 h incubation in humidified 5% CO_2 atmosphere at 37°C, the production of ROS was evaluated using $2',7'$-dichlorodihydrofluorescein diacetate (H_2DCFH-DA) (Sigma-Aldrich) staining, as described earlier [30–32].

2.10. Statistics.

Statistical analyses were performed with Graph pad prism 5 software. Representative data from three independent experiments are shown as mean value ± S.E.M. One-way Analysis Variance (ANOVA) followed by post hoc Tukey's test was used to determine the significance of the

difference between mean values relative to the control. The p value was calculated to determine significant differences (p value < 0.05).

3. Results

3.1. Phytochemistry. The chemical structures of the isolated phytochemicals were determined by exploiting the physical, mass spectra, and NMR data, followed by direct comparison of these data with those of similar reported compounds in the literature. Compounds were identified as trichadonic acid $C_{30}H_{48}O_3$ (**1**; white amorphous powder; m/z 456) [33], fridelan-3-one $C_{30}H_{50}O$ (**2**; white powder; m.p. 258°C; m/z 426) [33], 2-hydroxy-5-methoxyxanthone $C_{14}H_{10}O_4$ (**3**; yellow amorphous powder; m/z 242) [34], 1,3,6,7-tetrahydroxyxanthone or norathyriol $C_{13}H_8O_6$ (**4**; green-yellowish powder; m.p. 271°C; m/z 260) [35], 1,3,5,6-tetrahydroxyxanthone $C_{13}H_8O_6$ (**5**; yellow powder; m.p. 136°C; m/z 260) [36], betulenic acid $C_{30}H_{48}O_3$ (**6**; white powder; m.p. 318°C; m/z 456) [33], 3′-hydroxymethyl-2′-(4″-hydroxy-3″,5″-dimethoxyphenyl)-5′,6′:5,6-(6,8-dihydroxyxanthone)-1′,4′-dioxane $C_{24}H_{20}O_8$ (**7**; yellow powder; m.p. 264°C; m/z 436) [37, 38], and 3′-hydroxymethyl-2′-(4″-hydroxy-3″,5″-dimethoxyphenyl)-5′,6′:5,6-(xanthone)-1′,4′-dioxane $C_{2420}O_{10}$ (**8**; yellow amorphous powder; m/z 468) [37] (Figure 1). The 1D NMR spectra of these compounds are provided as Supplementary Materials.

3.2. Cytotoxicity of Phytochemicals and Doxorubicin. The cytotoxicity of crude extracts, fractions, and phytochemicals **1–5**, **7**, **8**, and doxorubicin was investigated using RRA towards 9 cancer cell lines and normal AML12 hepatocytes (Tables 1 and 2). The degree of resistance (D.R.) of the tested samples was determined as the ratio of the IC_{50} value of the resistant cell line divided by that of the corresponding parental sensitive cell line (Tables 1 and 2). Collateral sensitivity or hypersensitivity was deduced if the D.R. was below 1 while normal sensitivity was defined as a D.R. of 1 or around 1; cross resistance was considered as a D.R. above 1. The selectivity index (S.I.) was also calculated as the ratio of the IC_{50} value in normal AML12 hepatocytes by the corresponding values in HepG2 hepatocarcinoma cells (Tables 1 and 2).

The obtained IC_{50} values ranged from 11.43 μg/mL (against the P-gp-overexpressing CEM/ADR5000 leukemia cells) to 26.75 μg/mL (against HCT116 (p53$^{+/+}$) colon adenocarcinoma cells) for the crude extract HRB, from 15.65 μg/mL (against CEM/ADR5000 leukemia cells) to 41.17 μg/mL (against HCT116 (p53$^{+/+}$) cells) for HRBa, from 13.92 μg/mL (against U87MG.ΔEGFR glioblastoma cells) to 33.44 μg/mL (against HCT116 (p53$^{+/+}$) cells) for HRBa2, from 16.13 μg/mL (against U87MG glioblastoma cells) to 33.63 μg/mL (against HCT116 (p53$^{-/-}$) cells) for HRBa3, from 10.52 μg/mL (against U87MG.ΔEGFR cells) to 28.43 μg/mL (against HCT116 (p53$^{+/+}$) cells) for HRBa4, and from 28.30 μg/mL (against U87MG.ΔEGFR cells) to 69.48 μg/mL (against HepG2 cells) for HRBb (Table 1). Fractions HRBa1 and HRBa5 had selective activities (Table 1).

Triterpenoid **1**, xanthone **5**, and doxorubicin displayed cytotoxic effects towards the 9 tested cancer cell lines with IC_{50} values ranging from 14.44 μM (against CCRF-CEM cells) to 44.20 μM (against the resistant HCT116 (p53$^{-/-}$) cells) for **1**, from 38.46 μM (against CEM/ADR5000 cells) to 112.27 μM (against HCT116 (p53$^{-/-}$) cells) for **5**, and from 0.02 μM (against CCRF-CEM cells) to 122.96 μM (against CEM/ADR5000 cells) for doxorubicin (Table 2). Xanthones **3** and **4**, as well as xantholignans **7** and **8**, had selective cytotoxic effects (Tables 2).

Collateral sensitivity (D.R. below 1) of CEM/ADR5000 cells, *BCRP*-expressing MDA-MB-231 cells, and HCT116 (p53$^{-/-}$) cells to the mother botanical, HRB compared to their sensitive counterparts CCRF-CEM cells, MDA-MB-231 cells, and HCT116 (p53$^{+/+}$) cells, respectively, was observed. Hypersensitivity of all resistant cell lines to fraction HRBa4 and HRBb compared to their sensitive parental cell lines was also recorded (Table 1). Collateral sensitivity of *BCRP*-expressing MDA-MB-231 cells and U87MG.ΔEGFR cells to phytochemicals **1**, **3–5**, and **8** compared to their sensitive counterparts MDA-MB-231 cells and U87MG cells, respectively, was also observed (Table 2). Concerning the most active compound **1**, a little cross resistance of HCT116 (p53$^{-/-}$) cells compared to their sensitive counterparts HCT116 (p53$^{+/+}$) was observed with a D.R. of 2.55; however, this value was lower than that obtained with doxorubicin (D.R. of 3.73) (Table 2). Apart against HRBb, the S.I. of all samples was above 2 in HepG2 as compared with normal AML12 hepatocytes (Table 1). Compounds **1**, **3**, **5**, **8**, and doxorubicin had an S.I. above 2 in HepG2 as compared with normal AML12 hepatocytes (Table 1). Regarding the recorded IC_{50} values, trichadonic acid (**1**) had the best activity and was consequently selected, together with the crude extract, HRB, for further mechanistic studies.

3.3. Cell Cycle Distribution and Apoptosis. The crude extract (HRB) and triterpenoid **1**, as well as doxorubicin, caused dose-dependent alteration of CCRF-CEM cells' cycle distribution after 24 h treatment (Figure 2). Figure 2 shows that HRB and trichadonic acid (**1**) induced increase of cells in the sub-G0/$G1$ phase, varying from 1.68% ($1/4 \times IC_{50}$) to 24.30% ($2 \times IC_{50}$) for HRB and from 1.86% ($1/4 \times IC_{50}$) to 17.40% ($2 \times IC_{50}$) for compound **1**, while doxorubicin induced increase in the range of 3.28% ($1/4 \times IC_{50}$) to 12.05% ($2 \times IC_{50}$). This suggests that HRB and compound **1** induced apoptosis in CCRF-CEM cells. Increase of cells in the Go/$G1$ phase also suggests that both HRB and trichadonic acid caused cycle arrest in this phase; meanwhile, doxorubicin induced S and G2/M phase arrest (Figure 2). A concentration-dependent induction of apoptosis by HRB and compound **1**, as well as doxorubicin, was further confirmed by annexin V/PI staining (Figure 3). At $2 \times IC_{50}$ for example, HRB significantly ($p < 0.05$) induced late apoptosis (Q2-UR) while compound **1** significantly ($p < 0.05$) induced early apoptosis with, respectively, 14.6% annexin V (+)/PI (−) and 52.5% annexin V (+)/PI (+) cells (Figure 3).
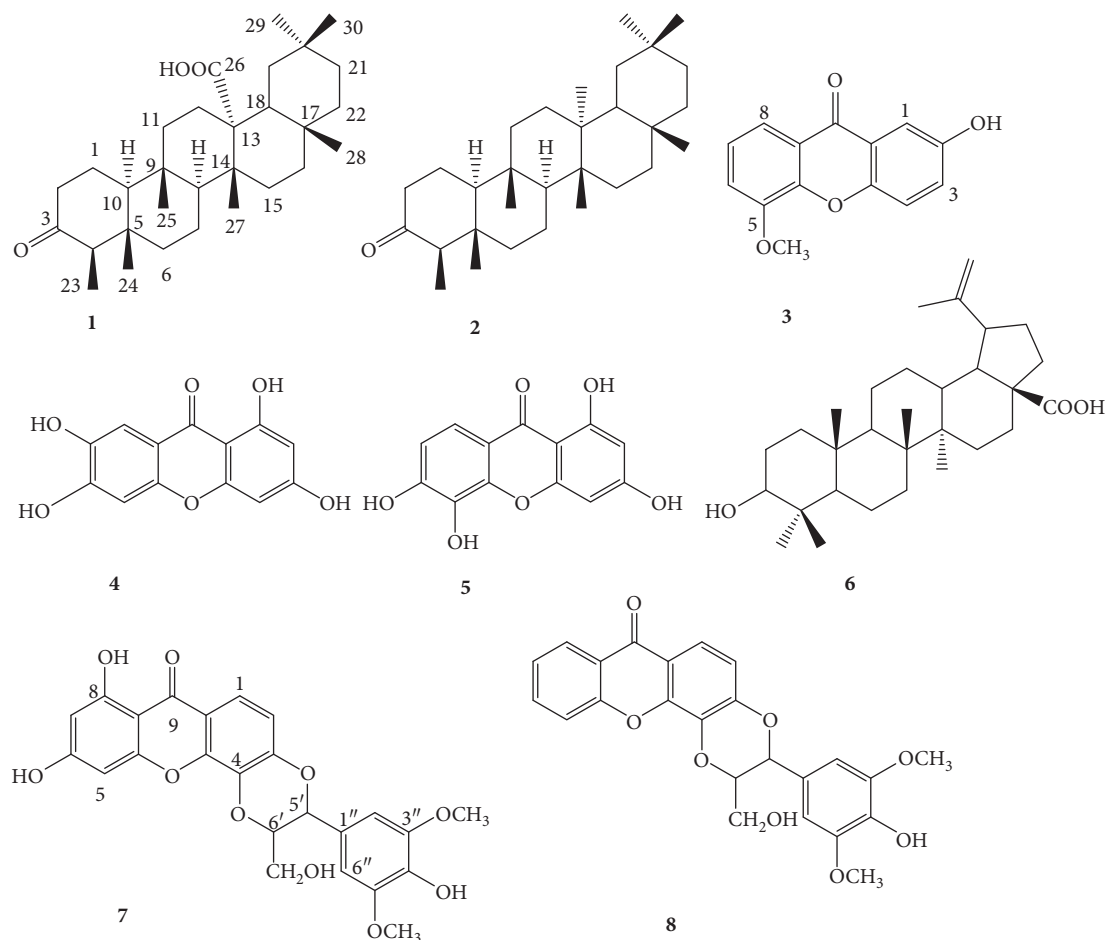
FIGURE 1: Chemical structures of phytochemicals isolated from the bark methanol extract of *Hypericum roeperianum*. **1**: Trichadonic acid; **2**: fridelan-3-one; **3**: 2-hydroxy-5-methoxyxanthone; **4**: 1,3,6,7-tetrahydroxyxanthone or norathyriol; **5**: 1,3,5,6-tetrahydroxyxanthone; **6**: betulenic acid; and **7**: 3′-hydroxymethyl-2′-(4″-hydroxy-3″,5″-dimethoxyphenyl)-5′,6′:5,6-(6,8-dihydroxyxanthone)-1′,4′-dioxane; 8 : 3′-hydroxymethyl-2′-(4″-hydroxy-3″,5″-dimethoxyphenyl)-5′,6′:5,6-(xanthone)-1′,4′-dioxane.

TABLE 1: Recorded IC_{50} values after 72 h incubation of drug-sensitive and MDR cancer cells lines with botanicals from the bark of *Hypericum roeperianum*.

Cell lines	Samples, IC_{50} values in μg/mL, and degrees of resistance* or selectivity index**							
	HRB	HRBa	HRBa1	HRBa2	HRBa3	HRBa4	HRBa5	HRBb
CCRF-CEM	**13.71 ± 0.26**	**15.65 ± 1.18**	46.42 ± 1.98	**17.87 ± 1.53**	**16.81 ± 4.02**	**16.27 ± 4.28**	57.15 ± 3.76	48.76 ± 2.83
CEM/ADR5000	**11.43 ± 0.88**	**18.56 ± 1.74**	>80	**20.18 ± 1.76**	23.03 ± 1.22	**13.55 ± 0.44**	>80	31.55 ± 2.28
Degree of resistance*	0.84	1.19	>1.72	1.13	1.37	0.83	>1.16	0.65
MDA-MB-231-*pcDNA*	**19.87 ± 1.77**	23.12 ± 1.65	72.23 ± 4.54	**20.42 ± 1.71**	28.32 ± 1.57	**18.13 ± 2.08**	68.91 ± 6.30	48.12 ± 1.99
MDA-MB-231-*BCRP*	**18.22 ± 0.81**	26.42 ± 3.01	63.16 ± 3.30	**19.89 ± 0.62**	24.41 ± 1.77	**17.66 ± 1.11**	74.32 ± 3.92	37.23 ± 4.51
Degree of resistance	0.92	1.14	0.87	0.97	0.86	0.97	1.08	0.77
HCT116 ($p53^{+/+}$)	26.75 ± 1.23	34.52 ± 1.74	59.10 ± 3.06	33.44 ± 3.62	30.76 ± 1.61	28.43 ± 3.01	>80	31.19 ± 1.26
HCT116 ($p53^{-/-}$)	**17.44 ± 2.01**	41.17 ± 3.14	>80	24.58 ± 3.48	33.63 ± 3.77	28.09 ± 1.75	>80	29.52 ± 0.98
Degree of resistance	0.65	1.19		0.74	1.09	0.99		0.95
U87MG	**12.42 ± 0.66**	**18.03 ± 1.77**	47.84 ± 4.36	**18.01 ± 1.19**	**16.13 ± 2.04**	**18.44 ± 2.11**	47.89 ± 2.24	46.55 ± 2.43
U87MG.Δ*EGFR*	**14.36 ± 1.48**	**20.12 ± 0.81**	59.60 ± 5.12	**13.92 ± 2.07**	18.72 ± 1.45	**15.52 ± 0.88**	55.20 ± 4.79	28.30 ± 1.11
Degree of resistance	1.16	1.12	1.25	0.77	1.16	0.84	1.15	0.60
HepG2	**17.45 ± 2.05**	29.17 ± 1.30	>80	**18.75 ± 1.41**	25.88 ± 1.56	**14.95 ± 1.34**	>80	69.48 ± 2.93
AML12	42.09 ± 1.17	>80	>80	61.34 ± 3.39	56.12 ± 2.67	65.17 ± 4.31	>80	>80
Selectivity index**	2.41	>2.74		3.27	2.17	4.56		1.15

(*): the degree of resistance was determined as the ratio of the IC_{50} value in the resistant divided by the IC_{50} in the sensitive cell line; CEM/ADR5000, MDA-MB-231-*BCRP*, HCT116 ($p53^{-/-}$), and U87MG.Δ*EGFR* were used as the corresponding resistant counterpart for CCRF-CEM, MDA-MB-231-*pcDNA*, HCT116 ($p53^{+/+}$), and U87MG, respectively; (**): the selectivity index was determined as the ratio of the IC_{50} value in the normal AML12 hepatocytes divided by the IC_{50} in HepG2 hepatocarcinoma cells; in bold: significant cytotoxic effect [7, 39, 40]; nd: not determined; HRB: crude methanol extract from the bark of *Hypericum roeperianum*, HRBa: portion obtained by exhaustion of HRB with ethyl acetate; HRBa1-5: fractions from HRBa; HRBb: residual fraction obtained after exhaustion of HRB with ethyl acetate. The data for doxorubicin used as positive control in similar experimental conditions are shown in Table 2.

TABLE 2: Recorded IC_{50} values following RRA for phytochemicals isolated from the bark of *Hypericum roeperianum* and reference drug, doxorubicin, towards drug-sensitive, MDR cancer cells lines and hepatocytes after 72 h incubation.

| Cell lines | Samples, IC_{50} values in μM, and degrees of resistance* or selectivity index** | | | | | | |
	1	3	4	5	7	8	Doxorubicin
CCRF-CEM	14.44 ± 0.53	16.80 ± 0.96	19.94 ± 2.12	38.58 ± 2.11	23.28 ± 1.46	16.31 ± 2.12	**0.02 ± 0.00**
CEM/ADR5000	18.27 ± 1.56	52.95 ± 3.08	23.21 ± 1.66	38.46 ± 4.07	54.04 ± 4.38	43.47 ± 2.97	122.96 ± 10.94
Degree of resistance*	1.26	3.15	1.16	1.00	2.32	2.66	6,683.00
MDA-MB-231-*pcDNA*	16.47 ± 0.74	43.80 ± 3.47	>153.85	75.15 ± 4.88	20.73 ± 1.32	36.89 ± 2.73	**0.13 ± 0.01**
MDA-MB-231-*BCRP*	14.95 ± 1.17	33.60 ± 1.99	20.38 ± 1.17	62.94 ± 5.32	22.16 ± 2.88	30.50 ± 1.88	**0.79 ± 0.08**
Degree of resistance	0.91	0.77	<0.13	0.84	1.07	0.83	6.14
HCT116 ($p53^{+/+}$)	17.36 ± 1.84	46.67 ± 3.38	40.17 ± 3.09	75.48 ± 6.10	>91.74	37.79 ± 2.92	**0.48 ± 0.06**
HCT116 ($p53^{-/-}$)	44.20 ± 3.21	>165.29	>153.85	112.27 ± 8.49	>91.74	>85.47	**1.78 ± 0.08**
Degree of resistance	2.55	>3.54	>6.15	1.49	nd	>2.26	3.73
U87MG	16.16 ± 1.09	74.44 ± 4.75	106.00 ± 6.74	61.42 ± 3.39	29.70 ± 1.77	35.50 ± 3.28	**0.26 ± 0.03**
U87MG.Δ*EGFR*	14.69 ± 1.55	44.98 ± 5.22	30.37 ± 2.91	59.04 ± 6.01	12.72 ± 0.75	30.61 ± 3.14	**0.98 ± 0.07**
Degree of resistance	0.91	0.60	0.29	0.96	0.43	0.86	3.79
HepG2	21.68 ± 3.18	44.21 ± 2.65	32.40 ± 3.72	64.73 ± 5.77	25.19 ± 1.69	31.29 ± 1.19	**4.56 ± 0.48**
AML12	47.34 ± 0.81	>165.29	45.35 ± 3.52	150.02 ± 7.03	20.89 ± 1.17	>85.47	52.90 ± 4.09
Selectivity index**	2.18	>3.74	1.40	2.32	0.83	>2.73	11.59

(*): the degree of resistance was determined as the ratio of the IC_{50} value in the resistant divided by the IC_{50} in the sensitive cell line; CEM/ADR5000, MDA-MB-231-*BCRP,* HCT116 ($p53^{-/-}$), and U87MG.Δ*EGFR* were used as the corresponding resistant counterparts for CCRF-CEM, MDA-MB-231-*pcDNA*, HCT116 ($p53^{+/+}$), and U87MG, respectively; (**): the selectivity index was determined as the ratio of the IC_{50} value in the normal AML12 hepatocytes divided by the IC_{50} in HepG2 hepatocarcinoma cells; in bold: significant cytotoxic effect [7, 39, 40], the cytotoxicity of compound **6** (betulenic acid) on these cell lines was previous reported [41], and this compound was no more tested in this study; no IC_{50} value was recorded at up to 100 μM with compound **2**; nd: not determined; **1**: trichadonic acid; **3**: 2-hydroxy-5-methoxyxanthone; **4**: 1,3,6,7-tetrahydroxyxanthone or norathyriol; **5**: 1,3,5,6-tetrahydroxyxanthone; **7**: 3′-hydroxymethyl-2′-(4″-hydroxy-3″,5″-dimethoxyphenyl)-5′,6′:5,6-(6,8-dihydroxyxanthone)-1′,4′-dioxane; and **8**: 3′-hydroxymethyl-2′-(4″-hydroxy-3″,5″-dimethoxyphenyl)-5′,6′:5,6-(xanthone)-1′,4′-dioxane.
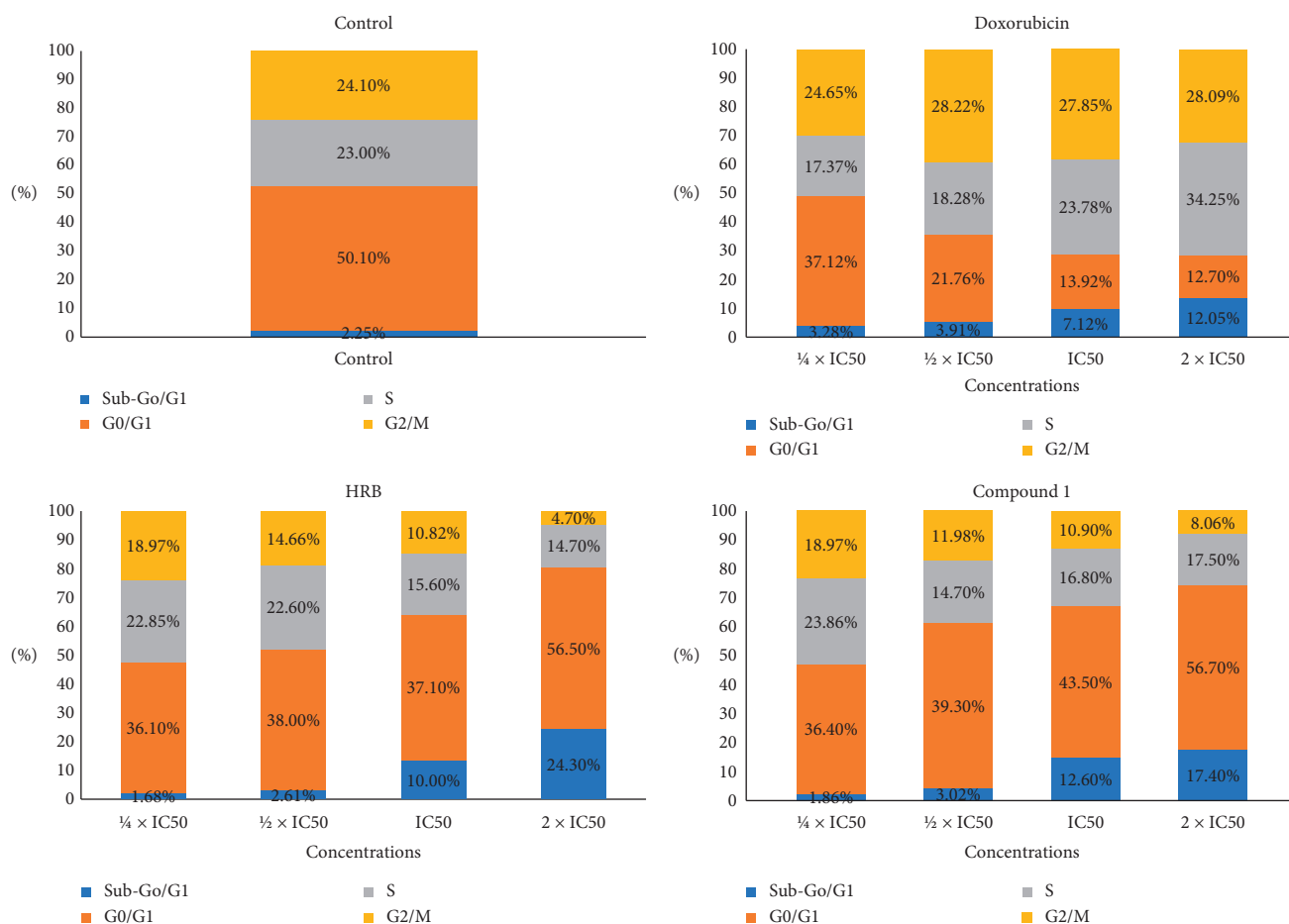

FIGURE 2: Distribution of the CCRF-CEM cells cycle after treatment with the crude extract (HRB), compound **1** (trichadonic acid), and doxorubicin. IC_{50} values were 14.44 μM for trichadonic acid and 0.02 μM for doxorubicin.
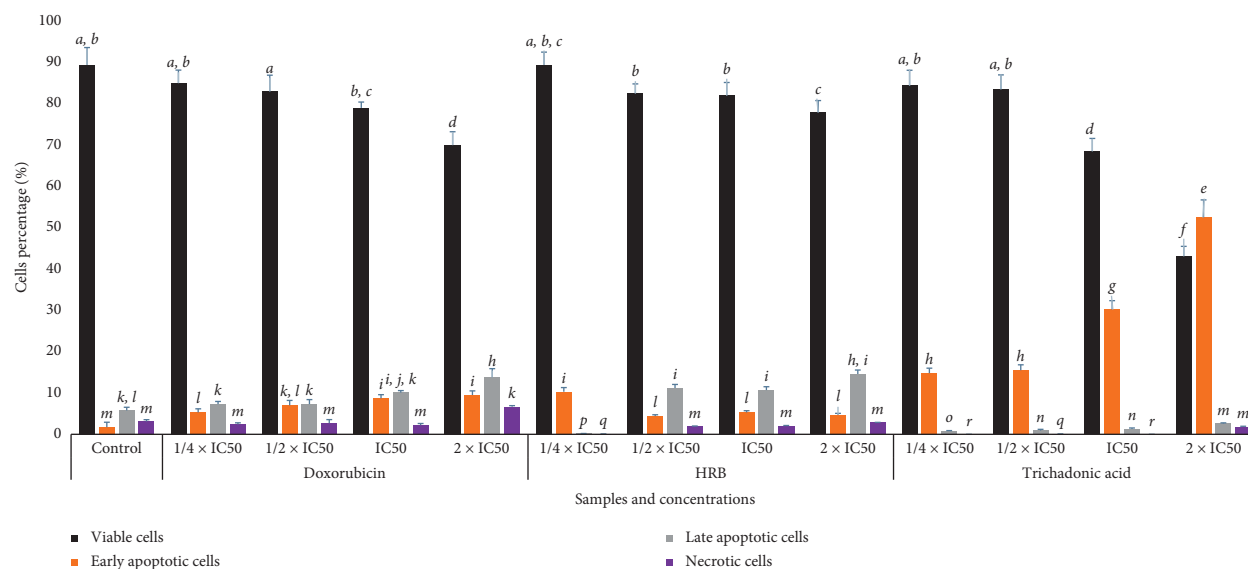
FIGURE 3: Apoptosis induced by the crude extract (HRB), trichadonic acid, and doxorubicin after 24 h on CCRF-CEM leukemia cells as determined by annexin V/PI assay. Apoptosis was assessed by flow cytometry after annexin V-PI double staining. IC$_{50}$ values were 13.71 μg/mL for HRB, 14.44 μM for trichadonic acid, and 0.02 μM for doxorubicin. Mean values ± SD of three independent experiments is shown. Data with different superscript letters are significantly different ($p < 0.05$).

3.4. Activation of Caspases and Production of ROS. In the presence of the tested samples, the activity of caspases in CCRF-CEM cells increased by 1.18-fold, 1.45-fold, and 1.35-fold for HRB and by 2.52-fold, 2.62-fold, and 2.23-fold for trichadonic acid (**1**), respectively, for caspases 3/7, 8, and 9 (Figure 4).

The production of reactive oxygen species (ROS) in CCRF-CEM cells treated with HRB, triterpenoid **1**, H$_2$O$_2$ (positive control), or DMSO was analyzed, and the results are depicted in Figure 5. The crude extract HRB significantly ($p < 0.05$) induced increase of ROS production in a range of 8.98% ($1/4 \times$ IC$_{50}$) to 71.92% ($2 \times$ IC$_{50}$); compound **1** also significantly ($p < 0.05$) induced increase of ROS production in a range of 12.35% (7.22 μM) to 68.12% (57.76 μM). The reference compound, H$_2$O$_2$, increased the ROS levels to 94.30% at 50 μM, while ROS production in nontreated cells was 0.6%.

4. Discussion

Taking into account the rapid development of resistance by cancer cell lines, the use of MDR phenotypes when screening phytochemicals is an interesting approach. Collateral or normal sensitivity (D.R. below or equal to 1) of MDR cells to phytochemicals combined to their good cytotoxicity could be better criteria to select substances for clinical studies. In the present work, four MDR cells lines, CEM/ADR5000 cells, MDA-MB-231-*BCRP* cells, HCT116 ($p53^{-/-}$) cells, and U87.MGΔ*EGFR* cells, were used, and their susceptibilities to isolated phytochemicals were compared with those of their parental sensitive counterparts, CCRF-CEM cells, MDA-MB-231 cells, HCT116 ($p53^{+/+}$) cells, and U87.MG cells, respectively (Tables 1 and 2). Interestingly, collateral sensitivity of CEM/ADR5000 cells, *BCRP*-expressing MDA-MB-231 cells, and HCT116 (p53$^{-/-}$) cells to HRB was

achieved, as well as the hypersensitivity of all resistant cell lines to fraction HRBa4 and HRBb compared to their sensitive parental cell lines (Table 1). Collateral sensitivity of *BCRP*-expressing MDA-MB-231 cells and U87MG.ΔEGFR cells to phytochemicals **1**, **3–5**, and **8** was observed, suggesting that they might be useful to fight drug resistance in breast cancer and glioblastoma (Table 2). This clearly indicates that these botanicals and phytochemicals can be exploited in the fight against recalcitrant cancers. The IC$_{50}$ values below 20 μg/mL or below 10 μM after incubation between 48 and 72 h have been set for promising cytotoxic botanicals and phytochemicals, respectively [39, 40]. Importantly, IC$_{50}$ values below 20 μg/mL were obtained with HRB against 8/9 tested cancer cells lines, HRBa2 and HRBa4 against 7/9 cancer cell lines, HRBa against 4/9 cancer cell lines, and HRBa3 against 3/9 cell lines (Table 1). It can, therefore, be confirmed that these botanicals are interesting cytotoxic agents. However, IC$_{50}$ values below the established threshold were not achieved with phytochemicals, though terpenoid **1** and xanthone **5** had cytotoxic effects towards the 9 tested cancer cell lines. However, their good selectivity indexes still suggest that they can still be good candidates to tackle cancers, especially when drug resistance is observed. To the best of our knowledge, the cytotoxicity of the crude extract and compounds **1**, **2**, **3**, **7**, and **8** on the studied cell lines is being reported, herein, for the first time. Betulinic acid (**6**) is a well-known cytotoxic compound and has previously been found active towards the cancer cell lines tested in the present work, with IC$_{50}$ values ranging from 7.65 μM (in CEM-ADR5000 cells) to 44.17 μM (in HepG2 cells) [41]. Although it was not further tested, herein, compound **6** can be ranked amongst the best active principles of *Hypericum roeperianum*. Also, the cytotoxicity of norathyriol (**4**) in JB6 P+ mouse skin epidermal cells was reported [42]. 1,3,5,6-Tetrahydroxyxanthone (**5**) had low
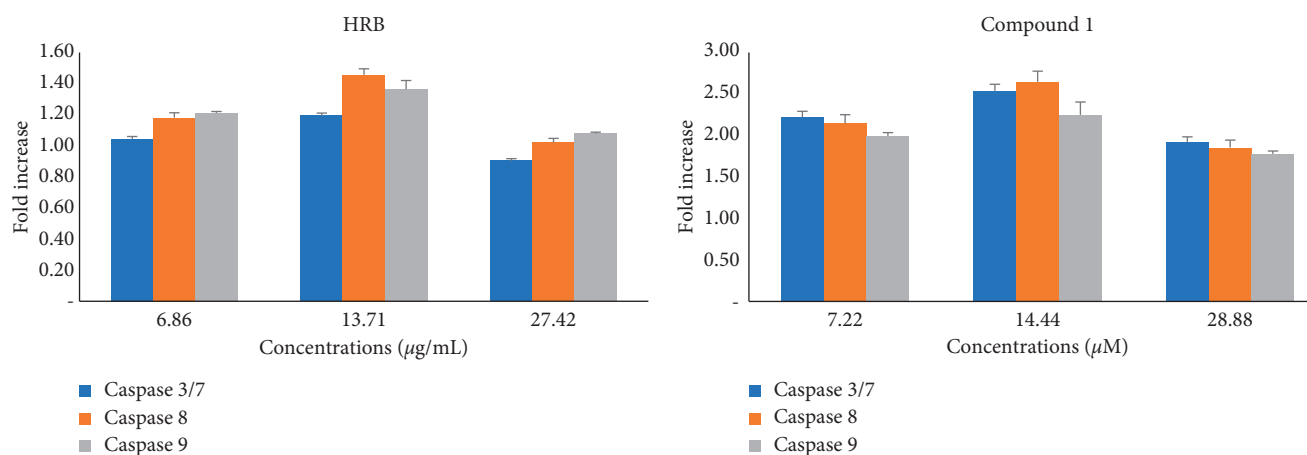
FIGURE 4: Caspases activities in CCRF-CEM cells treated with the crude extract (HRB) and trichadonic acid for 6 h IC$_{50}$ of HRB: 13.71 μg/mL and trichadonic acid: 14.44 μM; (A) caspase activity is expressed as percentage (%) compared to untreated cells. Mean ± SD of three independent experiments is shown.
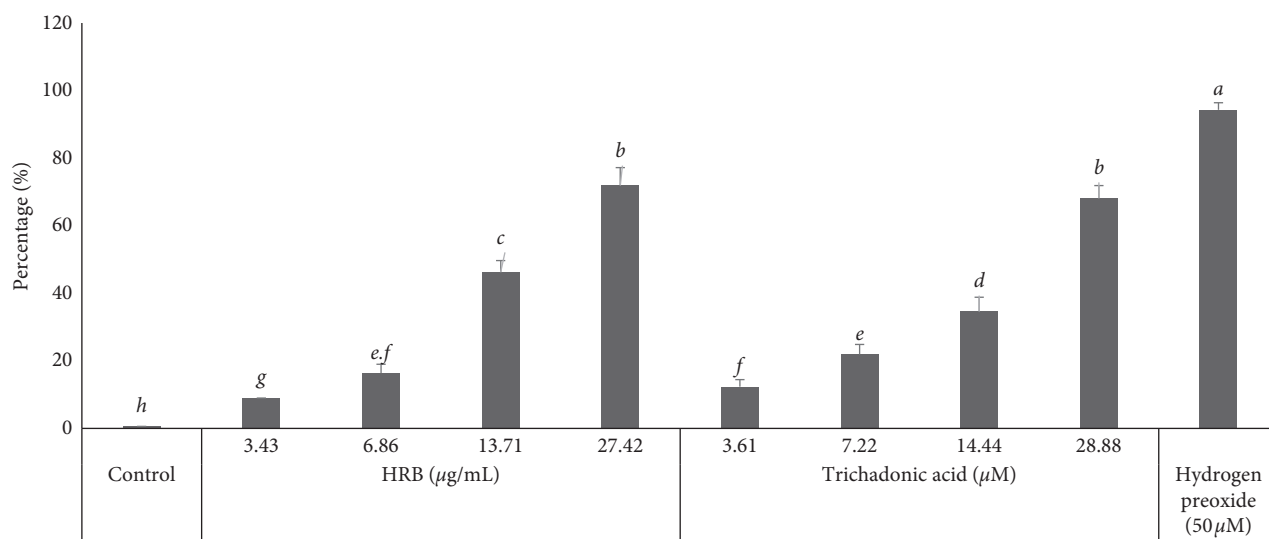
FIGURE 5: Effects of the crude extract (HRB), trichadonic acid, and hydrogen peroxide (H$_2$O$_2$) on the production of reactive oxygen species (ROS) in CCRF-CEM cells treated for 24 h. Mean ± SD of three independent experiments is shown. Data with different superscript letters are significantly different ($p < 0.05$).

cytotoxic effects against K562 leukemia cells with 12.98 μg/mL (49.92 μM) [43].

Apoptosis is a programmed cell death and is also the most investigated mechanism of action of antiproliferative drugs. In this study, it was found that both HRB and compound **1** induced apoptosis in CCRF-CEM cells with cell cycle arrest in the Go/G1 phase (Figures 2 and 3). Modulation of caspases activities is one of the events observed in the apoptotic process in cancer cell lines [44], making these enzymes a target for cytotoxic drug discovery [8, 45]. However, no significant increase in the activity of initiator caspases (caspases 8 and 9) or in that of the activator caspases (caspase 3/7) was observed (Figure 4). Phytochemical **1** induced 2.52-fold, 2.62-fold, and 2.23-fold increase of the activity of caspases 3/7, 8, and 9, respectively (Figure 4), suggesting that this molecule is a caspase modulator. Botanical HRB and compound **1** were also shown to induce

increase of ROS by up to 71.92% and 68.12%, respectively (2 × IC$_{50}$; Figure 5); this is an indication that one of the modes of action of this triterpenoid also includes the enhancement of ROS production in cancer cells.

Regarding the structure-activity relationship, it appears that pentacyclic triterpene **1** is different from **2** by the presence of the carboxyl group (-COOH) in C-13 (Figure 1); the presence of this −COOH group significantly enhanced the cytotoxic activity of triterpene **1**, with IC$_{50}$ values ranging from 14.44 μM to 44.20 μM in cancer cells tested whilst no IC$_{50}$ value at up to 100 μM was recorded with triterpene **2** (Table 1). Betulic acid, another pentacyclic triterpene with−COOH in C-17, previously displayed good cytotoxicity against all cancer cell lines tested in this work [41], illustrating the importance of the carboxyl function in the cytotoxicity of pentacyclic triterpenes. Concerning xanthones, though **5** was active in all tested cancer cell lines,

3-5 displayed moderate activities (Table 1). It was previously shown that additional hetrocycle in xanthone combined to prenylation improved the cytotoxicity of xanthones, with cudraxanthone I (additional hetrocycle combined to -C-8-prenylation) displaying significant cytotoxic effects (IC_{50} value below $10\,\mu M$) against all cancer cell lines tested in the present study [46]. This observation is also confirmed with another prenylated xanthone bearing additional herocycle, xanthone V1 [47]. The difference between the two xanthonolignoids **7** and **8** is the presence of two hydroxyl (-OH) groups in C-6 and C-7 (Compound **8**) (Figure 1). This difference seems to influence the selectivity, as compound **8** was active against HCT116 ($p53^{+/+}$) cells, with an IC_{50} value of $37.79\,\mu M$ compared to the IC_{50} value above $91.74\,\mu M$ obtained for compound **7** (against the same cell line (Table 1).

5. Conclusions

The present work demonstrated that *Hypericum roeperianum* is a source of cytotoxic compounds. Triterpenoids such as trichadonic acid (**1**) and betulinic acid (**6**), xonthones (2-hydroxy-5-methoxyxanthone (**3**), norathyriol (**4**), and 1,3,5,6-tetrahydroxyxanthone (**5**)), and xantholignoids (3′-hydroxymethyl-2′-(4″-hydroxy-3″,5″-dimethoxyphenyl)-5′,6′:5,6-(6,8-dihydroxyxanthone)-1′,4′-dioxane (**7**) and 3′-hydroxymethyl-2′-(4″-hydroxy-3″,5″-dimethoxyphenyl)-5′,6′:5,6-(xanthone)-1′,4′-dioxane (**8**)) are amongst the active constituents of this plant. Trichadonic acid (**1**) induced apoptosis in CCRF-CEM leukemia cells, through caspases activation and enhancement of ROS production. The crude extract, HRB, also induced apoptosis in CCRF-CEM cells, mediated by enhancement of ROS production. These compounds can potentially be useful in the fight against recalcitrant cancers.

Abbreviations

1: Trichadonic acid
2: Fridelan-3-one
3: 2-Hydroxy-5-methoxyxanthone
4: 1,3,6,7-Tetrahydroxyxanthone or norathyriol
5: 1,3,5,6-Tetrahydroxyxanthone
6: Betulenic acid
7: 3′-Hydroxymethyl-2′-(4″-hydroxy-3″,5″-dimethoxyphenyl)-5′,6′:5,6-(6,8-dihydroxyxanthone)-1′,4′-dioxane
8: 3′-Hydroxymethyl-2′-(4″-hydroxy-3″,5″-dimethoxyphenyl)-5′,6′:5,6-(xanthone)-1′,4′-dioxane; ABC, ATP-binding cassette; BCRP, breast cancer resistance protein; DMSO, dimethylsulfoxide; D.R., resistance; EGFR, epidermal growth factor receptor; FITC, flourescein isothiocynate; H_2O_2, hydrogen peroxide; H2DCFH-DA, 2′,7′-dichlorodihydrofluoresceine diacetate; HRB, methanol extract of the bark of *Hypericum roeperianum*; HRBa, portion obtained by exhaustion of HRB with ethyl acetate; HRBa1-5, fractions from HRBa; HRBb, Residual fraction obtained after exhaustion of HRB with ethyl acetate; IC_{50}, 50% inhibitory concentration; MDR, multidrug resistance; PBS, phosphate buffer saline; P-gp, P-glycoprotein; PI, propidium iodide; and ROS, reactive oxygen species

Data Availability

All data generated or analyzed during this study are included in this published article and its supplementary information files.

Conflicts of Interest

The authors declare that they have no conflicts of interest.

Authors' Contributions

SBT, FD, M-GGF, ATM, and VK carried out the experiments; IC recorded NMR data; FD, GTMB, and JDSM elucidated the chemical structures; ATM and VK wrote the manuscript; and all authors read and approved the final manuscript.

Acknowledgments

Supplementary Materials

Additional File: S1: NMR spectra and main chemical shifts of compounds: NMR spectra and main chemical shifts of the isolated compounds; S2: diagrams of annexin V/PI staining of CCRF-CEM with HRB and trichadonic acid. (*Supplementary Materials*)

References

[1] IARC, *Latest Global Cancer Data: Cancer Burden Rises to 18.1 Million New Cases and 9.6 Million Cancer Deaths in 2018*, International Agency for Research on Cancer, Lyon, France, 2020, https://www.who.int/cancer/PRGlobocanFinal.pdf.

[2] D. A. Vorobiof and R. Abratt, "The cancer burden in Africa," *South African Medical Journal=Suid-Afrikaanse Tydskrif Vir Geneeskunde*, vol. 97, no. 10, pp. 937–939, 2007.

[3] C. Fitzmaurice, C. Fitzmaurice, D. Dicker et al., "The global burden of cancer 2013," *JAMA Oncology*, vol. 1, no. 4, pp. 505–527, 2015.

[4] N. R. Farnsworth and D. D. Soejarto, "Global importance of medicinal plants," in *Conservation of Medicinal Plants*, pp. 25–51, Cambridge University Press, Cambridge, UK, 1991.

[5] R. F. Ludueña, "Immunsystem," *Klinische Biochemie*, vol. 178, pp. 207–230, 1997.

[6] N. P. Gullett, A. R. M. Ruhul Amin, S. Bayraktar et al., "Cancer prevention with natural compounds," *Seminars in Oncology*, vol. 37, no. 3, pp. 258–281, 2010.

[7] V. Kuete and T. Efferth, "African flora has the potential to fight multidrug resistance of cancer," *BioMed Research International*, vol. 2015, Article ID 914813, 2015.

[8] A. T. Mbaveng, V. Kuete, and T. Efferth, "Potential of Central, Eastern and Western Africa medicinal plants for cancer therapy: spotlight on resistant cells and molecular targets," *Frontiers in Pharmacology*, vol. 8, p. 343, 2017.

[9] M.-E. F. Hegazy, A. R. Hamed, A. M. El-Halawany et al., "Cytotoxicity of abietane diterpenoids from *Salvia multicaulis* towards multidrug-resistant cancer cells," *Fitoterapia*, vol. 130, pp. 54–60, 2018.

[10] A. T. Mbaveng, G. W. Fotso, D. Nginetedo et al., "Cytotoxicity of epunctanone and four other phytochemicals isolated from the medicinal plants Garcinia epunctata and Ptycholobium contortum towards multi-factorial drug resistant cancer cells," *Phytomedicine*, vol. 48, pp. 112–119, 2018.

[11] A. T. Mbaveng, B. L. Ndontsa, V. Kuete et al., "A naturally occuring triterpene saponin ardisiacrispin B displayed cytotoxic effects in multi-factorial drug resistant cancer cells via ferroptotic and apoptotic cell death," *Phytomedicine*, vol. 43, pp. 78–85, 2018.

[12] V. Kuete, A. T. Mbaveng, L. P. Sandjo, M. Zeino, and T. Efferth, "Cytotoxicity and mode of action of a naturally occurring naphthoquinone, 2-acetyl-7-methoxynaphtho[2,3-b]furan-4,9-quinone towards multi-factorial drug-resistant cancer cells," *Phytomedicine*, vol. 33, pp. 62–68, 2017.

[13] V. Kuete, L. P. Sandjo, D. E. Djeussi et al., "Cytotoxic flavonoids and isoflavonoids from *Erythrina sigmoidea* towards multi-factorial drug resistant cancer cells," *Investigational New Drugs*, vol. 32, no. 6, pp. 1053–1062, 2014.

[14] F. A. Adem, V. Kuete, A. T. Mbaveng et al., "Cytotoxic benzylbenzofuran derivatives from *Dorstenia kameruniana*," *Fitoterapia*, vol. 128, pp. 26–30, 2018.

[15] F. A. Adem, A. T. Mbaveng, and V. Kuete, "Cytotoxicity of isoflavones and biflavonoids from *Ormocarpum kirkii* towards multi-factorial drug resistant cancer," *Phytomedicine*, vol. 58, Article ID 152853, 2019.

[16] V. Kuete, H. Fouotsa, A. T. Mbaveng, B. Wiench, A. E. Nkengfack, and T. Efferth, "Cytotoxicity of a naturally occurring furoquinoline alkaloid and four acridone alkaloids towards multidrug-resistant cancer cells," *Phytomedicine*, vol. 22, no. 10, pp. 946–951, 2015.

[17] V. Kuete, L. P. Sandjo, A. T. Mbaveng, M. Zeino, and T. Efferth, "Cytotoxicity of compounds from *Xylopia aethiopica* towards multi-factorial drug-resistant cancer cells," *Phytomedicine*, vol. 22, no. 14, pp. 1247–1254, 2015.

[18] A. T. Mbaveng, G. T. M. Bitchagno, V. Kuete, P. Tane, and T. Efferth, "Cytotoxicity of ungeremine towards multi-factorial drug resistant cancer cells and induction of apoptosis, ferroptosis, necroptosis and autophagy," *Phytomedicine*, vol. 60, Article ID 152832, 2019.

[19] M. Iwu, *Handbook of African Medicinal Plants*, CRC Press, Boca Raton, FL, USA, 1993.

[20] H. M. Burkill, *The Useful Plants of West Tropical Africa*, Vol. 2, Royal Botanic Gardens, Kew, UK, 1985.

[21] M. J. Moshi, C. J. van den Beukel, and O. J. Hamza, "Brine shrimp toxicity evaluation of some Tanzanian plants used traditionally for the treatment of fungal infections," *African Journal of Traditional Complementary and Alternative Medicine*, vol. 4, no. 2, pp. 219–225, 2007.

[22] F. Damen, O. M. F. Demgne, G. T. M. Bitchagno et al., "A new polyketide from the bark of *Hypericum roeperianum* Schimp." *Natural Product Research*, pp. 1–7, 2019.

[23] G. Rath, O. Potterat, S. Mavi, and K. Hostettmann, "Xanthones from Hypericum roeperanum," *Phytochemistry*, vol. 43, no. 2, pp. 513–520, 1996.

[24] A. Kimmig, V. Gekeler, M. Neumann et al., "Susceptibility of multidrug-resistant human leukemia cell lines to human interleukin 2-activated killer cells," *Cancer Research*, vol. 50, no. 21, pp. 6793–6799, 1990.

[25] T. Efferth, A. Sauerbrey, A. Olbrich et al., "Molecular modes of action of artesunate in tumor cell lines," *Molecular Pharmacology*, vol. 64, no. 2, pp. 382–394, 2003.

[26] J.-P. Gillet, T. Efferth, D. Steinbach et al., "Microarray-based detection of multidrug resistance in human tumor cells by expression profiling of ATP-binding cassette transporter genes," *Cancer Research*, vol. 64, no. 24, pp. 8987–8993, 2004.

[27] L. A. Doyle, W. Yang, L. V. Abruzzo et al., "A multidrug resistance transporter from human MCF-7 breast cancer cells," *Proceedings of the National Academy of Sciences*, vol. 95, no. 26, pp. 15665–15670, 1998.

[28] J. O'Brien, I. Wilson, T. Orton, and F. Pognan, "Investigation of the Alamar Blue (resazurin) fluorescent dye for the assessment of mammalian cell cytotoxicity," *European Journal of Biochemistry*, vol. 267, no. 17, pp. 5421–5426, 2000.

[29] V. Kuete, A. H. L. Nkuete, A. T. Mbaveng et al., "Cytotoxicity and modes of action of 4′-hydroxy-2′,6′-dimethoxychalcone and other flavonoids toward drug-sensitive and multidrug-resistant cancer cell lines," *Phytomedicine*, vol. 21, no. 12, pp. 1651–1657, 2014.

[30] D. A. Bass, J. W. Parce, L. R. Dechatelet, P. Szejda, M. C. Seeds, and M. Thomas, "Flow cytometric studies of oxidative product formation by neutrophils: a graded response to membrane stimulation," *Journal of Immunology (Baltimore, Md.:1950)*, vol. 130, no. 4, pp. 1910–1917, 1983.

[31] A. Cossarizza, R. Ferraresi, L. Troiano et al., "Simultaneous analysis of reactive oxygen species and reduced glutathione content in living cells by polychromatic flow cytometry," *Nature Protocols*, vol. 4, no. 12, pp. 1790–1797, 2009.

[32] V. Kuete, S. B. Tankeo, M. E. M. Saeed, B. Wiench, P. Tane, and T. Efferth, "Cytotoxicity and modes of action of five Cameroonian medicinal plants against multi-factorial drug resistance of tumor cells," *Journal of Ethnopharmacology*, vol. 153, no. 1, pp. 207–219, 2014.

[33] S. B. Mahato and A. P. Kundu, "13C NMR spectra of pentacyclic triterpenoids-A compilation and some salient features," *Phytochemistry*, vol. 37, no. 6, pp. 1517–1575, 1994.

[34] M. L. Cardona, J. R. Pedro, E. Seoane, and R. Vidal, "Xanthone constituents of *Hypericum canariensis*," *Journal of National Products*, vol. 48, no. 3, pp. 467–469, 2004.

[35] C. Çirak, "Hypericin in *Hypericum lydium* boiss. growing in Turkey," *Biochemical Systematics and Ecology*, vol. 34, no. 12, pp. 897–899, 2006.

[36] M.-J. Don, Y.-J. Huang, R.-L. Huang, and Y.-L. Lin, "New phenolic principles from *Hypericum sampsonii*," *Chemical & Pharmaceutical Bulletin*, vol. 52, no. 7, pp. 866–869, 2004.

[37] M. Abou-shoer, A.-A. Habib, C.-J. Chang, and J. M. Cassady, "Seven xanthonolignoids from *Psorospermum febrifugum*," *Phytochemistry*, vol. 28, no. 9, pp. 2483–2487, 1989.

[38] M. L. Cardona, M. I. Fernández, J. R. Pedro, E. Seoane, and R. Vidal, "Additional new xanthones and xanthonolignoids from *Hypericum* canariensis," *Journal of Natural Products*, vol. 49, no. 1, pp. 95–100, 1986.

[39] J. Boik, *Natural Compounds in Cancer Therapy*, Oregon Medical Press, Princeton, MN, USA, 2001.

[40] G. Brahemi, F. R. Kona, A. Fiasella et al., "Exploring the structural requirements for inhibition of the ubiquitin E3 ligase breast cancer associated protein 2 (BCA2) as a treatment for breast cancer," *Journal of Medicinal Chemistry*, vol. 53, no. 7, pp. 2757–2765, 2010.

[41] A. T. Mbaveng, F. Damen, and J. D. Simo Mpetga, "Cytotoxicity of crude extract and isolated constituents of the *Dichrostachys cinerea* bark towards multifactorial drug-resistant cancer cells," *Evidence- Based Complementary and Alternative Medicine*, vol. 2019, Article ID 8450158, 2019.

[42] J. Li, M. Malakhova, M. Mottamal et al., "Norathyriol suppresses skin cancers induced by solar ultraviolet radiation by targeting ERK kinases," *Cancer Research*, vol. 72, no. 1, pp. 260–270, 2012.

[43] N. H. Zamakshshari, G. C. L. Ee, I. S. Ismail, Z. Ibrahim, and S. H. Mah, "Cytotoxic xanthones isolated from *Calophyllum depressinervosum* and *Calophyllum buxifolium* with antioxidant and cytotoxic activities," *Food and Chemical Toxicology*, vol. 133, Article ID 110800, 2019.

[44] Y. Fuchs and H. Steller, "Programmed cell death in animal development and disease," *Cell*, vol. 147, no. 4, pp. 742–758, 2011.

[45] B. Howley and H. O. Fearnhead, "Caspases as therapeutic targets," *Journal of Cellular and Molecular Medicine*, vol. 12, no. 5A, pp. 1502–1516, 2008.

[46] V. Kuete, L. P. Sandjo, J. L. N. Ouete, H. Fouotsa, B. Wiench, and T. Efferth, "Cytotoxicity and modes of action of three naturally occurring xanthones (8-hydroxycudraxanthone G, morusignin I and cudraxanthone I) against sensitive and multidrug-resistant cancer cell lines," *Phytomedicine*, vol. 21, no. 3, pp. 315–322, 2014.

[47] V. Kuete, H. K. Wabo, and K. O. Eyong, "Anticancer activities of six selected natural compounds of some Cameroonian medicinal plants," *PLoS One*, vol. 6, no. 8, Article ID e21762, 2011.

Research Article

In Vitro Antioxidant and Antidiabetic Potentials of *Syzygium caryophyllatum* L. Alston

Herath Pathiranage Thathmi Wathsara,[1] **Hasitha Dhananjaya Weeratunge,**[2]
Mohamed Naeem Ahammadu Mubarak,[3] **Pahan Indika Godakumbura,**[1]
and Pathmasiri Ranasinghe [2]

[1]*Department of Chemistry, Faculty of Applied Sciences, University of Sri Jayewardenepura, Nugegoda, Sri Lanka*
[2]*Herbal Technology Section (HTS), Modern Research & Development Complex (MRDC), Industrial Technology Institute (ITI),
503A Halbarawa Gardens, Malabe, Sri Lanka*
[3]*Residue Analysis Laboratory, Industrial Technology Institute (ITI), 363, Bauddhaloka Mawatha, Colombo 07, Sri Lanka*

Correspondence should be addressed to Pathmasiri Ranasinghe; pathmasiri@iti.lk

Syzygium caryophyllatum L. Alston (Family: Myrtaceae, Sinhala: Heendan) is a red-listed plant that has been used in traditional medicine in Sri Lanka for the treatment of diabetes, but it is yet to be exploited for its potential uses as a functional food or a source of supplements. The present study focused on the evaluation of antidiabetic property of *S. caryophyllatum* fruits and leaves assessing antioxidant, antiglycation, and antiamylase activities and functional mineral element composition. The crude extracts (CR) of leaves and fruits were fractionated into hexane (Hex) ethyl acetate (EA) and aqueous (AQ) and evaluated for bioactivities along with the crude extracts. The isolated fraction (C_3) of Hex fraction of fruit showed significantly high ($p < 0.05$) antiamylase activity with IC_{50} value 2.27 ± 1.81 μg/mL where the Hex fraction of fruits exhibited the IC_{50} value as 47.20 ± 0.3 μg/mL which was higher than acarbose (IC_{50}: 87.96 ± 1.43 μg/mL). The EA fraction of leaves showed highest values for DPPH radical scavenging activity, ferric reducing antioxidant power, and oxygen radical absorbance capacity. Significantly high ($p < 0.05$) ABTS radical scavenging activity and iron chelating activity were observed in Hex fraction of fruit. The composition of volatiles in leaf oil was studied with GC-MS, and 58 compounds were identified. Inductively coupled plasma-mass spectrometry data revealed the presence of biologically significant trace elements such as Fe, Zn, Mg, Cu, Se, and Sr in leaves and fruits. It is concluded that the Hex fraction of *S. caryophyllatum* fruits will be a good source for the formulation of supplements for diabetic management with further evaluation of potency and efficacy.

1. Introduction

The prevalence of diabetes mellitus has shown a rapid increase over the years, and according to the reports of the WHO, individuals suffering from diabetes mellitus worldwide will show a marked increase of up to 592 million in 2035 from 422 million in 2014. Further in 2015, 1.6 million deaths were estimated to be directly or indirectly caused by diabetes. At present, developing countries are much affected by the more predominant form of diabetes—Type 2 diabetes that accounts for increased morbidity and disability causing a threat to the economic growth in most developing countries. However, reports revealed that more than 80% of

deaths resulting from diabetes in developing countries are due to rapid urbanization and poor healthcare facilities [1].

Diabetes Mellitus (DM) is a metabolic disorder of multiple etiology characterized by chronic hyperglycemia which is mainly caused by one or combination of factors including the ineffectiveness of insulin, deficiency of insulin secretion, and insulin resistance of the cells, in particular, skeletal muscle tissues [2]. Changes in food patterns and lifestyle such as high intake of calories, less exercise, and physiological stress conditions are also closely associated with the development and progression of DM [3].

Prolonged hyperglycemic conditions in diabetes patients induce nonenzymatic glycation, which is a reaction between

the amino group of proteins and the carbonyl group of reducing sugar to form a fluorescent, Advanced Glycation End-products (AGEs) [4]. Apart from elevated sugar levels in the blood, exposure to exogenous free radicals and consumption of processed foods with a high content of fructose may also accelerate the accumulation of AGEs [5]. Studies have proven that hyperglycemia and signal-transducing receptor interactions of AGEs formation induce increased production of free radicals leading to oxidative stress [6, 7]. This in turn leads to various pathological conditions, such as cancer, neurological disorders, atherosclerosis, hypertension, type 2 diabetes, acute respiratory distress syndrome, idiopathic pulmonary fibrosis, chronic obstructive pulmonary disease, and asthma [6].

Studies have further revealed that the imbalance of several essential trace elements leads to the development and progression of DM. Further clinical studies have suggested that patients with diabetes have an increased risk of trace element deficiency. Hence, it is recommended to increase the dietary intake of some trace elements or as a dietary supplement to manage this condition during DM [8]. The mineral elements play a pivotal role in numerous basic physiological functions of the human body and the deficiency thus leads to a variety of extensive diseases and disorders [9]. Several mineral elements have been identified as the cofactors of antioxidative enzymes and play an important role in protecting the insulin-secreting pancreatic β-cells [8]. Thus management of type 2 DM includes reduction of postprandial glucose concentrations by inhibition of α-amylase and α-glucosidase enzymes which delays the digestion of carbohydrates, thus, lowering the hyperglycemic condition.

In recent years, the usage and the vitality of natural products have created great curiosity among the scientific community. This is mainly due to the benefits of natural products such as high effectiveness, low risk of side effects, low cost, and abundant availability.

Ethnobotanical information reveals that there is a wide array of plants that possessed potential antidiabetic properties and antioxidant properties [10, 11]. In this regard, over 200 pure compounds from herbal plants are scientifically proven to have hypoglycemic activity [12].

Syzygium is a genus from the Myrtaceae family possessing 1200–1800 species. *Syzygium caryophyllatum* (*Sinhala*: Heendan) is one of the species that has been classified as endangered species under the International Union for Conservation of Nature (IUCN) and is native to Sri Lanka and India [13]. In India, *S. caryophyllatum* plant has been studied for its antibacterial and antioxidant activities using some *in vitro* antioxidant assays [14]. However, this is the 1st Sri Lankan study to report the antioxidant activities and antidiabetic activities of *S. caryophyllatum*. In traditional folklore medical practices, the decoction of *S. caryophyllatum* is used in the treatment for ailments of diabetes mellitus [15]. In Sri Lanka, *S. caryophyllatum* is considered as an underutilized wild fruit amidst all its beneficial properties due to the lack of reported data on its nutritional value, poor awareness on the beneficial roles of the fruit, upcoming modern agricultural practices, and over imported fruits [16].

Therefore, the present study aimed to evaluate *in vitro* bioactivities such as antioxidant, antiamylase, and antiglycation and quantify mineral elements and volatile oil compositions of *Syzygium caryophyllatum* in Sri Lanka. Furthermore, the outcome of this study will be used to determine whether *Syzygium caryophyllatum* fruits and leaves are potential sources of dietary supplement in managing DM and its complications.

2. Materials and Methods

2.1. Chemical and Reagents. Folin-Ciocalteu reagent (FC Reagent), gallic acid, quercetin, acarbose, 6-hydroxy-2-5-7-8-tetramethylchroman-2carboxylic acid (Trolox), ethylenediaminetetraacetic acid (EDTA), 1,1-diphenyl-2-picrylhydrazyl (DPPH), 2, 2-azino-bis (3ethylbenzothiazoline-6-sulfonic acid) diammonium salt (ABTS), potassium persulphate, 2, 2′-azobis (2-amidinopropane) dihydrochloride (AAPH), sodium fluorescein, 2,4,6 tripyridyl-s-triazine (TPTZ), and α-amylase (*Bacillus amyloliquefaciens*) were purchased from Roche Diagnostics (USA), and 3,5-dinitrosalycilic acid, 4, 4′-disulfonic acid sodium salt (ferrozine), soluble starch, bovine serum albumin (BSA), D-glucose, and trichloro-acetic acid (TCA) were purchased from Sigma-Aldrich (USA). All other chemicals used for the preparation of buffers and solvents were in the analytical grade. Spectrophotometric assays were conducted using 96-well microplate readers (Spectra Max Plus384, Molecular Devices, USA, and SPECTRAmax-Gemini EM, Molecular Devices Inc., USA). The mineral analysis was done using microwave digester CEM Mar 5, USA, using the Easy Prep digestion program and ICP-MS (Agilent 7900, USA).

2.2. Plant Materials. Fresh leaves and ripened fruits (Figure 1) were collected into sterile polypropylene bags from the areas of Homagama and Malabe (Colombo district, Sri Lanka) during the period from April to May 2016. The plant materials were botanically identified by the botanist, Dr. Chandima Wijesiriwardena, Principle Research Scientist, Industrial Technology Institute, Sri Lanka, and voucher specimens (leaves WF10-1 and fruits-WF10-2) were deposited at the Herbal Technology Section (HTS), Industrial Technology Institute (ITI), Sri Lanka. The collected materials were washed with running water followed by distilled water, cleaned, air dried, and ground to obtain a fine powder. The powder was packed in polypropylene bags and stored at −20°C for further analyses.

2.3. Preparation of Extracts

2.3.1. Preparation of Leaf Crude Extract of Syzygium caryophyllatum. The moisture content of the powdered leaves was recorded by moisture analyzer (moisture 13.53%). The powdered sample (225 g dry weight of sample) was extracted by the reflux apparatus for 3 hours and filtered using a muslin cloth and later with Whatman number 1 filter paper. The filtrate was treated with 70% ethanol (1 : 3, extract: ethanol) and centrifuged to remove the precipitate. The extract was concentrated in a vacuum below 50°C and neutralized to pH 7 with 0.01 M HCl.

(a)

(b)

(c)

FIGURE 1: Different parts of the *Syzygium caryophyllatum* plant: (a) leaf, (b) flowers, and (c) fruits.

2.3.2. Preparation of Fruit Crude Extract of Syzygium caryophyllatum.

The ripen fruits (30 g dry weight of sample) without seed were extracted with ethanol by overnight cold extraction with stirring. The ethanol extract was concentrated in a vacuum at 40°C.

The crude extracts of leaves and fruits were fractionated into hexane and ethyl acetate by using separation funnels, and all concentrated samples were stored at −20°C prior to the analyses. The extracts were evaporated to dryness by rotary evaporator, and a known amount of sample was dissolved in DMSO for further analyses.

2.4. Compound Isolation from Hexane Fraction of Syzygium caryophyllatum Fruits.

The fraction was separated using column chromatography with different organic solvents as the mobile phase. A column of 75 cm height and 2.5 cm diameter was packed with silica gel 100–200 mesh with hexane as a solvent in the wet packing method. Compound isolation was carried out in two different methods by using different solvents on the isolation procedure.

2.4.1. Hexane and Ethyl Acetate Solvents on Isolation Procedure (Hex and EA).

The 50 mg of Hex fraction of fruits was separated by column by increasing polarity of eluent hexane and ethyl acetate $100 : 0$ and $0 : 100$, respectively. The two separated isolates were tested for α-amylase inhibition activity.

2.4.2. Hexane, Dichloromethane, and Ethyl Acetate Solvents on Isolation Procedure (Hex, DCM, and EA).

Column chromatography was performed using 200 mg of Hex fraction of fruits to obtain fractions by increasing polarity using a gradient elution technique as follows: Fractions (FR) 1–10 (Hex), FR 11–12 (Hex : DCM = 3 : 1), FR 13 (Hex : DCM = 2 : 1), FR 14–19 (DCM), and FR 20–22 (DCM : EA = 95 : 5) to obtain 51.8 mg (C_1: combined fractions 1–13), 95.7 mg (C_2: combined fractions 14–19), and 6.8 mg (C_3: combined fractions 20–22), respectively. All combined fractions were tested for α-amylase inhibition activity.

Flowchart of the overall methodology is shown in Figure 2.

Leaves and fruits of *Syzygium caryophyllatum* plant were extracted, fractionated, and subjected for phytochemical analysis, antioxidant, antiamylase, antiglycation potentials analysis, and compounds isolation. Chemical compositions of *Syzygium caryophyllatum* leaf oil were analyzed by GC-MS and mineral composition of leaves and fruits were analyzed by ICP-MS.

2.5. Estimation of Phytochemical Compounds

2.5.1. Determination of Total Polyphenol Content (TPC).

The total polyphenol content (TPC) was determined using the Folin-Ciocalteu (FC) reagent method [17] with minor modification using 96-well microplates. Freshly prepared $110 \mu L$ of
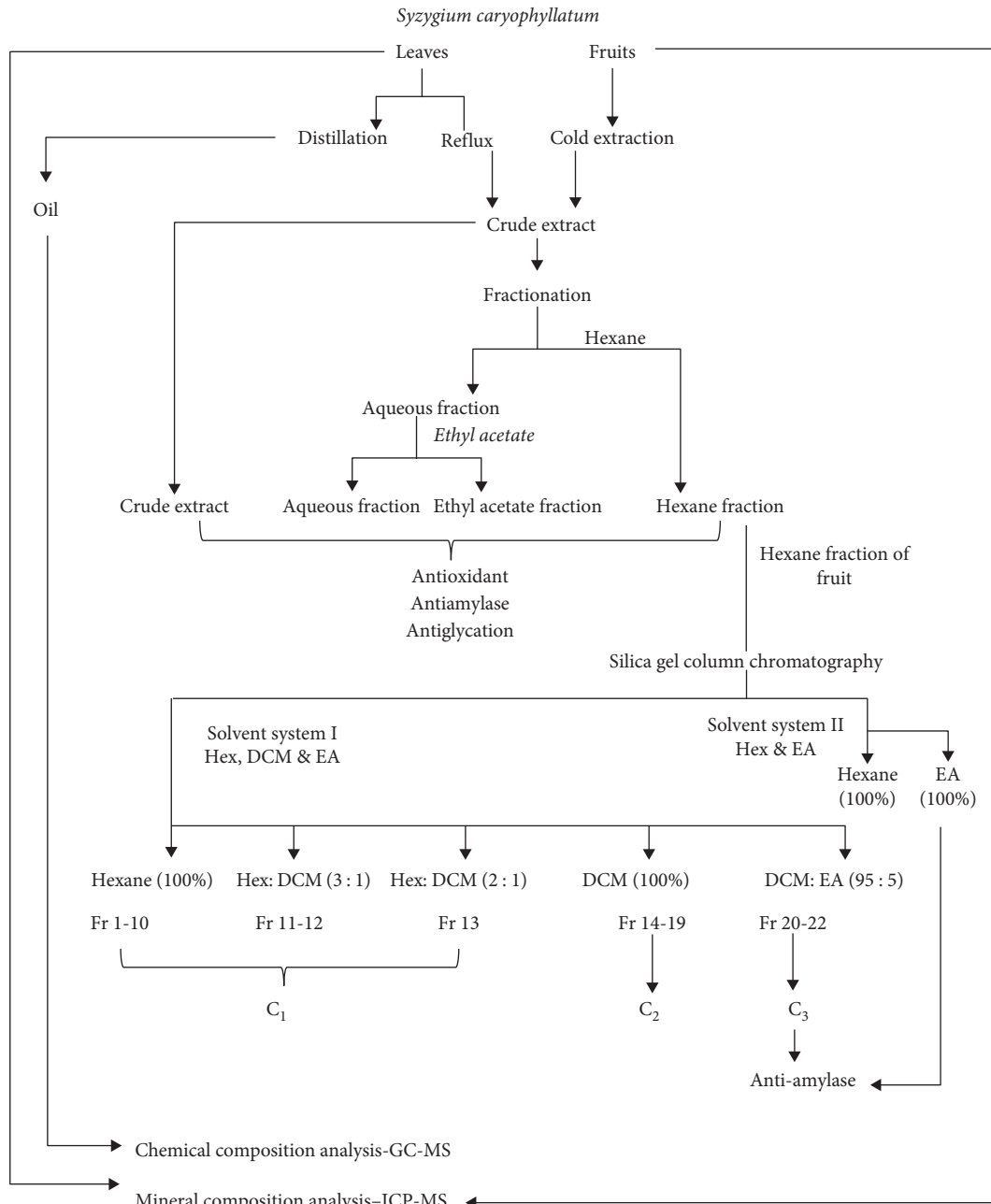
FIGURE 2: Flow chart depicting the methodology of the study.

FC Reagent was added to 20 μL of the sample. The mixture was treated with 10% sodium carbonate and incubated at room temperature for 30 min and absorbance was measured at 765 nm. Gallic acid was used as a reference standard, and the results were expressed as milligram gallic acid equivalent per gram of sample (mg GAE/g of sample).

2.5.2. Determination of Total Flavonoid Content (TFC).
The total flavonoid content (TFC) was determined using an aluminum chloride colorimetric method using 96-well microplates [18]. Extracts were dissolved in methanol, and 100 μL of the sample was mixed with 100 μL of 2% aluminum chloride. The mixture was incubated at room temperature for 10 min and absorbance was measured at 415 nm. Quercetin was used as a reference standard, and the results were expressed as milligram quercetin equivalent per gram of sample (mg QE/g of sample).

2.6. Evaluation of Antioxidant Activity

2.6.1. Ferric Reducing Antioxidant Power (FRAP) Assay.
The assay method was based on the reduction of Fe^{3+} to Fe^{2+} by the electron donation ability of antioxidants resulting in an intense blue-colored complex (Fe^{2+}-tripyridyltriazine)

[18]. The FRAP reagent was prepared freshly by mixing acetate buffer (300 mM, pH 3.6) solution of TPTZ in HCl and $FeCl_3$ (20 mM) in $10:1:1$ ratio and incubated at $37°C$. Two hundred microliters of the reaction mixture (FRAP reagent and sample) was incubated at room temperature, and absorbance was measured at 600 nm. Vitamin E analogue Trolox was used as the reference standard where the results were expressed as mg of Trolox equivalent per gram of extract (mg TE/g of extract).

2.6.2. DPPH Radical Scavenging Assay.

The radical scavenging activity was determined by using 1, 1-diphenyl-2-picrylhydrazyl (DPPH) stable radical method [18]. The method is based on the reduction of purple-colored 1, 1-diphenyl-2-picrylhydrazyl to a yellow-colored diphenylpicrylhydrazine. The reaction volume of 200 μL containing sample (50 μL), methanol, and DPPH were incubated at room temperature for 10 min, and absorbance was measured at 517 nm. A percentage inhibition versus concentration was plotted, and the concentration of the sample required for 50% inhibition was determined and represented as EC_{50} value. The following formula was used to calculate the percent inhibition:

$$\%\text{Radical scavenging activity} = \frac{(C_{AB} - S_{AB})}{C_{AB}} \times 100, \quad (1)$$

where C_{AB} is the absorbance of the control, and S_{AB} is the absorbance of the sample.

2.6.3. ABTS Radical Scavenging Activity.

The $ABTS^+$ radical cation ($ABTS^+$) scavenging activity assay was performed [19] with some modifications in 96-well microplates. Plant extracts were prepared in phosphate buffer solutions and were allowed to react with $ABTS^+$ radicals in a microwell plate for 10 min. Absorbance was measured in 734 nm and Trolox was used as the standard. The following formula was used to calculate the percent inhibition:

$$\%\text{Radical scavenging activity} = \frac{(C_{AB} - S_{AB})}{C_{AB}} \times 100, \quad (2)$$

where C_{AB} is the absorbance of the control, and S_{AB} is the absorbance of the sample.

The antiradical activity was expressed as EC_{50}, the concentration required to cause 50% inhibition of $ABTS^+$ radicals.

2.6.4. Oxygen Radical Absorbance Capacity (ORAC) Assay.

The ORAC assay is a hydrogen atom transfer- (HAT-) based assay which measures the depletion of fluorescence intensity of a fluorescent probe upon the generation of peroxy radicals due to the oxidation of azo compounds. In the presence of an antioxidant compound, the decaying of fluorescent intensity is retarded. The overall decay is calculated by the difference between the area under the fluorescence decay curve (AUC) of the sample of interest and AUC of blank [20]. The reaction volume of 200 μL (pH 7.4) containing fluorescein (100 μL) and sample (50 μL) was preincubated at $37°C$ for 5 min. The 2,2'-azobis (2-amidinopropane) dihydrochloride (AAPH)

solution was added (50 μL) to the mixture, and the plate (black 96 well plates) was immediately placed in a fluorescent microplate reader (SPECTRAmax-Gemini EM, Molecular Devices Inc, USA). The decay of fluorescence was recorded every minute for 35 min, and the excitation and emission wavelengths were obtained at 494 nm and 535 nm, respectively. Phosphate buffer (75 mM, pH 7.4) replacing the sample was used as the blank, and Trolox was used as the standard antioxidant. Results were expressed as mg of Trolox equivalent per gram of extract.

2.6.5. Ferrous Ion Chelating Activity.

The ferrous ion chelating (FIC) activity was measured by the decrease in the absorbance at 562 nm of the iron (II)-ferrozine complex [21]. EDTA was used as the reference standard, and all the samples and standards were prepared in distilled water. The sample was mixed with 1 mM ferrous sulfate and distilled water followed by 1 mM ferrozine solution. The ability of the sample to chelate ferrous ions was calculated relative to the control (distilled water instead of the sample) by the following formula. The results were expressed as mg EDTA equivalent per gram of extract.

$$\%\text{Chelating activity} = \frac{(C_{AB} - S_{AB})}{C_{AB}} \times 100, \quad (3)$$

where S_{AB} is the absorbance of the sample and C_{AB} is the absorbance of the control.

2.7. Determination of α-Amylase Inhibition Activity.

The α-amylase inhibition activity was carried out using the dinitrosalicylic (DNS) method [22], where the inhibition activity was measured by quantifying the maltose liberated under the assay conditions. The enzyme inhibitory activity was expressed as a decrease in units of maltose liberated. A modified dinitrosalicylic acid (DNS) method was adopted to estimate the maltose equivalent. The reaction volume containing 40 μL of 1% (w/v) starch solution and 775 μL of 100 mM sodium acetate buffer was preincubated with 135 μL of the sample at $40°C$ shaking water bath for 10 min. The mixture was further incubated with 50 μL of the α-amylase enzyme (5 μg/mL) at $40°C$ shaking water bath for 15 min. The reaction was terminated by adding 500 μL DNS reagent, and the mixture was placed in a boiling water bath for 5 min followed by cooling in an ice bath. Absorbance was measured at 540 nm using a 96-well microplate reader. Antiamylase activity (inhibition %) was calculated using the following equation:

$$\text{Inhibition}(\%) = \frac{[A_C - (A_S - A_b)]}{A_C} \times 100, \quad (4)$$

where A_C is the absorbance of the control, A_S is the absorbance of the sample, and A_b is the absorbance of the sample blank.

2.8. BSA-Glucose Glycation Inhibitory Activity Assay.

Antiglycation activity assay was performed with some modifications to the previous methodology [23] for CR

extracts of leaves and fruits of *Syzygium caryophyllatum*. A mixture of 800 μg/mL BSA, 400 mM glucose, and 80 μL of the sample in 50 mM phosphate buffer (pH 7.4) containing sodium azide (0.02%) was incubated at 60°C for 40 h. The 600 μL of the reaction mixture was transferred to 1.5 mL microcentrifuge tubes and 60 μL of 100% (w/v) TCA was added, and sample mixtures were centrifuged at 15,000 rpm at 4°C for 4 min. The resultant advanced glycation end products-BSA (AGEs-BSA) precipitate was then dissolved in 1 mL of phosphate buffer saline (pH 10), and the fluorescence intensity was measured at an excitation and emission wavelengths of 370 nm and 440 nm using a 96-well fluorescence microplate reader (SpectraMax, Gemini EM, Molecular Devices, Inc., USA). Rutin was used as the positive control and antiglycation activity (% inhibition) was calculated using the following equation followed by the calculation of IC_{50} value:

$$\text{Inhibition} (\%) = \frac{[F_c - F_b] - [F_s - F_{sb}]}{[F_c - F_b]} \times 100, \quad (5)$$

where F_c is the fluorescence of the control, F_b is the fluorescence of BSA, F_s is the fluorescence of the sample, and F_{sb} is the fluorescence of the sample blank.

All the above *in vitro* bioassay procedures were validated at Herbal Technology Section, Industrial Technology Institute, Sri Lanka (ISO: 9005 certified Laboratory).

2.9. Gas Chromatography-Mass Spectrometry (GC-MS) Analysis.

The extracted essential oil from the leaves was subjected to GC-MS analysis to identify volatile compounds. The analysis was carried out by using TRACE 1300 coupled to ISQ QD mass spectrophotometer instrument (Thermo Fisher Scientific, Milan, Italy). The sample was injected into Thermo-scientific TG-WAX capillary column (30 m × 0.25 mm × 0.25 μm) fused with silica having polyethylene glycol as the stationary phase with helium as the carrier gas (1 mL/min). The temperature of the injector was maintained at 250°C. The GC oven temperature was initially programmed at a temperature of 60°C and was ramped up to 220°C at the rate of 5°C/min. GC-MS interface temperature was maintained at 250°C. The mass detector was operated in EI mode in a scan mass range of m/z 40–450. The identification of compounds was ascertained by comparing the mass spectral values with the known compounds in NIST 11, USA mass spectral database.

2.10. Preparation of Plant Extracts for Mineral Content Determination.

Approximately 0.5 g of homogenized sample was weighed into easy prep high-pressure microwave vessel, and 10.0 mL of 65% nitric acid was added. The easy prep microwave digestion program was followed to digest the samples by using a microwave digester (CEM MARS 5, USA). The digested sample was quantitatively transferred and filtered using No. 542 Whatman filter paper followed by washing with deionized water and volume up to 25 mL. The prepared solution was used to analyze mineral content by ICP-MS (Agilent 7900, USA).

2.11. Statistical Analysis.

Statistical analysis was performed using Graph Pad Prism (version 7). All experimental data was analyzed by one-way analysis of variance (ANOVA). ANOVA's Turkey multiple comparison test was used to compare the mean values. Pearson's correlation coefficient was used for the correlation analysis, and in all cases, p values less than 0.05 ($p < 0.05$) were considered statistically significant. The quantitative results of phytochemicals, antioxidant potentials, and enzyme inhibition values were expressed as mean ± standard deviation (SD).

3. Results

S. caryophyllatum, fruits, and leaves were extracted according to the method described above and fractionated into nonpolar and polar solvents with increasing polarity, hexane, and ethyl acetate, respectively. This solvent–solvent partitioning procedure was allowed to generate hexane (Hex) fraction, ethyl acetate (EA) fraction, and aqueous (AQ) fraction which was labelled and stored in −20°C prior to analysis. The yield was estimated to the dry weight, which ranged from 0.6 mg to 31.2 g, where the highest yield was recorded in crude (CR) extract of fruits (31.2 g) and the lowest was recorded in Hex fraction of leaves (0.6 mg). The weights of the CR extracts, Hex, EA, and AQ fractions are given in Table 1, and the yield was calculated as a percentage.

All the crude extracts and fractions were subjected to further analysis except the hexane fraction of leaves of *Syzygium caryophyllatum* due to the unavailability of adequate sample yield.

3.1. Total Polyphenol Content (TPC) and Total Flavonoid Content (TFC) of Leaves and Fruit Extracts of Syzygium caryophyllatum Plant Extracts.

Total polyphenol content was expressed as milligram gallic acid equivalent per gram of sample (mg GAE/g) and the total flavonoid content as milligram quercetin equivalent per gram of sample (mg QE/g). Total polyphenol values varied from 0.0923 mg GAE/g of sample to 8.18 mg GAE/g of sample and from 1.72 mg GAE/g of sample to 8.92 mg GAE/g of sample for leaves and fruits, respectively. Polyphenol contents of samples were differed significantly ($p < 0.05$). Table 2 presents the TPC and TFC values for crude and fractions of samples. The highest TPC value was recorded in CR extract of fruits followed by CR extract of leaves and AQ fraction of leaves. Flavonoid content of the tested samples varied significantly ($p < 0.05$) among extracts. TFC ranged from 0.001 mg QE/g of sample to 2.03 mg QE/g of sample, and the highest TFC value was reported in CR extract of fruits with value as 2.02 ± 0.19 mg QE/g of the sample followed by Hex fraction and EA fraction of fruits with values 0.80 ± 0.05 mg QE/g of sample and 0.37 ± 0.01 mg QE/g of sample, respectively.

3.2. In Vitro Antioxidant Properties of Different Extracts of Syzygium caryophyllatum.

The antioxidant properties of crudes and fractions of leaves and fruits of *Syzygium caryophyllatum* were determined using DPPH, ABTS, ORAC, FRAP, and iron chelation assay methods. The results

TABLE 1: The yield of *Syzygium caryophyllatum* plant extracts.

Scientific name	Part of plant	Extract	Weight of concentrated extract (g)	Yield %
Syzygium caryophyllatum	Leaves	CR	17.500	7.0
		Hex	<0.001	<0.1
		EA	0.114	0.1
		AQ	15.984	7.1
	Fruits	CR	31.200	62.0
		Hex	1.950	2.6
		EA	1.531	2.0
		AQ	10.165	13.6

CR = crude extract, Hex = hexane fraction, EA = ethyl acetate fraction, AQ = aqueous fraction.

TABLE 2: Total polyphenol content (TPC) and total flavonoid content (TFC) in different extracts of *Syzygium caryophyllatum*.

Scientific name	Part of plant	Extract	TPC (mg GAE/g of sample)	TFC (mg QE/g of sample)
Syzygium caryophyllatum	Leaves	CR	8.12 ± 0.46^a	0.16 ± 0.01^a
		EA	0.09 ± 0.01^b	<0.01
		AQ	7.12 ± 0.16^c	0.18 ± 0.02^{ab}
	Fruits	CR	8.83 ± 0.62^{ad}	2.02 ± 0.19^c
		Hex	3.42 ± 0.29^e	0.80 ± 0.05^d
		EA	1.73 ± 0.76^f	0.37 ± 0.01^e
		AQ	2.16 ± 0.12^g	0.10 ± 0.01^{af}

Results expressed as mean ± standard deviation, CR = crude extract, Hex = hexane fraction, EA = ethyl acetate fraction, AQ = aqueous fraction. Mean values within a column superscripted by different letters are significantly different at $p < 0.05$.

obtained are depicted in Table 3 where the significant differences ($p < 0.05$) were observed between CR extracts of leaves and fruits and among different fractions of leaves and fruits.

3.2.1. DPPH Radical Scavenging Activity.
Results revealed that the crude extract and fractions of *S. caryophyllatum* have the ability to scavenge radicals and depicted a dose-response relationship. DPPH radical scavenging activity of different fractions of *S. caryophyllatum* differed significantly ($p < 0.05$). The EA fraction of leaves exhibited the lowest EC_{50} value followed by Hex and EA fraction of fruits with values $91.2 \pm 4.28 \, \mu g/mL$, $100.97 \pm 8.19 \, \mu g/mL$, and $135.53 \pm 9.83 \, \mu g/mL$, respectively. The results obtained from the fractions showed that EA fractions of leaves and Hex fractions of fruits exhibited high antioxidant activities compared to other fractions. It shows that the accumulation of a variety of antioxidant compounds depends on the polarity of the solvent. Therefore, the compounds responsible for the high radical scavenging activity of *S. caryophyllatum* leaves are mainly medium polarity compounds. The dose-response relationships of *S. caryophyllatum* leaves and fruits are given in Figures 3(a) and 3(b).

3.2.2. ABTS$^+$ Radical Scavenging Activity.
The highest radical scavenging activity was reported in Hex fraction of fruits with EC_{50} value $15.01 \pm 0.65 \, \mu g/mL$ followed by AQ fraction of *S. caryophyllatum* leaves and AQ fraction of *S. caryophyllatum* fruits, and the EC_{50} values were 27.03 ± 2.06 and $31.45 \pm 1.43 \, \mu g/mL$, respectively. It was found that fruits and leaves showed a significant difference ($p < 0.05$) among

fractions. The CR extracts and fractions of leaves and fruits showed significant difference and dose-dependent inhibition on ABTS radical scavenging activity (Figures 4(a) and 4(b)).

3.2.3. Ferric Reducing Antioxidant Power (FRAP).
The CR extracts of leaves and fruits differed significantly ($p < 0.05$) in their FRAP values: CR extract of leaves: $48.27 \pm 8.11 \, mg \, TE/g$ of extract and CR extract of fruits: $6.81 \pm 1.17 \, mg \, TE/g$ of extract. The FRAP values of the fractions ranged from $14.81 \, mg \, TE/g$ of the extract to $270.41 \, mg \, TE/g$ of extract. EA fraction of leaves was reported as the highest among the tested fractions in leaves and fruits, where the AQ fraction of fruits exhibited the lowest values. These results suggested that EA fraction of leaves and fruits exhibited the highest ferric reducing property among tested fractions, which explains the important behavior of the polar compounds in its reducing property.

3.2.4. Oxygen Radical Absorbance Capacity (ORAC).
The ORAC values of fractions ranged from $17.23 \, mg \, TE/g$ of the extract to $347.32 \, mg \, TE/g$ of extract. The highest activity was recorded in EA fraction of leaves following the AQ fraction of leaves and the lowest was recorded in AQ fraction in fruits. The CR extract of leaves exhibited a significantly higher ($p < 0.05$) activity compared to the CR extract of fruits with values 221.00 ± 34.96 and $45.98 \pm 2.58 \, mg \, TE/g$ of extract, respectively.

3.2.5. Iron Chelating Activity.
The highest iron chelating ability of CR extract was reported in leaves with values $33.2 \pm 1.68 \, mg \, EDTA/g$ of extract and fruits were reported as $13.73 \pm 0.69 \, mg \, EDTA/g$ of extract. The Hex fraction of

TABLE 3: Antioxidant potentials of leaves and fruits of *Syzygium caryophyllatum*.

Scientific name	Part of plant	Extract	ORAC mg TE/g of extract	FRAP mg TE/g of extract	EC$_{50}$ DPPH μg/mL	EC$_{50}$ ABTS μg/mL	Iron chelation mg EDTA/g of extract
Syzygium caryophyllatum	Leaves	CR	221.00 ± 34.96[a]	48.27 ± 8.11[a]	500.20 ± 44.33[a]	107.93 ± 15.07[a]	33.2 ± 1.68[a]
		EA	344.31 ± 3.37[b]	262.26 ± 43.93[b]	91.20 ± 4.28[b]	40.61 ± 2.76[b]	36.01 ± 6.98[a]
		AQ	320.97 ± 20.62[bc]	73.42 ± 12.58[c]	251.05 ± 17.52[c]	27.04 ± 2.06[c]	56.17 ± 7.98[b]
	Fruit	CR	45.98 ± 2.58[d]	6.81 ± 1.17[d]	873.72 ± 12.52[d]	128.08 ± 6.12[d]	13.73 ± 0.69[c]
		Hex	32.77 ± 1.41[e]	53.91 ± 12.30[a]	100.97 ± 8.19[e]	15.01 ± 0.65[e]	74.82 ± 2.66[d]
		EA	118.65 ± 7.60[f]	63.07 ± 10.17[e]	135.53 ± 9.83[f]	89.54 ± 3.88[f]	8.28 ± 0.40[e]
		AQ	20.93 ± 4.49[g]	15.45 ± 0.68[f]	946.42 ± 65.04[g]	31.45 ± 1.45[g]	—

Results are expressed as mean ± standard deviation, $n = 3$. Mean values within a column superscripted by different letters are significantly different at $p < 0.05$. CR = crude, Hex = hexane, EA = ethyl acetate, AQ = aqueous. ORAC: oxygen radical absorbance capacity; FRAP: ferric reducing antioxidant power; ABTS: ABTS radical scavenging activity; DPPH: DPPH radical scavenging activity.

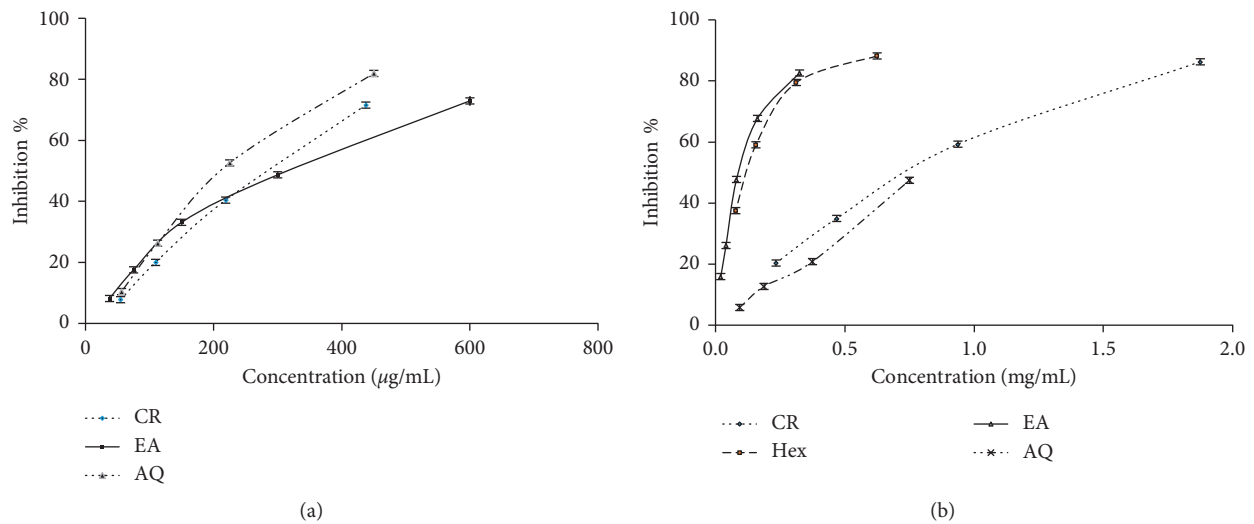
(a)

(b)

FIGURE 3: Dose-response curves for DPPH radical scavenging activity of *Syzygium caryophyllatum*: (a) leaves and (b) fruits (CR = crude, Hex = hexane, EA = ethyl acetate, AQ = aqueous).
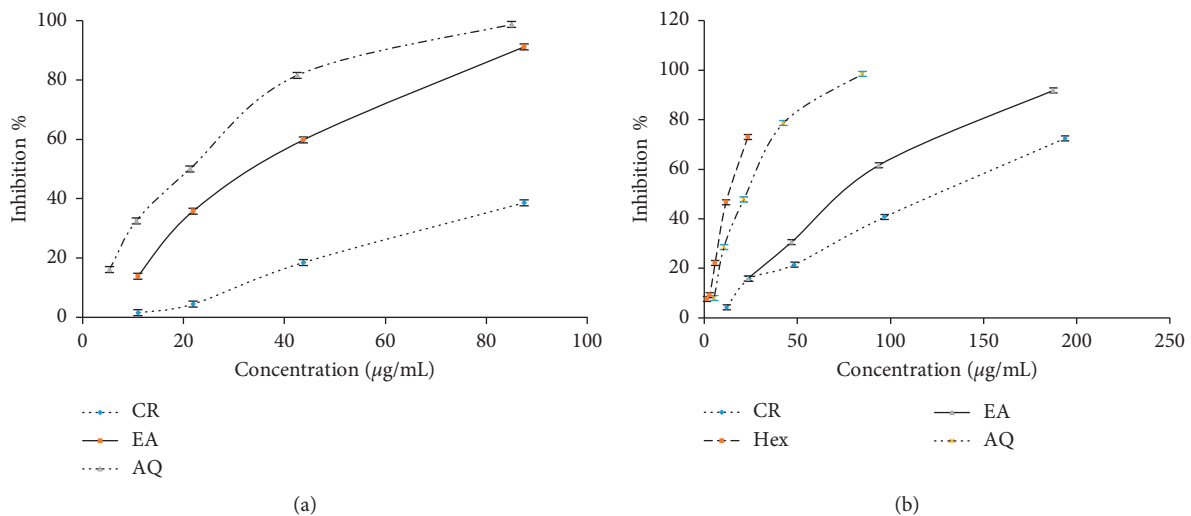

(a)

(b)

FIGURE 4: Dose-response curves for ABTS + radical scavenging activity of *Syzygium caryophyllatum*: (a) leaves and (b) fruits (CR = crude, Hex = hexane, EA = ethyl acetate, AQ = aqueous).

fruits exhibited the highest iron-chelating ability among the tested fractions with value 74.82 ± 2.66 mg EDTA/g of extract, and the lowest was reported in EA fraction of fruits with value 8.28 ± 0.40 mg EDTA/g of extract, respectively. The AQ fraction of *Syzygium caryophyllatum* fruits did not show a significant chelating activity where the highest concentration (2.15 mg/mL) exhibited 16.05% inhibition.

3.3. Correlation Analysis between Polyphenol Content and DPPH Radical Scavenging Activity of Syzygium caryophyllatum Fruits.

The correlation coefficient between TPC content and DPPH of *Syzygium caryophyllatum* fruits exhibited a significant ($p < 0.05$) positive correlation with Pearson r value 0.9921 (Figure 5).

3.4. The α-Amylase Inhibitory Activity.

The α-amylase inhibition potentials of CR extract, Hex, EA, and AQ fraction of leaves and fruits were analyzed. Fruits exhibited significant inhibition of α-amylase activities where the leaves did not exhibit significant inhibitory activities. The Hex fraction of *S. caryophyllatum* fruits was reported to have the highest inhibitory activity with IC$_{50}$ value 47.20 ± 0.3 μg/mL followed by CR extract, EA fraction, and AQ fraction with IC$_{50}$ values 218.26 ± 5.38 μg/mL, 618.85 ± 18.55 μg/mL, and 1014.55 ± 85.55 μg/mL, respectively. Interestingly, the Hex fraction of fruits demonstrated potent α-amylase inhibition activity (IC$_{50}$; 47.20 ± 0.3 μg/mL) compared to the standard drug acarbose (IC$_{50}$; 87.96 ± 1.43 μg/mL). The percentage of α-amylase inhibitions of crudes and fractions was plotted against concentration (Figure 6) where it showed a dose-dependent increase in percentage activity of CR extract and three types of fractions of fruits.

3.4.1. The α-Amylase Inhibitory Activity of Isolated Fractions of Hexane Fraction of Syzygium caryophyllatum Fruits

(1) Hexane and Ethyl Acetate Solvents on Isolation Procedure. The inhibition potential of compound mixtures of EA fraction was evaluated for α-amylase inhibitory activity. The highest tested concentration was 200 μg/mL followed by 100 μg/mL, 50 μg/mL, and 25 μg/mL. The similar inhibition potentials were observed for the first three concentrations, and the % inhibition values were $57.63 \pm 0.18\%$, $55.99 \pm 1.60\%$, and $57.30 \pm 0.18\%$, respectively, where the inhibition potential of 25 μg/mL was observed as a rapid drop to the inhibition $12.78 \pm 0.45\%$. Further inhibition potentials were evaluated between 50 μg/mL and 25 μg/mL (Table 4). The α-amylase inhibitory activity of the tested fraction showed a poor linear response ($R^2 = 0.6384$); hence, IC$_{50}$ was not calculated.

(2) Dichloromethane and Ethyl Acetate Solvents on Isolation Procedure. The α-amylase inhibitory activity of different combined fractions was analyzed (C$_1$, C$_2$, and C$_3$). The inhibitory activities of C$_1$ and C$_2$ fractions did not exhibit significant inhibitory activities where the fraction C$_3$ showed significant ($p < 0.05$) inhibitory activity for the
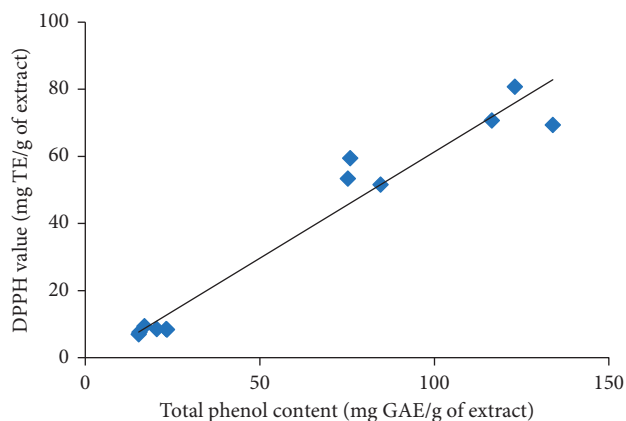

FIGURE 5: Correlation of *Syzygium caryophyllatum* fruits TPC versus DPPH values ($p < 0.05$).

screened concentrations. The fraction C$_3$ was dose-dependent and IC$_{50}$ value was 2.27 ± 1.81 μg/mL.

The summary of α-amylase inhibitory activity of hexane fraction and its chromatographic fraction is given in Table 5.

3.5. Antiglycation Activity.

The antiglycation activity of crude extracts of leaves and fruits was screened for three concentrations 200, 100, and 50 μg/mL (Table 6). The CR extract of leaves exhibited the highest inhibitory activity ($93.61 \pm 8.53\%$ at a concentration of 200 μg/mL) followed by CR extract of *S. caryophyllatum* fruits ($47.97 \pm 2.63\%$). The standard drug rutin exhibited antiglycation activity with IC$_{50}$ value as 34.23 ± 3.18 μg/mL. The IC$_{50}$ value of CR extract of leaves was 57.83 ± 7.91 μg/mL. However, for fruits, similar inhibitions were observed for different doses; hence, IC$_{50}$ value could not be calculated.

3.6. Chemical Compositions of Syzygium caryophyllatum Leaf Essential Oil.

Syzygium caryophyllatum leaves yielded essential oil upon hydrodistillation. GC-MS analysis identified 58 compounds from the essential oil and the retention time and area % of the identified major peaks are listed in Table 7. The major compounds identified in the leaves were phytol with a 24.66% peak area (retention time: 34.44), α-cadinol with a 3.87% peak area (retention time: 27.81), α-guaiene with a 3.84% peak area (retention time: 26.29), cyclosiolongifolene, 9,10-dehydro with a 3.82% peak area (retention time: 28.26), humulene with a 3.36% peak area (retention time: 16.45), and caryophyllene with a 3.21% peak area (retention time: 14.79), respectively. The GC-MS chromatogram of *Syzygium caryophyllatum* leaf oil is presented in Figure 7.

3.7. Mineral Compositions.

Functionally important micro-minerals such as selenium (Se), iron (Fe), strontium (Sr), manganese (Mn), cobalt (Co), copper (Cu), and the toxic heavy metals such as arsenic (As), cadmium (Cd), chromium (Cr), and lead (Pb) were evaluated (Table 8). The ICP-MS
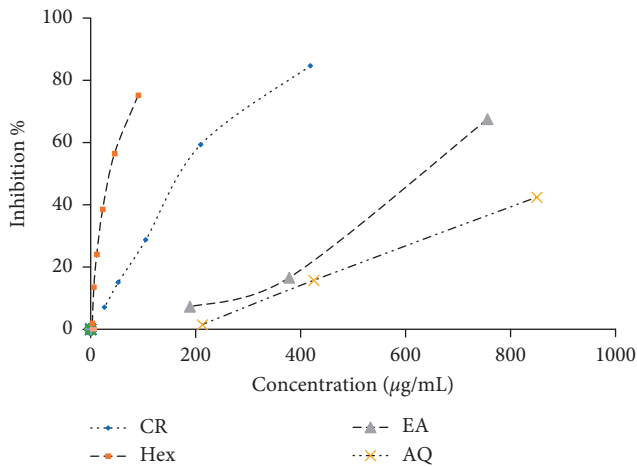
FIGURE 6: Dose-response relationship of crude and fractions of *Syzygium caryophyllatum* fruits for alpha-amylase inhibitory activity (CR = crude, Hex = hexane, EA = ethyl acetate, AQ = aqueous).

TABLE 4: The α-amylase inhibitory activity of isolated compound mixtures of Hex fraction of *Syzygium caryophyllatum* fruits (hexane and ethyl acetate solvents on isolation procedure).

Assay concentration μg/mL	Inhibition %
200	57.63 ± 0.18^a
100	55.99 ± 1.60^a
50	57.30 ± 0.18^a
45	23.39 ± 0.21^b
40	22.45 ± 0.79^b
35	21.43 ± 0.19^b
30	14.33 ± 0.83^c
25	12.78 ± 0.45^c

Results are expressed as mean $\pm$ standard deviation, $n = 3^*$. Mean values within a column superscripted by different letters are significantly different at $p < 0.05$.

TABLE 5: The α-amylase inhibitory activity of hexane fraction and its chromatographic fraction of *Syzygium caryophyllatum* fruits.

Sample	IC$_{50}$ (μg/mL)
Hex fraction	$47.20^a \pm 0.30$
Hex : EA, (0 : 100)	NLR
C$_3$, DCM : EA (95 : 5)	$2.27^b \pm 1.81$
Standard drug acarbose	$87.96^c \pm 1.43$

Results are expressed as mean $\pm$ standard deviation, $n = 3^*$. NLR = no linear response. Mean values within a column superscripted by different letters are significantly different at $p < 0.05$. Hex = hexane, EA = ethyl acetate, DCM = dichloromethane, C$_3$ = combined fraction 3.

data ranged from 0.09 to 4537.0 mg/kg of sample. Sodium (Na) was found to be the highest (leaves: 4357.68 mg/kg of the sample) while Se was found to be the lowest (fruits: 0.09 mg/kg of the sample). The leaves were found to have the highest concentration of the tested minerals compared to the fruits. The second richest macroelement was found to be K (leaves: 3559.25 mg/kg and fruits: 2944.28 mg/kg) followed by Mg (leaves: 2580.40 mg/kg) and Ca (leaves: 1843.52 mg/kg). The maximum amount of Al, Mn, Fe, and Zn was found

to be in leaves with values 524.45 mg/kg, 298.82 mg/kg, 221.98 mg/kg, and 21.60 mg/kg, respectively. Among the tested microelements, Sr was found to be the richest with a value of 32.889 mg/kg in leaves which is significantly ($p < 0.05$) different from fruits (2.70 mg/kg). The Cu and Cr were found in similar small concentrations in leaves (Cu: 4.91 mg/kg and Cr: 4.03 mg/kg) and fruits (Cu: 5.23 mg/kg and Cr: 4.65 mg/kg). The maximum concentration of Se was determined to be 0.85 mg/kg in leaves and the fruits exhibited the lowest concentration with a value of 0.09 mg/kg. The investigation of the level of Co revealed that the maximum concentration of the element exists as 0.128 mg/kg in leaves while in the fruits it was not detected at the detection limit of 0.05 mg/kg.

The analysis of toxic heavy metals revealed the presence of a maximum concentration of Pb in leaves (1.02 mg/kg) and the lowest in fruits (0.15 mg/kg). Besides, the concentrations of toxic heavy metals such as Cd and As were not detected in leaves and fruits (limit of detection: 0.05 mg/kg).

4. Discussion

Diabetes mellitus (DM) is a complex metabolic disorder characterized by hyperglycemia which is mainly associated with malfunctions and abnormalities in carbohydrate, protein, and fat metabolism. Digestion and absorption of carbohydrates to the blood stream also have a significant influence on DM. Further, the increased production of reactive oxygen species (ROS) under DM accelerates the protein glycation process [24]. The production and accumulation of glycated proteins have shown a strong association with complications of DM [25]. Thus, the management of DM is directed toward addressing multiple targets including reduction of postprandial carbohydrate levels in the blood, improvement in the homeostatic and metabolic process of carbohydrates and lipids, an improvement on the efficiency of antioxidant defense, and control of protein glycation [26].

In this regard, WHO recommends functional ingredients and supplements with multiple functional properties including antidiabetic and the antiradical properties in the control of the DM [27].

In this study, functional properties including α-amylase inhibition, protein glycation inhibition, and antioxidant activities of *S. caryophyllatum* fruit and leaf extracts have been investigated along with chemical constituents and mineral analyses. The results revealed the potential of *S. caryophyllatum* as a source of supplement for DM management. To the best of our knowledge, the present study is the first study reported in Sri Lanka on functional activities of *S. caryophyllatum* fruit and leaf extracts. Crude extracts of both fruits and leaves showed significant antioxidant and moderate antiglycation activities. However, only fruit extracts showed α-amylase inhibitory activity. Even though both fruits and leaves CR were tested against α-glucosidase enzyme inhibitory activity, none of them showed a significant inhibitory activity at a maximum dose of 400 μg/mL (data not shown). Solvent–solvent partitioning of both CR was used to separate and valuate the most potent fractions with α-amylase inhibition activity.

TABLE 6: Antiglycation activity of crude extracts of *Syzygium caryophyllatum*.

	% Inhibition			
Crude extract	Concentration (μg/mL)			IC$_{50}$ (μg/mL)
	50	100	200	
Leaves	54.88 ± 3.10[a]	79.87 ± 5.94[a]	93.61 ± 8.50[a]	57.83 ± 7.91
Fruits	41.31 ± 7.89[b]	56.66 ± 8.36[b]	47.97 ± 2.63[b]	—
Standard rutin	IC$_{50}$ = $34.23 \pm 3.18 \mu$g/mL			

Results are expressed as mean $\pm$ standard deviation, $n = 3$*. Mean values within a column superscripted by different letters are significantly different at $p < 0.05$.

TABLE 7: Major compounds detected in *Syzygium caryophyllatum* leaf essential oil.

Peak	Compound	Formula and *mol wt	RT	Area %	SI	RSI
1	Caryophyllene	$C_{15}H_{24}$, 204,	14.79	3.21	954	954
2	Humulene	$C_{15}H_{24}$, 204,	16.45	3.36	907	907
3	α-Cadinol	$C_{15}H_{26}O$, 222,	27.81	3.87	923	928
4	Cyclosiolongifolene, 9,10-dehydro	$C_{17}H_{26}O_2$, 202	28.26	3.82	790	800
5	Phytol	$C_{20}H_{40}O$, 296,	34.44	24.66	927	927

*Mol wt = molecular weight.
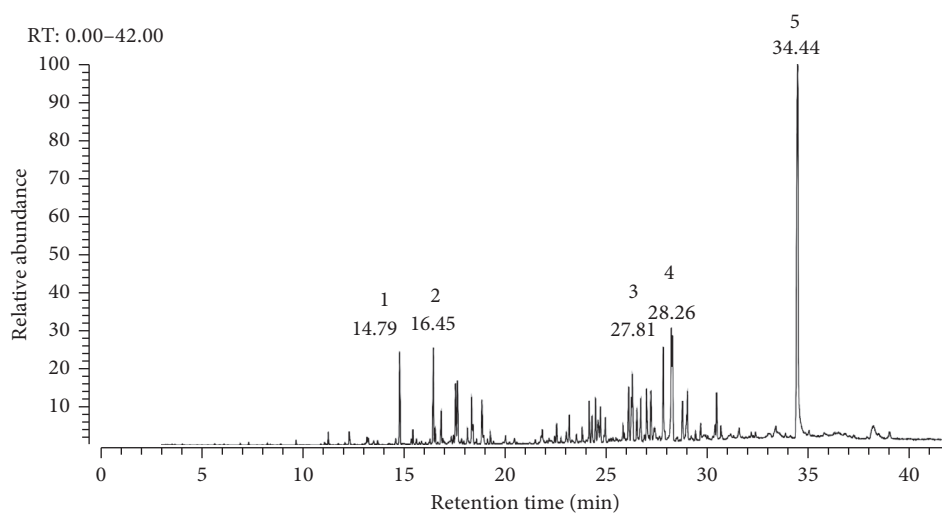
FIGURE 7: GC-MS chromatogram of *Syzygium caryophyllatum* leaf essential oil.

TABLE 8: Mineral compositions of leaves and fruits of *Syzygium caryophyllatum*.

		Mineral elements (mg/kg per sample)														
		K	Fe	Na	Ca	Mg	Mn	Cu	Zn	Cr	Zn	Sr	Se	Pb	As	Cd
Syzygium	Leaves	3559.25	221.98	4357.68	1843.52	2580.39	298.82	4.91	21.60	4.03	21.59	32.89	0.85	1.02	ND	ND
caryophyllatum	Fruits	2944.28	49.55	756.21	149.27	855.55	18.14	5.23	7.75	4.65	7.75	2.70	0.09	0.15	ND	ND
RDA		3.5 g	9–15 mg	1.5 g	1 g	280–350 mg	50–60 μg									

*ND: not detected; limit of detection: 0.05 mg/kg; RDA: recommended daily intake.

Hexane fraction of fruit extract exhibited the highest inhibition activity with IC$_{50}$ value $47.20 \pm 0.37 \mu$g/mL and is significantly higher compared to acarbose (IC$_{50}$: $87.96 \pm 1.43 \mu$g/mL). Therefore, it was further separated by column chromatography. The fraction C_3, which was isolated on elution with DCM : EA, 95 : 5, exhibited a significant ($p < 0.05$) α-amylase inhibitory activity with an IC$_{50}$ value of $2.27 \pm 1.81 \mu$g/mL. The compound or the mixture of compounds responsible for the α-amylase inhibition activity may be in the C_3 compound mixture which is required to be subjected to further isolation and identification. Inhibition may be due to the presence of potential alpha-amylase inhibitors such as alkaloids, tannin, polyphenols, and flavonoids. These inhibitors can also act as starch blockers as they block the hydrolysis of 1,4,-glycosidic linkages of starch and oligosaccharides [28]. Hex fraction of *S. caryophyllatum* fruit

extract which can be easily prepared even at a commercial scale may be a very good source for the formulation of supplements for DM management.

Hyperglycemic conditions in DM promote the formation of AGEs that leads to the complications of DM. *In vivo* studies have revealed the involvement of potent glycation inhibitors in the prevention of diabetic complications [29]. In this regard, studies show that pyridoxamine slows down nephropathy in DM, and aminoguanidine reduces the development of albuminuria in diabetic rats [30]. Further, protocatechualdehyde (PCA) has been shown to improve the development of lens opacity (cataract) with a positive effect on glycemic control. PCA was found to be 80% more effective than aminoguanidine in preventing AGE-related complications of DM [30].

However, there are no available reports on the antiglycation activity of *S. caryophyllatum* leaves and fruits. The results of the present study also demonstrate moderate activity for CR extracts for leaf and weak activity for fruits.

Dietary antioxidants are essential to strengthen the oxidative defense system of the body particularly under hyperglycemic conditions. In this regard, the antioxidant activity of *S. caryophyllatum* fruits and leaves was evaluated using four different methods which are having different modes of action.

Free radical scavenging methods such as DPPH and ABTS were used and EC_{50} values of both assays suggested potent radical scavenging activity of *S. caryophyllatum* fruits and leaf extracts. The DPPH, nitrogen centered stable free radical, has been used to determine the free radical scavenging activity. The reduction of DPPH in methanol leads to discoloration from violet to yellow by either hydrogen or electron donation.

A previous study on DPPH radical scavenging activity of the *S. caryophyllatum* leaves has reported DPPH inhibition activity in methanol extract with 81.97%, followed by EA (78.69%) and Hex fraction (34.34%) at the concentration of $100 \mu g/mL$ [14]. Annadurai et al. [31] have reported DPPH scavenging activity for the EA fraction of *S. caryophyllatum* leaves as 86.14% inhibition at a concentration of $400 \mu g/mL$. Subramanian et al. [14] and the present study show similar results for the EA fraction with a value of 72.92% inhibition at the concentration of $150 \mu g/mL$. A previous study carried out by sequential extraction method for leaves and fruits has reported having IC_{50} value for DPPH scavenging activity in methanol as $34.9 \pm 1.2 \mu g/mL$ and $69.4 \pm 0.7 \mu g/mL$, respectively, which showed high activity compared to the present study [15].

The scavenging activity against cationic radical indicates the capability of crude and fractions to act as electron or hydrogen donors. Previous studies have reported having ABTS radical scavenging activity with IC_{50} values of $13.2 \pm 0.03 \mu g/mL$ for leaves and $120.2 \pm 0.4 \mu g/mL$ for fruit pulp in methanol extract [15]. Though previous studies have used methanolic extracts, in this study, ethanol/water was used to prepare the extract as the main focus was on the formulation of a supplement. In this regard, the Hex fraction of the fruit extract exhibited higher ABTS radical scavenging

activity (EC_{50}: $15.01 \pm 0.65 \mu g/mL$) compared to the results reported in a previous study [15].

The differences observed among these studies are generally accepted, as the samples were from different geographic locations with different degrees of biotic and abiotic stress conditions that are associated with biosynthesis and expression of secondary metabolites [32].

In the FRAP assay, the reduction of the ferric-TPTZ complex to ferrous-TPTZ by accepting electrons from the sample was measured as the total amount of antioxidants. Compounds that exhibit the ferric reducing activity indicate that their ability to act as electron donors reduces the oxidized intermediates of the lipid peroxidation process. In this study, EA fraction of leaves reported the highest value among the tested fractions in leaves and fruits, which reveals the best-reducing property.

The ORAC assay is based on hydrogen atom transfer mechanism (HAT) and the inhibition of oxidation of fluorescein by peroxide radicals generated from 2,2'-azobis (2-amidino-propane) dihydrochloride (AAPH) with an antioxidant action. According to the present study, ORAC assay results implied that there is no correlation with other antioxidant assays. This fact still requires more supporting pieces of evidence as there is no available reported data on ORAC assay for the *S. caryophyllatum* fruit and leaf extracts.

The Fe^{2+} chelation assay is considered as an indirect antioxidant activity measurement which indicates the potential to inhibit Fenton reaction. The Fe^{2+} chelation was estimated quantitatively with ferrozine. The test procedure results in the formation of a red-colored complex with Fe^{2+} that reduces its color in the presence of a chelating agent. This is due to the interruption caused by the formed complex. Extracts and fractions exhibited the metal iron-chelating power, where the Hex fraction of fruits exhibited the highest iron chelation capacity. This is suggestive of the presence of bioactive molecules with chelating abilities in addition to the polyphenolics.

Strong antioxidant and antimicrobial potentials of the leaf oil of *S. caryophyllatum* along with GC-MS analysis have been reported for Indian plants by Soni et al. [33] and Nadarajan et al. [34]. The major compounds revealed by the present study are phytol, caryophyllene, humulene, globulol, and α-cadinol. The composition of leaf volatiles of *S. caryophyllatum* reported in this study relates and corresponds to those reported in the previous study. The previous study has reported 55 compounds in the winter season and 129 compounds in the summer season with promising antibacterial activity [34]. The major identified compound in winter essential oil was α-cadinol, and in summer, the essential oil was caryophyllene oxide where the phytol was the major compound in the present study [34]. Further, few common compounds such as α-cadinol, caryophyllene oxide, globulol, and phytol were also found.

Mineral deficiencies impose a major burden on public health and maintenance of healthy physiology. Therefore, supplementation is the best choice in order to fulfil the daily mineral requirement especially when an individual is suffering from a health complication such as DM. Some dietary minerals including Cr, Mg, Ca, Mn, K, Zn, and Se play a key

role in physiological processes related to DM [35]. Magnesium deficiency is related to the risk of atherosclerosis, hypertension, cardiac arrhythmias, stroke, alterations in lipid metabolism, insulin resistance, metabolic syndrome, type 2 diabetes mellitus, osteoporosis, and depression.

Zinc is an important microelement with definite roles in metabolism and growth and it is also essential and vital for the smooth functioning of over 200 enzymes [36]. Zinc deficiency adversely affects the growth of T and B cells and apoptosis, growth retardation, and cognitive impairment [37]. Further, Zn is involved in the synthesis and secretion of insulin, and it is a structural part of Zn-dependent antioxidant enzymes such as superoxide dismutase [38]. Copper is an essential microelement that acts as a cofactor of many redox enzymes and as catalysts for iron absorption [36].

Chromium is an essential microelement for the biosynthesis of DNA, which regulates cell division and growth [39]. The Cr is also necessary for the regulation of normal glucose metabolism and the deficiency of Cr is related to impaired glucose tolerance [35]. Selenium plays a critical role in antioxidant defense due to its presence in the active center of antioxidative enzymes (glutathione peroxidase (GPX) and thioredoxin reductase (TrxRs)). This essential microelement impairs lipid peroxidation and protects cells against damage to genetic material [40]. A previous study carried out by Subramanian et al. [41] for the leaves of S. caryophyllatum reported having 99.275 ± 0.022 mg/kg, 17.302 ± 0.010 mg/kg, 45.498 ± 0.072 mg/kg, 47.344 ± 0.002 mg/kg, 7.634 ± 0.050 mg/kg, and 0.253 ± 0.003 mg/kg of Fe, Zn, Cu, Mn, Pb, and Cd, respectively [41]. The content of Na and K reported was absent and also Zn, significantly high Cu and low Mn levels and Cd were detected, and a higher amount of Pb was reported compared to the present study [41].

The results of the present study exhibited that the content of the mineral elements differs significantly among the parts of the similar plants. Furthermore, with comparison to the reported data, it reveals that the levels of mineral elements vary from different geographical locations due to the variation in soil types, agricultural and industrial activities, local growing conditions, plant interactions, and weather [8]. Nonetheless, studies have revealed that the metal-tolerant plants (metallophytes) possess the effects for phytoremediation through exposure to heavy metal stress showing varying degrees of therapeutically active constituents [42].

Thus, the risk analysis is required in plants before any preparation as the wild fruity plants are favored in controlling the growth and processing of the environment.

5. Conclusions

The present study concludes that the leaves and the fruits of Syzygium caryophyllatum plant possess antioxidant, antiamylase, and antiglycation activities and are a rich pool of essential mineral elements such as Zn, Mn, Cu, and Sr, which together may act to reduce the risk of associated diabetic complications and other noncommunicable diseases. Studies on isolation and characterization of the bioactive

compound in leaves and fruit extracts are important for confirmation of the pharmacological properties of the responsible active compounds. Further, it can be concluded that Syzygium caryophyllatum leaves and fruits are potent natural sources that possess the potential to be developed into a natural supplement to aid the management process of type 2 diabetes mellitus.

Data Availability

The data used to support the findings of this study are available from the corresponding author upon request.

Conflicts of Interest

The authors declare that they have no conflicts of interest.

Acknowledgments

References

[1] World Health Organization, "Diabetes," World Health Organization, Geneva, Switzerland, 2016, http://www.who.int/mediacentre/factsheets/fs312/en/.

[2] El Nahas, A. Meguid, and A. K. Bello, "Chronic kidney disease: the global challenge," The Lancet, vol. 365, no. 9456, pp. 331–340, 2005.

[3] H. Kolb and S. Martin, "Environmental/lifestyle factors in the pathogenesis and prevention of type 2 diabetes," BMC Medicine, vol. 15, no. 1, p. 131, 2017.

[4] A. Phaniendra, D. B. Jestadi, and L. Periyasamy, "Free radicals: properties, sources, targets, and their implication in various diseases," Indian Journal of Clinical Biochemistry, vol. 30, no. 1, pp. 11–26, 2015.

[5] M. Odjakova, E. Popova, M. Al Sharif, and R. Mironova, "Plant-derived agents with anti-glycation activity," Glycosylation, pp. 223–256, IntechOpen, London, UK, 2012.

[6] R. S. Tupe, N. M. Sankhe, S. A. Shaikh et al., "Aqueous extract of some indigenous medicinal plants inhibits glycation at multiple stages and protects erythrocytes from oxidative damage-an in vitro study," Journal of Food Science and Technology, vol. 52, no. 4, pp. 1911–1923, 2015.

[7] H. P. Gunawardena, R. Silva, R. Sivakanesan, P. Ranasinghe, and P. Katulanda, "Poor glycaemic control is associated with increased lipid peroxidation and glutathione peroxidase activity in type 2 diabetes patients," Oxidative Medicine and Cellular Longevity, vol. 2019, Article ID 9471697, 10 pages, 2019.

[8] M. Sium, P. Kareru, J. Keriko, B. Girmay, G. Medhanie, and S. Debretsion, "Profile of trace elements in selected medicinal plants used for the treatment of diabetes in Eritrea," The Scientific World Journal, vol. 2016, Article ID 2752836, 7 pages, 2016.

[9] I. N. Leroux, A. P. S. d. S. Ferreira, F. P. Paniz et al., "Brazilian preschool children attending day care centers show an inadequate micronutrient intake through 24-h duplicate diet," Journal of Trace Elements in Medicine and Biology, vol. 54, pp. 175–182, 2019.

[10] E. Jarald, S. B. Joshi, and D. Jain, "Diabetes and herbal medicines," *Iranian Journal of Pharmacology & Therapeutics*, vol. 7, pp. 97–106, 2008.

[11] E. Idm'hand, F. Msanda, and K. Cherifi, "Ethno-pharmacological review of medicinal plants used to manage diabetes in Morocco," *Clinical Phytoscience*, vol. 6, pp. 1–32, 2020.

[12] A. Singh and T. Marar, "Inhibitory effect of extracts of syzygiumcumini and psidiumguajava on glycosidases," *Journal of Cell and Tissue Research*, vol. 11, no. 1, p. 2535, 2011.

[13] K. Kala, V. T. Antony, M. S. Sheemole, and A. Saji, "Analysis of bioactive compounds present in syzygiumcaryophyllatum (L.) alston fruit," *International Journal of Pharmaceutical Sciences Review and Research*, vol. 36, pp. 239–243, 2016.

[14] R. Subramanian, P. Subbramaniyan, and V. Raj, "Phyto-chemical screening, total phenolic contents and antioxidant activity ofSyzygium caryophyllatumandSyzygium densiflorum," *Journal of Biologically Active Products from Nature*, vol. 4, no. 3, pp. 224–235, 2014.

[15] N. Stalin and S. P. Sudhakar, "Screening of phytochemical and pharmacological activities of Syzygiumcaryophyllatum (L.) Alston," *Clinical Phytoscience*, vol. 4, no. 1, pp. 1–3, 2018.

[16] K. V. Peter, "Underutilized and underexploited crops," vol. 3, p. 177, New India Publishing Agency, New Delhi, India, 2008.

[17] V. L. Singleton, R. Orthofer, and R. M. Lamuela-Raventós, "[14] Analysis of total phenols and other oxidation substrates and antioxidants by means of folin-ciocalteu reagent," *Oxidants and Antioxidants Part A*, vol. 299, pp. 152–178, 1999.

[18] P. Ranasinghe, G. Premakumara, C. Wijayarathna, and W. Ratnasooriya, "Antioxidant activity of," *Tropical Agricultural Research*, vol. 23, no. 2, pp. 117–125, 2012.

[19] R. Re, N. Pellegrini, A. Proteggente, A. Pannala, M. Yang, and C. Rice-Evans, "Antioxidant activity applying an improved ABTS radical cationdecolourization assay," *Free Radical Biology and Medicine*, vol. 26, no. 9-10, pp. 1231–1237, 1999.

[20] B. Ou, M. Hampsch-Woodill, and R. L. Prior, "Development and validation of an improved oxygen radical absorbance capacity assay using fluorescein as the fluorescent probe," *Journal of Agricultural and Food Chemistry*, vol. 49, no. 10, pp. 4619–4626, 2001.

[21] P. Carter, "Spectrophotometric determination of serum iron at the submicrogram level with a new reagent (ferrozine)," *Analytical Biochemistry*, vol. 40, no. 2, pp. 450–458, 1971.

[22] G. A. S. Premakumara, W. K. S. M. Abeysekera, W. D. Ratnasooriya, N. V. Chandrasekharan, and A. P. Bentota, "Antioxidant, anti-amylase and anti-glycation potential of brans of some Sri Lankan traditional and improved rice (Oryzasativa L.) varieties," *Journal of Cereal Science*, vol. 58, no. 3, pp. 451–456, 2013.

[23] N. Matsuura, T. Aradate, C. Sasaki et al., "Screening system for the Maillard reaction inhibitor from natural product extracts," *Journal of Health Science*, vol. 48, no. 6, pp. 520–526, 2002.

[24] A. B. Oyenihi, N. L. Brooks, O. O. Oguntibeju, and G. Aboua, "Antioxidant-antidiabetic agents and human health," *OluwafemiOguntibeju*, IntechOpen, London, UK, 2014, https://www.intechopen.com/books/antioxidant-antidiabetic-agents-and-human-health/antioxidant-rich-natural-products-and-diabetes-mellitus.

[25] V. P. Singh, A. Bali, N. Singh, and A. S. Jaggi, "Advanced glycation end products and diabetic complications," *The Korean Journal of Physiology & Pharmacology*, vol. 18, no. 1, pp. 1–14, 2014.

[26] M. I. Kazeem, J. O. Adamson, and I. A. Ogunwande, "Modes of inhibition of α-amylase and α-glucosidase by aqueous extract of MorindalucidaBenth leaf," *BioMed Research International*, vol. 2013, Article ID 527570, 6 pages, 2013.

[27] C. S. Rabeque and S. Padmavathy, "Hypoglycaemic effect of *Syzygium caryophyllatum* (L.) alston on alloxan induced diabetic albino mice," *Asian Journal of Pharmaceutical and Clinical Research*, vol. 6, no. 4, pp. 203–205, 2013.

[28] G. Keerthana, M. K. Kalaivani, and A. Sumathy, "In-vitro alpha amylase inhibitory and anti-oxidant activities of ethanolic leaf extract of Croton bonplandianum," *Asian Journal of Pharmaceutical and Clinical Research*, vol. 6, no. 4, pp. 32–36, 2013.

[29] J. S. Ramkissoon, F. M. Mahomoodally, A. Ahmed, and H. A. Subratty, "Natural inhibitors of advanced glycation end-products," *Nutrition & Food Science*, vol. 42, no. 6, pp. 397–404, 2012.

[30] G. Abbas, A. S. Al-Harrasi, H. Hussain, J. Hussain, R. Rashid, and M. I. Choudhary, "Anti-glycation therapy: discovery of promising anti-glycation agents for the management of diabetic complications," *Pharmaceutical Biology*, vol. 54, no. 2, pp. 198–206, 2016.

[31] G. Annadurai, B. R. P. Masilla, S. Jothiramshekar, E. Palanisami, S. Puthiyapurayil, and A. K. Parida, "Antimicrobial, antioxidant, anticancer activities of *Syzygiumcaryophyllatum* (L.) Alston," *International Journal of Green Pharmacy (IJGP)*, vol. 6, no. 4, pp. 285–288, 2012.

[32] C. M. Andre, M. Oufir, L. Hoffmann et al., "Influence of environment and genotype on polyphenol compounds and in vitro antioxidant capacity of native Andean potatoes (Solanumtuberosum L.)," *Journal of Food Composition and Analysis*, vol. 22, no. 6, pp. 517–524, 2009.

[33] A. M. R. I. T. A. Soni and P. R. A. V. E. E. N. Dahiya, "Phytochemical analysis, antioxidant and antimicrobial activity of Syzygiumcaryophyllatum essential oil," *Asian Journal of Pharmaceutical and Clinical Research*, vol. 7, no. 2, pp. 202–205, 2014.

[34] S. Nadarajan and S. S. Pujari, "Leaf essential oil composition and biochemical activity of an endangered medicinal tree syzygiumcaryophyllatum (L.) alston, (wild black plum)," *Journal of Essential Oil Bearing Plants*, vol. 17, no. 3, pp. 371–379, 2014.

[35] M. N. Piero, J. M. Njagi, C. M. Kibiti, J. J. N. Ngeranwa, E. N. M. Njagi, and P. M. Miriti, "The role of vitamins and mineral elements in management of type 2 diabetes mellitus: a review," *South Asian Journal of Biological Science*, vol. 2, pp. 107–115, 2012.

[36] N. K. Singh, C. B. Devi, T. S. Singh, and N. R. Singh, "Trace elements of some selected medicinal plants of Manipur," *Indian Journal of Natural Products and Resources*, vol. 1, no. 2, pp. 227–231, 2010.

[37] A. P. Prasad, "Impact of the discovery of human zinc deficiency on health," *Journal of the American College of Nutrition*, vol. 28, no. 3, pp. 257–265, 2009.

[38] R. Jayawardena, P. Ranasinghe, P. Galappatthy, R. L. D. K. Malkanthi, G. R. Constantine, and P. Katulanda, "Effects of zinc supplementation on diabetes mellitus: a systematic review and meta-analysis," *Diabetology & Metabolic Syndrome*, vol. 4, no. 1, p. 13, 2012.

[39] K. O. Soetan, C. O. Olaiya, and O. E. Oyewole, "The importance of mineral elements for humans, domestic animals and plants-A review," *African Journal of Food Science*, vol. 4, no. 5, pp. 200–222, 2010.

[40] J. Pieczy, P. Sylwia, K. Orywal, B. Mroczko, and H. Grajeta, "Is maternal dietary selenium intake related to antioxidant status and the occurrence of pregnancy complications?" *Journal of Trace Elements in Medicine and Biology*, vol. 54, pp. 110–117, 2019.

[41] R. Subramanian, P. Subbramaniyan, and V. Raj, "Determination of some minerals and trace elements in two tropical medicinal plants," *Asian Pacific Journal of Tropical Biomedicine*, vol. 2, no. 2, pp. 555–558, 2012.

[42] R. A. Street, "Heavy metals in medicinal plant products—an African perspective," *South African Journal of Botany*, vol. 82, pp. 67–74, 2012.

Research Article

Aqueous Root Bark Extract of *Daniellia oliveri* (Hutch. & Dalz.) (Fabaceae) Protects Neurons against Diazepam-Induced Amnesia in Mice

**Galba Jean Beppe, Lea Blondelle Kenko Djoumessie, Eglantine Keugong Wado [ID],
Hervé Hervé Ngatanko Abaïssou, Balbine Kamleu Nkwingwa, Jorelle Linda Damo Kamda,
Roland Rebe Nhouma, and Harquin Simplice Foyet [ID]**

Department of Biological Sciences, Faculty of Science, University of Maroua, P.O. Box 814, Maroua, Cameroon

Correspondence should be addressed to Harquin Simplice Foyet; fharquins@gmail.com

Daniellia oliveri (DO) is a traditional medicinal plant used for the treatment of diseases such as inflammation, schizophrenia, and epilepsy in Nigeria, Kenya, Congo, and Cameroon. This study was carried out to evaluate the potential neuroprotection effect of the aqueous root bark extract of *Daniellia oliveri* against diazepam-induced amnesia in mice. Thirty-six adult male mice were distributed into six groups: the three test groups received *Daniellia oliveri* root bark extract (100, 200, and 300 mg/kg), the normal control group received distilled water (10 ml/kg), a positive control group received piracetam (150 mg/kg), and the negative control received diazepam (2.5 mg/kg). Learning and memory were evaluated using the radial arm maze and the T-maze. Biomarkers of oxidative stress were also quantified in mice brains. Statistical analyses were performed using two-way ANOVA followed by Tukey's post hoc test. *Daniellia oliveri* root bark aqueous extract decreased the number of working memory errors and number of reference memory errors in amnesic mice evaluated in the radial arm maze. Also, an increase in glutathione activity and a decrease in malondialdehyde levels were noted in the hippocampi homogenate of the extract-treated mice as compared to the diazepam-demented but untreated group. Moreover, pretreatment with *Daniellia oliveri* aqueous root bark extract reversed the decrease in hippocampal cell density observed in the nontreated diazepam group. Taken together, these results suggest that the aqueous extract of DO leaves possesses antioxidant potential and might provide an opportunity for the management of neurological abnormalities in amnesic conditions.

1. Introduction

Amnesia is a neuropsychological pathology which results in the partial or total loss of memory. The pathology occurs when complex neurobiological processes, involved in learning and short- or long-term storage of information, are disrupted [1]. It is the main cause of dementia syndrome, which accounts for at least 70% of the cases [2]. The distribution of the new cases has reached 4.9 million (49%) in Asia, 2.5 million (25%) in Europe, 1.7 million (18%) in America, and 0.8 million (8%) in Africa [2]. Cameroon is not immune to this pathology with a prevalence of 2.85% in the

city of Yaoundé [3]. Causes of this pathology are poorly known until now; however, age, environmental, and genetic factors are considered as risk factors to the occurrence of this disease.

Diazepam (DZP) is a benzodiazepine (allosteric modulators GABA receptor) which is well tolerated in organism and employed in the treatment of memory disorders, psychomotor disorders, sedation, dependence, and anxiety rebound [4]. Acute administration of DZP causes anterograde amnesia [5], while intravenous administration significantly impairs free recall based on the dose used [6]. Pretreatment with diazepam (2.0–16.0 mg/kg *i.p.*) or

scopolamine (3.0 mg/kg *i.p.*) causes an alteration of the anterograde memory, in a dose-dependent manner [4, 7]. According to Maria et al. [8], intraperitoneal injection (*i.p.*) of 2.5 mg/kg DZP induces amnesia in rodents by hyperpolarization of neurons, decreased excitability, and increased lipid peroxidation [9, 10]. The current treatment options, such as surgery and synthetic drugs, are limited in their ability to improve neuronal function because they fail to repair damaged neurons or improve neural regeneration [11]. Due to the adverse side effects of standard antiamnesic drugs line, rivastigmine, donepezil, and galantamine, alternative therapies consisting of plant-derived medications, are increasingly being used to relieve neurodegenerative disorders [12].

Daniellia oliveri is a plant which grows in the Amazonia, certain part of America, and some Africans countries including Cameroon. Roots of this plant are used in traditional medicine to treat anxiety and schizophrenia [13]. Leaves decoction and stem bark infusion have been used as diuretic and aphrodisiac and applied as skin lotion. Dry leaves powder is also administered to treat yellow fever, back ache, and headache and for wound healing. The dried root and stem bark have been used in Ivory Coast as chewing stick and the water extract of the stem bark showed antibacterial activity [14]. Hexane and methanolic extracts of the bark showed analgesic and anti-inflammatory activities, while the methanolic extract of the stem bark showed smooth muscle relaxant activity [15]. Gaston and Daget [16] reported the presence of glycosides, flavonoids, saponins, rutin, quercitrin, and quercimeritrin in leaves. Saponins and flavonoids are recognized as anti-inflammatory and antioxidant compounds which could impart many health benefits and thereby reduce the risk of many chronic illnesses like degenerative disorder [17, 18]. This study was carried out to investigate the neuroprotective effects of *D. oliveri* root bark aqueous extract, in the diazepam-induced amnesia (DZP) mouse model.

2. Materials and Methods

2.1. Chemicals.
Diazepam, acetylthiocholine iodide, 5,5-dithiobis (2-nitro-benzoic acid) (DTNB), 2-thiobabituric acid (TBA), and piracetam were purchased from Sigma-Aldrich, USA. All drugs and extracts were freshly prepared in saline on the day of experiments.

2.2. Plant Material and Plant Extract.
Daniellia oliveri root bark was collected in Lara (Far North Region, Cameroon) in the month of December 2017 and authentificated at the National Herbarium, Yaoundé, where a voucher specimen was deposited under the reference number 14890/SRF/Cam-YA. After collection, *Daniellia oliveri* (DO) root bark was shade-dried for 5 days and pulverized into a fine powder. The extraction procedure used was as previously described by Soro et al. [19]. Briefly, 150 g pulverized sample material was introduced in 1 L of distilled water and boiled for 30 min. The filtrate was passed through a Whatman filter paper N° 4 and the solvent was eliminated from the extract

using a temperature controlled oven (50°C for 24 hours). The powder obtained was weighed and the extraction yield was determined (1.85%).

2.3. Experimental Animals.
Adult male Swiss mice aged 3 months (weighing 18–26 g) were obtained from the National Veterinary Laboratory of Garoua, Cameroon. Mice were acclimatized for 14 days, housed in polyacrylic cages (6 animals/cage) under natural dark-light cycle and provided with water and food *ad libitum*. Prior to and after treatment, mice were fasted for 12 and 7 h. Animal treatment and care was in accordance with the guidelines of the Cameroonian Bioethics Committee (Reg N° FWA-IRB00001954) and following NIH-Care and Use of Laboratory Animals Manual (8th Edition). Each animal was tested in only one behavioral test and tests were made to minimize animal suffering.

Mice were randomly divided into 6 groups of 6 animals each and subjected to the following treatment schedule (Figure 1). The normal control group received distilled water (DW) only (10 mL/kg *p.o.*), the negative control group received a single administration of diazepam (2.5 mg/kg, *i.p.* + DW) on day 14, the positive control group received a single dose of piracetam (150 mg/kg, *p.o.*), and different test groups received extract (DZP + 100, 200, and 300 mg/kg *p.o.* of DO) for 14 days. Diazepam was administered to all groups except the normal control 30 minutes after treatment on day 14. Behavioral tests were launched 30 minutes after diazepam administration.

2.4. Behavioral Test

2.4.1. Radial Arm Maze Task.
The radial arm maze used in the present study consisted of eight arms, numbered from 1 to 8 (48 cm × 12 cm), extending radially from a central area (32 cm in diameter). The apparatus was placed 50 cm above the floor. At the end of each arm, there was a food cup that had a single 50 mg food pellet. Before the performance of the maze task, animals were kept on restricted diet designed to keep their body weight at 85% of their free-feeding weight over a week, with water being available *ad libitum*. Before the actual training began, each mouse was simultaneously placed in the radial maze and allowed to explore for 5 min and take food freely. The food was initially available throughout the maze but was gradually restricted to the food cup. The animals were trained for 7 days to run to the end of the arms and consume the bait. The animals were trained for maze task performance by conducting daily training trials for 5 min, during which they do not receive any drug. The training trial continued until all the 4 baits had been consumed or until 5 min had elapsed. Completely trained animals were chosen for the study. Briefly, each animal was placed individually in the center of the maze and subjected to working and reference memory tasks, in which the same four arms (1, 3, 5, and 7) were baited for each daily training trial. The other four arms (2, 4, 6, and 8) were never baited. An arm entry was counted when all four limbs of the mouse were within an arm. Measures were made on the number of working memory errors (entering an arm containing food,
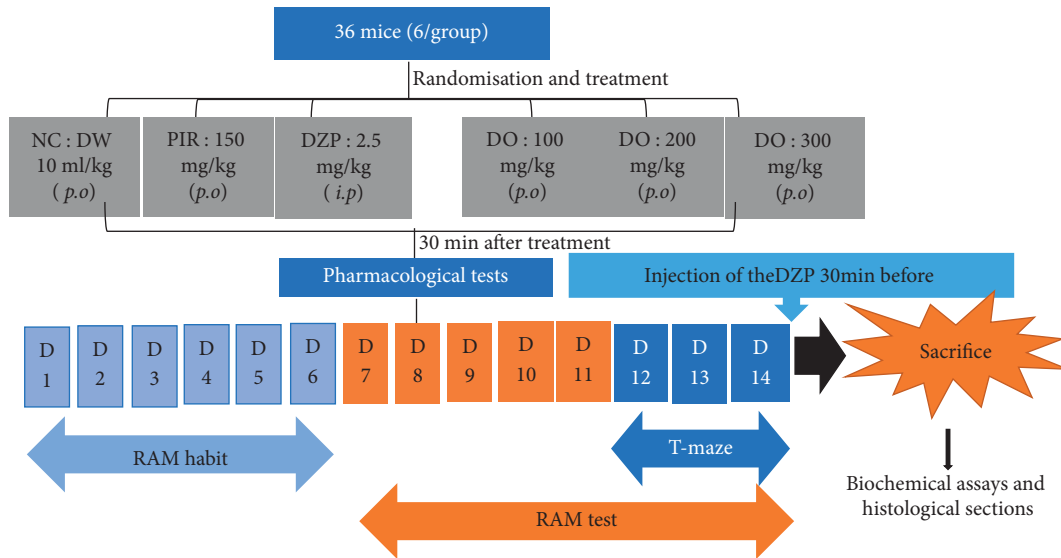
Figure 1: Experimental design. NC = neutral control, DW = distilled water, D = days, DO = *Daniellia oliveri*, and RAM = radial arm maze.

but previously entered) and reference memory errors (entering an arm that was not baited). The time taken to consume all four baits was also recorded. Reference memory was regarded as a long-term memory for information that remains constant over repeated trials (memory for the positions of baited arms), whereas working memory was considered a short-term memory in which the information to be remembered changes in every trial (memory for the positions of arms that had already been visited in each trial) [20].

2.4.2. T-Maze Task.
The T-maze test evaluates the ability of the rodent to memorize its first choice. It is a behavioral approach to study the following aspects of cognition: alternation behavior, location recognition, object recognition, spatial discrimination, working memory, and reference memory which is measured here [21]. The T-maze used in this study consisted of a T-shaped device, made of wood, painted white. It consists of a departure compartment and two arrival arms 30 cm long, 10 cm wide, and 25 cm high. Aluminum doors were placed at the exit of the departure compartment and at the entrance of each arrival corridor to control access to the various areas of the maze. At the end of each arrival compartment was a small cup containing a bait.

Two days before the start of the experiments, animals were progressively deprived of food to maintain them at 85% of their weight. Mice were placed one after the other in the starting arm of the T-maze. After each trial, the maze was cleaned with 70% ethanol, to eliminate residual odours left by the preceding mice. This test was carried out over three days during which habituation, acquisition, and retention phases were assessed each day, respectively [21].

The habituation phase consisted of a single session of free-choice trial. A mouse was placed in the start arm and allowed to explore the maze for 5 min. The preferred and discriminated arms of each mouse were noted. During the acquisition phase which was performed the next day, mice

were subjected to a forced-choice trial. The discriminated arm was blocked by a guillotine door. Once the animal was released from the starting arm, it was allowed to explore the maze by entering the preferred arm and returning to the start arm. During retention, all the guillotine doors were opened and mice were free to explore all the arms. In all the sessions, each mouse was evaluated for 5 min and the time spent in arms and number of returns to start arm were recorded. The floor of the apparatus was cleaned with 70% ethanol between trials to eliminate olfactory cues [22].

2.5. Biochemical Assay.
After the behavioral tests, all mice were deeply anesthetized (using sodium pentobarbital, 100 mg/kg b.w., *i.p.*) and decapitated and whole brains were removed. The hippocampus was carefully excised. The hippocampal sample was homogenized (1 : 10) in ice-cold 0.1 M phosphate buffer (pH 7.4). The homogenate was centrifuged (15 min) and the supernatant was used to evaluate malondialdehyde (MDA) and reduced glutathione (GSH) levels.

2.5.1. Determination of MDA.
The level of lipid peroxides was measured by thiobarbituric acid reaction previously described by Ohkawa et al. [23]. 200 μL of supernatant added and briefly mixed with 1 mL of 50% trichloroacetic acid in 0.1 M HCl and 1 mL of 26 mM thiobarbituric acid after the vortex mixing sample was maintained at 95°C for 20 min. Furthermore, samples were centrifuged at 9609 rpm for 10 min and supernatants were read at 532 nm. A calibration curve was constructed using MDA as standard and the results were expressed as nmol/organ of tissues.

2.5.2. Determination of GSH.
It was measured following the method described by Fukuzawa and Tokumura [24]. 200 μL of supernatant was added to 1.1 mL of 0.25 M sodium phosphate buffer (pH = 7.4) followed by the addition of

130 μl DTNB 0.04%. Finally, the mixture was brought to a final volume of 1.5 mL with distilled water and absorbance was read in a spectrophotometer at 412 nm and results were expressed as μg GSH/μg organ.

2.6. Histology of the Tissues. On day 14, after the acquisition of hippocampi, whole brains were collected, fixed in 10% formalin for a week. Fifty (50) mm coronal sections were made from the brain in the hippocampus region using the Mouse Brain Atlas with the following coordinate (anterior/ posterior D 2.0 mm, medial/lateral D 1.5 mm, and dorsal/ ventral AP D 2.0 mm) [25]. Hippocampi sections were collected in nine-well plates. The dehydration of these sections consisted in introducing tissues in ascending concentrations of ethanol followed by immersion in xylol and then embedding in paraffin. Paraffin sections of the brain were deparaffinised and rehydrated through washes in descending concentration series of alcohol. Hippocampi were then stained using hematoxylin and eosin stains. The brain sections were thereafter photographed and images were captured using a digital camera attached to a light microscope (Scientico, Haryana, India).

2.7. Statistical Analysis. All the results were expressed as mean ± SEM. The data were analyzed by one-way ANOVA (T-maze) and two-way ANOVA (RAM) followed by Tukey and Bonferroni post hoc tests, respectively. All analyses were performed using Graph Pad Prism 5.00 software, San Diego, California, USA. Results were considered significant at $p < 0.05$.

3. Results

3.1. Effect of D. oliveri Root Bark Aqueous Extract on Working and Spatial Reference Memory in the Radial Arm Maze. To investigate whether the aqueous extract of *D. oliveri* (100, 200, and 300 mg/kg) affects spatial memory formation, the mice were evaluated in the radial arm maze task. For reference memory errors, ANOVA revealed a significant time difference ($p < 0.01$) (Figure 2). Additionally, Tukey's post hoc analysis revealed significant differences between the normal control and DZP groups ($p < 0.01$), normal control and DZP + DO (100 mg/kg) groups ($p < 0.01$), DZP and DZP + DO (200 mg/kg) groups ($p < 0.01$), and DZP and DZP + DO (300 mg/kg) groups ($p < 0.01$). There were no significant differences between different doses of extract ($p > 0.05$). Moreover, the time taken to consume all the baits significantly increased ($p < 0.001$) in untreated mice compared to the normal control group (Figure 3). The administration of *D. oliveri* root back aqueous extract significantly ($p < 0.001$) reduced this time in DZP + DO (100 mg/kg) groups ($p < 0.001$), DZP + DO (200 mg/kg) groups ($p < 0.01$), and DZP + DO (300 mg/kg) groups ($p < 0.001$) compared to DZP group.

For working memory errors, Tukey's post hoc analysis revealed significant differences between the normal control and DZP groups ($p < 0.001$), DZP and DZP + DO (100 mg/ kg) groups ($p < 0.001$), DZP and DZP + DO (200 mg/kg) groups ($p < 0.001$), and DZP and DZP + DO (300 mg/kg) groups ($p < 0.001$) on the 7th day of the treatment (Figure 4).

3.2. Effect of D. oliveri Root Bark Aqueous Extract on Long-Term Memory in T-Maze Task. The T-maze test was performed to confirm the potential effect of DO on long-term memory. ANOVA revealed that acute administration of diazepam significantly ($p < 0.05$) increased the time spent in the preferred arm as compared to the control group (Figure 5). Animals treated with *D. oliveri* aqueous extract 200 mg/kg for 14 days resulted in a significant ($p < 0.05$) increase of this time in the preferred arm compared to demented group. The treatment of animals with piracetam significantly increased ($p < 0.001$) the time spent in preferred arm in comparison with the untreated group. In addition, the number of returns in the starting arm increased significantly ($p < 0.001$) in untreated animals compared to the normal control ones (Figure 6). It was also observed that the administration of *D. oliveri* root bark aqueous extract, 100 and 200 mg/kg, significantly ($p < 0.001$) reduced these numbers as compared to the untreated group. No significant ($p > 0.05$) difference was noted with the 300 mg/kg doses of the extract.

3.3. Effect of DO on MDA Content and Reduced GSH Level. Brain malondialdehyde (MDA) concentration was significant ($p < 0.001$) in the negative control group mice compared to the normal control (Figure 7(a)). The treatment of the animals with the aqueous extract of *D. oliveri* at dose of 100 mg/kg for 14 days significantly ($p < 0.01$) reduced the concentration of MDA compared to animals receiving diazepam.

The hippocampal concentration of malondialdehyde was significantly ($p < 0.001$) decreased in the animals treated with piracetam in comparison with the untreated group.

Glutathione concentration (GHS) decreases nonsignificantly ($p > 0.05$) in the group of mice that received diazepam with respect to normal control mice (Figure 7(b)). The pretreatment of mice with *Daniellia oliveri* root bark aqueous extract 200 mg/kg for 14 days significantly ($p < 0.001$) increased this concentration in comparison with the demented group. This parameter was also increased nonsignificantly ($p > 0.05$) in animals that were given piracetam compared to the demented group which was not subjected to any treatment.

3.4. Effects of Daniellia oliveri on Hippocampi Histological Sections. The effects of *Daniellia oliveri* aqueous root bark extract administration on the micromorphology of the hippocampus are illustrated in Figure 8. The analysis of the histological sections performed shows that in animals treated with DZP and receiving distilled water, the layer of granular cells at the dentate gyrus exhibits an abnormal architecture with some signs of cellular degeneration (red arrow) compared to that of the healthy control. In animals treated with DZP but did not receive the plant extract at doses of 100 and 300 mg/kg, the coronal sections revealed a
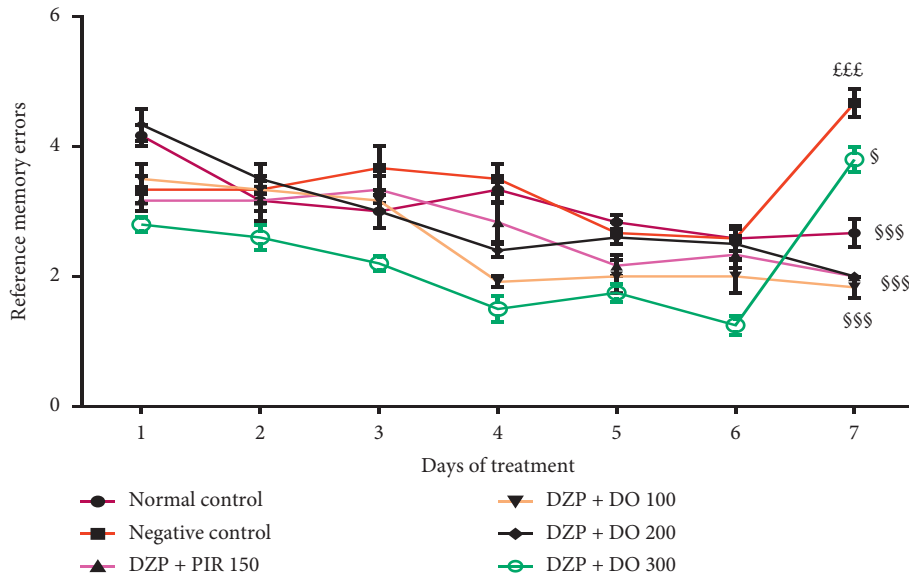
FIGURE 2: Effect of the aqueous extract of *D. oliveri* root on the reference memory of amnesic mice in the radial maze test. Each bar represents the mean ± ESM, $n = 6$. $^{£££}p < 0.001$ = significant difference compared to the normal control; $^{§}p < 0.05$ and $^{§§§}p < 0.001$ = significant difference compared to negative control. DZP 2.5 + DW = diazepam (2.5 mg/kg) + distilled water; PIR 150 = piracetam (150 mg/kg); DO 100, 200, 300 = *Daniellia oliveri* (100, 200, 300 mg/kg).
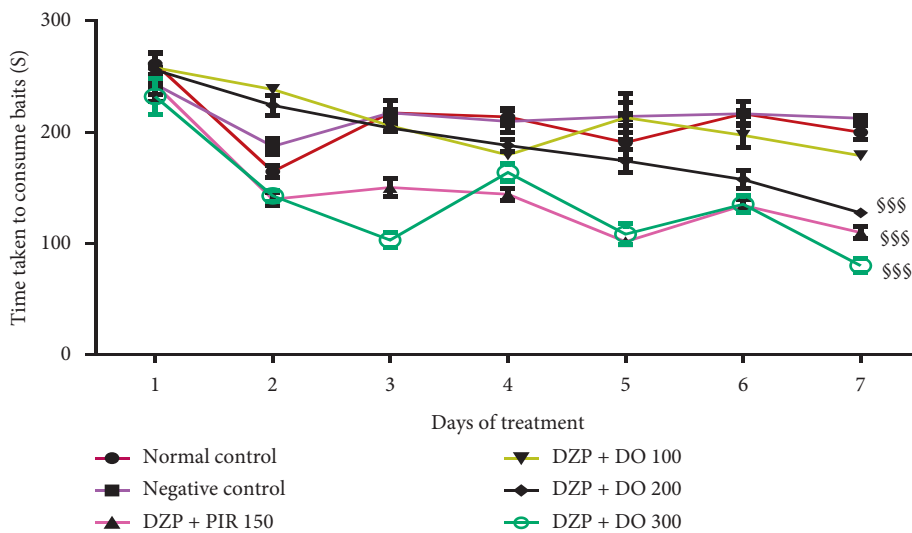

FIGURE 3: Effects of the aqueous root extract of *D. oliveri* on the time taken to consume the baits in the radial maze test. Each bar represents the mean ± ESM, $n = 6$. $^{§§§}p < 0.001$ = significant difference compared to the negative control. DZP 2.5 + DW = diazepam (2.5 mg/kg) + distilled water; PIR 150 = piracetam (150 mg/kg); DO 100, 200, and 300 = *Daniellia oliveri* (100, 200, 300 mg/kg).

normal architecture. However, signs of cellular degeneration still persist in the coronal section of animals treated with plant extract at a dose of 100 mg/kg.

4. Discussion

The aim of this study was to evaluate the neuroprotective effects of the aqueous extract of *Daniellia. oliveri* root bark on diazepam-induced amnesia model in mice. To achieve this, behavioral tests such as the radial maze and the T-maze were used, oxidative stress parameters (malondialdehyde and reduced glutathione) were evaluated in hippocampi

homogenates, and the histological sections of the hippocampus were performed.

Diazepam is an anxiolytic and hypnotic which binds to GABA-A receptors to exert its effects [26, 27]. However, it is possible to experimentally induce amnesia, which is either temporary (in the case of episodic memory) or reversible (for semantic memory) with benzodiazepines [28]. The results of this work show an increase of the number of reference memory errors (entering an arm that was not baited) and working memory (entering an arm containing food, but previously entered) in diazepam-treated animals compared to animals in the neutral control group in the
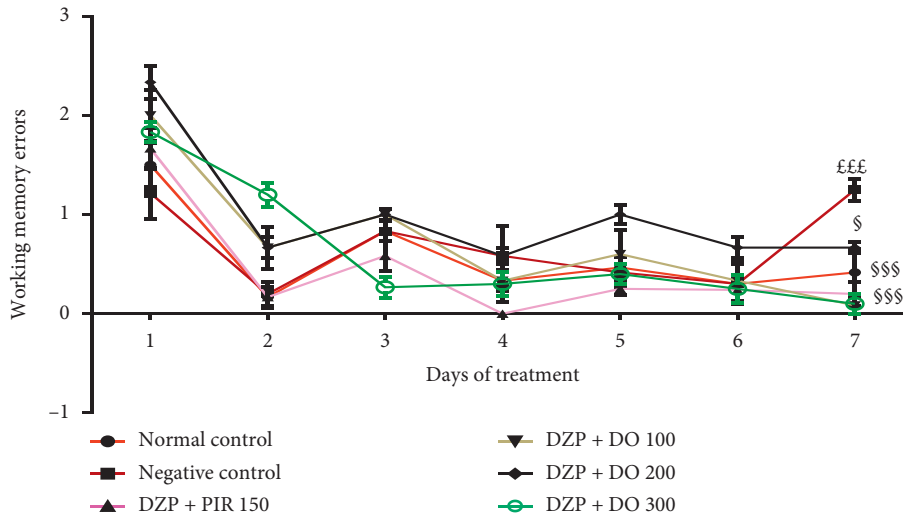
FIGURE 4: Effects of the aqueous extract of *D. oliveri* root bark on the number of working memory errors on in the radial maze test. Each bar represents the mean ± ESM, $n = 6$. $^{£££}p < 0.001$ = significant difference compared to the normal control; $^{§§§}p < 0.001$ = significant difference compared to the negative control. DZP 2.5 + DW = diazepam (2.5 mg/kg) + distilled water; PIR 150 = piracetam (150 mg/kg); DO 100, 200, and 300 = *Daniellia oliveri* (100, 200, and 300 mg/kg).
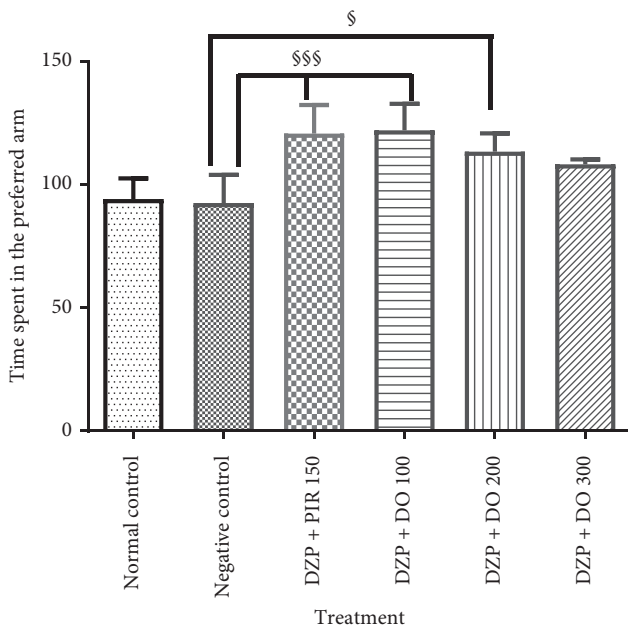

FIGURE 5: Effects of the aqueous extract of *D. oliveri* roots on the time spent in the preferred arm of the T-maze test. Each bar represents the average ± ESM, $n = 6$. $^{§}p < 0.05$ and $^{§§§}p < 0.001$ = significant difference compared to negative control. DZP 2.5 + DW = diazepam (2.5 mg/kg) + distilled water; PIR 150 = piracetam (150 mg/kg); DO 100, 200, and 300 = *Daniellia oliveri* (100, 200, and 300 mg/kg).
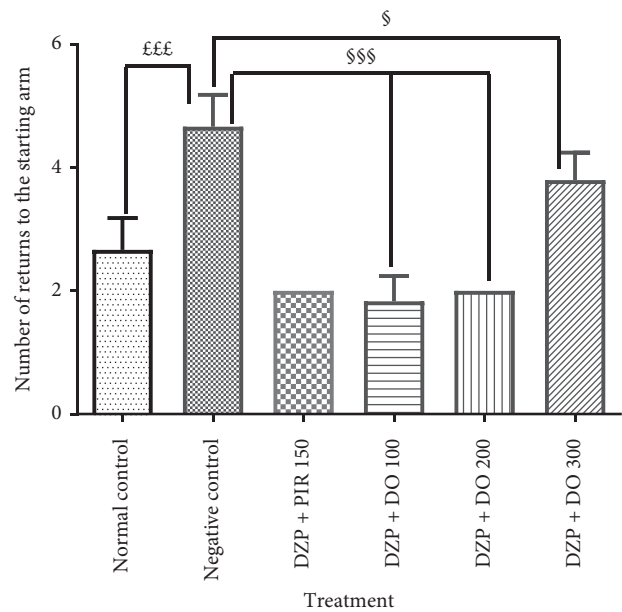

FIGURE 6: Effects of the aqueous extract of *D. oliveri* roots on the number of starting arm return of the T-maze test. Each bar represents the mean ± ESM, $n = 6$. $^{£££}p < 0.001$ significant difference compared to the normal control; $^{§§§}p < 0.001$ and $^{§}p < 0.05$ significant difference compared to negative control. N control = normal control; DZP 2.5 + DW = diazepam (2.5 mg/kg) + distilled water; PIR 150 = piracetam (150 mg/kg); DO 100, 200, and 300 = *Daniellia oliveri* (100, 200, and 300 mg/kg).

radial maze. Also, an increase was noted in the number of returns to the starting arm and a decrease of the time spent in the preferred arm in the diazepam-treated animals compared to the neutral control animals when they were subjected to the T-maze test. An increment in the time spent in the discriminated arm and a decrement in the time spent in the preferred arm are indications of impaired memory [29]. These observations were completely reversed

by pretreatment with the aqueous extract of *D. oliveri* for 14 days. In fact, in the radial maze test, the aqueous extract of *D. oliveri* roots bark at different tested doses significantly ($p < 0.001$) reduced the number of working and reference memory errors, thus translating an improvement of the working and reference memory, respectively, in amnesic mice. In addition, there was a decrease ($p < 0.001$) in the
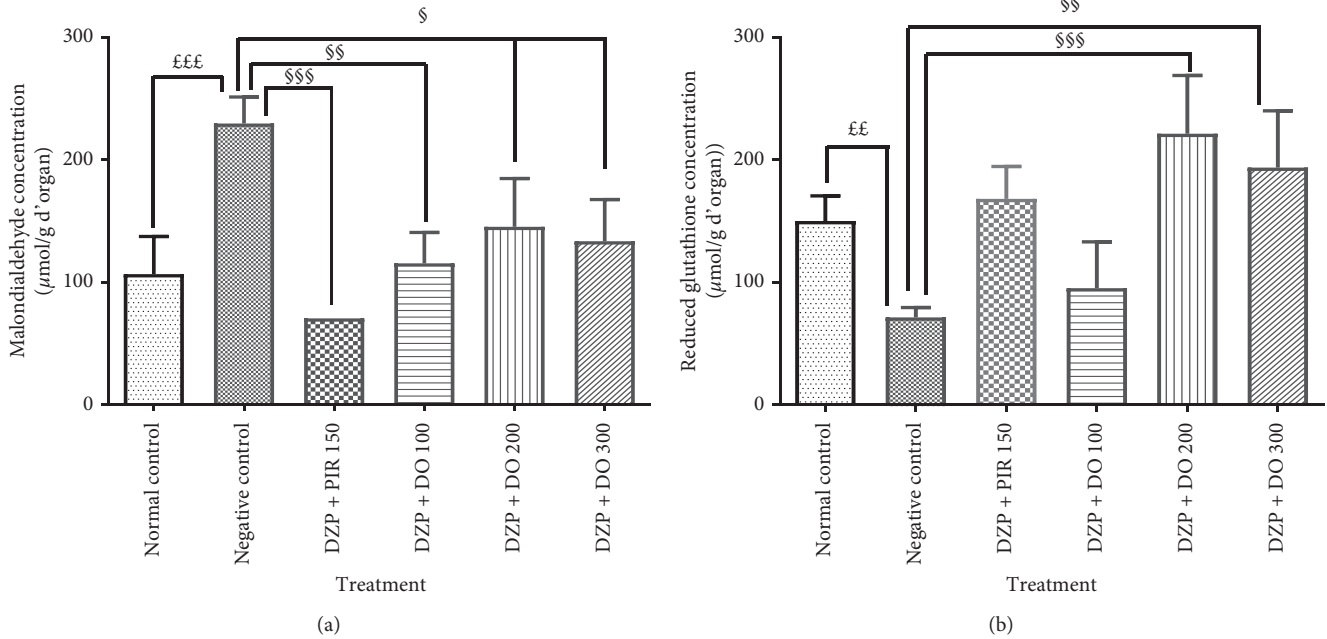
(a)

(b)

FIGURE 7: Effects of the aqueous extract of the root bark of *Daniellia oliveri* on the brain concentration of MDA (a) and reduced glutathione (b). Each bar represents the mean ± ESM, $n = 6$. $^{£££}p < 0.001$; significant difference compared to the normal control; $^{§}p < 0.05$, $^{§§}p < 0.01$, and $^{§§§}p < 0.001$; significant difference compared to the negative control. DZP $2.5 + DW =$ diazepam $(2.5 \, mg/kg) +$ distilled water; PIR $150 =$ piracetam $(150 \, mg/kg)$; DO 100, 200, and 300 = *Daniellia oliveri* (100, 200, and 300 mg/kg).
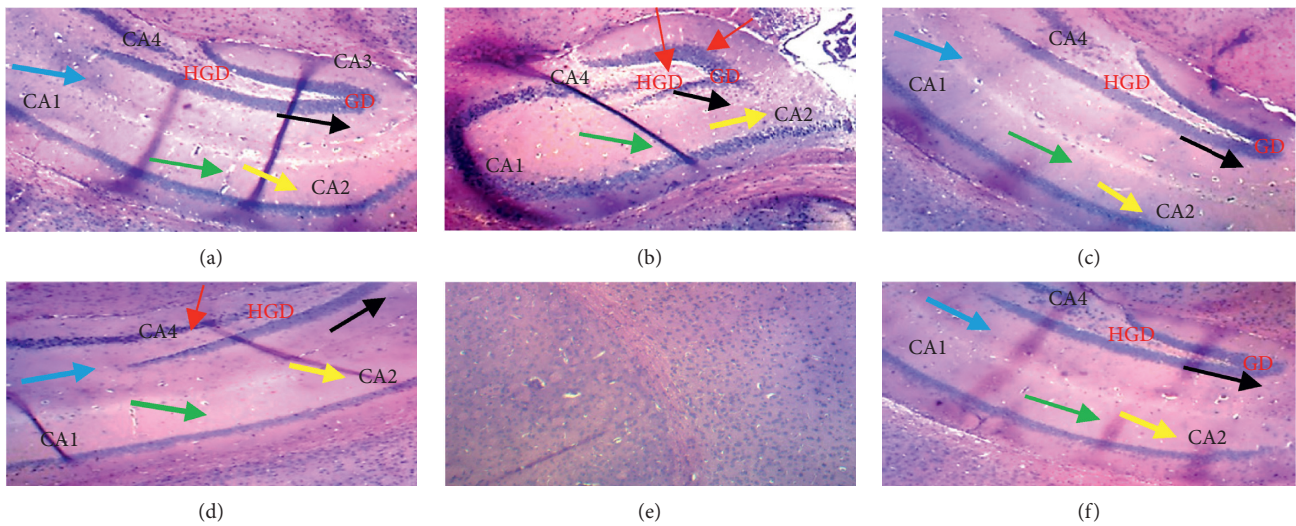

FIGURE 8: Effects of *D. oliveri* extract on hippocampi sections of mice brains. Coronal sections: hematoxylin and eosin-40x magnification; CA = cornus ammonis, GD = dentate gyrus, and HGD: dentate gyrus hilus. Yellow arrow: stratum oriens; green arrow: layer of pyramidal cells (contains the cell bodies of the pyramidal cells of the cornus ammonis. The density of the blue color corresponds to the density of the cell bodies of pyramidal neurons); blue arrow: stratum lacunosum-moleculare (contains pyramidal cell segments); black arrow: molecular layer of the dentate gyrus. ML: molecular layer of dentate gyrus. (a) Normal (DW 10 ml/kg). (b) DZP 2.5 mg/kg + DW. (c) DZP + PIR 150 mg/kg. (d) DZP + DO 100 mg/kg. (e) DZP + DO 200 mg/kg. (f) DZP + DO 300 mg/kg.

time taken to consume all baits. Moreover, in the T-maze, the results obtained show a significant increase ($p < 0.05$) in the time spent in the preferred arm and a significant decrease ($p < 0.001$) in the number of returns to the starting arm with all the doses of the extract. According to Chapouthier et al. [30], the increase in the time spent in the preferred arm and a reduction in the time spent in the discriminated arm reflect a good functioning of the memory. Furthermore, Farshchi et al. [29] reported that a decrease in the number of returns to the starting arm suggests an improvement in memory. These observations suggest that the aqueous extract of *D. oliveri* roots could

play an important role in memorization and more specifically by improving short-term and long-term memory. Pervious study has reported the presence of saponins, flavonoids, tannins, and alkaloids in the extract of *D. Oliveri*. These compounds are endowed with numerous pharmacological properties [16]. Indeed, Diaby [31] demonstrated that the aqueous extract of *Daniellia oliveri* bark had antiepileptic properties. In addition, the oleoresin isolated from this plant is an anti-inflammatory and antioxidant agent [32]. Therefore, the neuroprotective effect of this extract could be attributed to these groups of compounds. In order to elucidate how the extract act, the aqueous extract of the root bark of *Daniellia oliveri*, biochemical assays were carried out in homogenates of the hippocampus of amnesic mice.

DZP induces amnesia by generating reactive oxygen species [7]. The brain has increased susceptibility to oxidative stress because it contains high concentrations of polyunsaturated fatty acids vulnerable to lipid peroxidation and also has modest antioxidant capacity [33]. In addition, the high oxygen consumption in the brain, the metabolism of catecholamines, and the release of neurotransmitters are considered as important sources of free radicals and are therefore associated with significant oxidative damage [4]. Free radicals and related molecules are often classified together as reactive oxygen species (ROS) [33]. The formation of ROS in nerve cells is numerous, so cells must maintain an effective antioxidant system to protect against the overload of ROS and the resulting damage [7]. During oxidative stress, the production of ROS increases and exceeds the capacity of endogenous free radical scavengers such as GSH, CAT, and SOD [9, 10]. It has also been reported that ROS formation is involved in the neurotoxicity of many xenobiotics [4]. In this research, diazepam caused a significant change in the MDA content and GSH activities in the hippocampus. This observation was completely reversed by the pretreatment of animals with DO extract. However, concomitant administration of *D. oliveri* and diazepam not only reduced MDA concentration but also increased GSH concentration and enzymatic activity in the hippocampus of mice. GSH, CAT, and SOD are major enzymes that fight free radicals in the body. Indeed, GSH is vital for detoxifying heavy metals; the thiol group reacts with the salts of these heavy metals, creating with them a very strong sulfur-metal bond so that they are subsequently excreted without causing any harm to the organism [34]. The observed effect may be due to the radical scavenging properties of flavonoids contained in *D. oliveri*. The present results thus demonstrated the correlation between the antiamnesic effects of the aqueous extract of *D. oliveri* root bark against diazepam-induced amnesia and its antioxidant capacity.

Neurons provide the transmission of a bioelectric signal called nerve impulse. They have two physiological properties: excitability, that is, the ability to respond to stimuli and convert them into nerve impulses and conductivity, that is to say, the ability to transmit impulses nervous [35]. Any disturbance (degeneration) of a neuron at the level of the hippocampus leads to difficulty or inability to learn [36]. The histological section results showed a decrease in the density of the neurons of animals in the group receiving only diazepam compared to animals in the neutral control group. In contrast, DO (300 mg/kg) treated animals' hippocampi were protected from cell death associated to diazepam administration. The aqueous extract of *D. oliveri* root barks at a dose of 300 mg/kg therefore protects the neurons against diazepam-induced amnesia in mice. The aqueous extract of *D. oliveri* root bark could therefore act either as a DZP receptor antagonist or by inhibiting lipid peroxidation while increasing the antioxidant status. All these properties would be attributable once again to the various compounds (glycosides, flavonoids, rutin, quercitrin, tannins, saponins, and glycosides) contained in this plant. Stud phytochemical screening is still going on to identify and specify the compounds responsible of the observed effects.

5. Conclusion

The present study strongly demonstrates that *D. oliveri* root bark aqueous extract of 200 and 300 mg/kg effectively enhances memory processes, restores antioxidant brain status, and may confer neuroprotection by the alleviation diazepam-induced oxidative damage. These results suggest that the aqueous extract of *D. oliveri* root bark may possibly be used as a promising natural product for the prevention of memory disorders. The result of this study supports the traditional claim of the plant's use for schizophrenia, epilepsy, and studies currently being conducted to delineate the toxicological profile of this plant.

Data Availability

The data used to support the findings of this study are available from the corresponding author upon reasonable request.

Disclosure

Conflicts of Interest

The authors declare that they have no conflicts of interest related to the publication of this study.

Acknowledgments

References

[1] R. L. Rech, M. N. M. de Lima, V. A. Garcia, L. A. Alcalde, G. Vedana, and N. Schröder, "Reversal of age-associated memory impairment by rosuvastatin in rats," *Experimental Gerontology*, vol. 45, no. 5, pp. 351–356, 2010.

[2] Dubois and B. Michon, *Actualités de la Maladie d'Alzheimer*, Vol. 67, Elsevier Masson, Paris, France, 2015.

[3] C. K. Tegueu, S. Nguefack, J. Doumbe, Y. F. Fogang, P. Mbonda, and E. Mbond, "The spectrum of neurological disorders presenting at a neurology clinic in yaoundé, Cameroon," *Pan African Medical Journal*, vol. 14, pp. 123–231, 2013.

[4] C. S. B. Alexandra, F. Vlad, A. T. Vlad et al., "Curcumin reverses the diazepam-induced cognitive impairment by modulation of oxidative stress and ERK 1/2/NF-kB pathway in brain," *Hindawi Oxidative Medicine and Cellular Longevity*, Article ID 3037876, vol. 2017, pp. 1–16, 2017.

[5] R. G. Lister, "The amnesic action of benzodiazepines in man," *Neuroscience & Biobehavioral Reviews*, vol. 9, no. 1, pp. 87–94, 1985.

[6] J. A. Harris and R. F. Westbrook, "Benzodiazepine-induced amnesia in rats: reinstatement of conditioned performance by noxious stimulation on test," *Behavior and Neuroscience*, vol. 112, no. 1, pp. 183–192, 1998.

[7] S. Ferdousy, A. Rahman, A. Mamun, J. Aklima, and H. Kamirul, "Antioxidative and neuroprotective effects of Leea macrophylla methanol root extracts on diazepam-induced memory impairment in amnesic Wistar albino rat," *Clinical Phytoscience*, vol. 2, p. 17, 2016.

[8] M. T. Georgieva-Kotetarova, I. Ivanka, and I. I. Kostadinova, "Effect of atorvastatin and rosuvastatin on learning and memory in rats with diazepam-induced amnesia," *Folia Medical*, vol. 55, no. 2, pp. 58–65, 2013.

[9] S. Mani, *Production of Reactive Oxygen Species and its Implication in Human Diseases*, Vol. 1, Springer, New Delhi, India, 2015.

[10] D. B. Zorov, M. Juhaszova, and S. J. Sollott, "Mitochondrial reactive oxygen species (ROS) and ROS-induced ROS release," *Physiological Reviews*, vol. 94, no. 3, pp. 909–950, 2014.

[11] T. Wang, S. Y. Shan, B. Han, L. M. Zhang, and F. H. Fu, "Salvianolic acid A exerts anti amnesic effect on diazepam-induced anterograde amnesia in mice," *Neurochemistry Research*, vol. 36, no. 1, pp. 103–108, 2013.

[12] E. Ernst, "Herb-drug interactions: potentially important but woefully under-researched," *European Journal of Clinical Pharmacology*, vol. 56, no. 8, pp. 523-524, 2000.

[13] H. M. Burkill, "The useful plants of west tropical Africa," *Kew, Royal Botanic Gardens*, University Press of Virginia, Charlottesville, VA, USA, 1995.

[14] P. Dealaveau, A. Desrignes, E. Adoux, and A. M. Tessier, "Phytochemical and antimicrobial activities of the *Daniellia oliveri* leaves," *Annales Pharmaceutiques Françaises*, vol. 37, p. 185, 1995.

[15] D. N. Onwukaema and F. Udoh, "Anti-ulcer activity of the stem bark of *Daniellia oliveri*," *Nigerian Journal of Natural Products and Medicine*, vol. 3, pp. 39–41, 1999.

[16] A. Gaston and P. Daget, "La base FLOTROP et L'inventaire de la flore des paturages d'Afrique sahelienne," *Systematics and Geography of Plants*, vol. 71, no. 2, pp. 337–344, 2001.

[17] P. Sur, T. Chaudhuri, J. R. Vedasiromoni, A. Gomes, and D. K. Ganguly, "Antiinflammatory and antioxidant property of saponins of tea [Camellia sinensis (L) O. Kuntze] root extract," *Phytotherapy Research*, vol. 15, no. 2, pp. 174–176, 2001.

[18] F. Poumarad, S. J. Hosseinimehr, and N. Shahabimajd, "Antioxidant activity, phenol and flavonoid contents of some selected Iranian medicinal plants African," *Journal of Biotechnology*, vol. 5, pp. 1142–1145, 2006.

[19] T. Y. Soro, J. C. Mian, S. Coulibaly, S. A. Nene-Bi, and F. Traore, "Anti-inflammatory activity of the aqueous extract of *Daniellia oliveri* (Fabaceae)," *International Archives of Integrated Medicine*, vol. 3, pp. 1–9, 2015.

[20] G. J. Beppe, A. B. Dongmo, H. S. Foyet et al., "Memory-enhancing activities of the aqueous extract of *Albizia adianthifolia* leaves in the 6-hydroxydopamine-lesion rodent model of Parkinson's disease," *BMC Complementary and Alternative Medicine*, vol. 13, pp. 141-142, 2014.

[21] R. Deacon, J. Nicholas, and P. Rawlins, "T-maze alternation in the rodent," *Nature Protocols*, vol. 1, pp. 8–12, 2006.

[22] S. Okada, H. Igata, T. Sasaki, and Y. Ikegaya, "Spatial representation of hippocampal place cells in a T-maze with an aversive stimulation," *Frontiers in Neural Circuits Journal*, vol. 11, pp. 100–110, 2017.

[23] H. Ohkawa, N. Ohishi, and K. Yagi, "Assay for lipid peroxides in animal tissues by thiobarbituric acid reaction," *Analytical Biochemistry*, vol. 95, no. 2, pp. 351–358, 1979.

[24] K. Fukuzawa and A. Tokumurai, "Glutathione peroxidase activity in tissues of vitamin E-deficient mice," *Journal of Nutritional Science and Vitaminology*, vol. 22, no. 5, pp. 405–407, 1976.

[25] A. Smith and J. Bruton, "Histological staining procedure," *World Journal of Medicine*, vol. 18, pp. 1–86, 1977.

[26] C. E. Griffin, A. M. Kaye, F. R. Bueno, and A. D. Kaye, "Benzodiazepine pharmacology and central nervous system-mediated effects," *The Ochsner Journal*, vol. 13, no. 2, pp. 214–223, 2013.

[27] M. Lader, "Benzodiazepine harm: how can it be reduced?" *British Journal of Clinical Pharmacology*, vol. 77, no. 2, pp. 295–301, 2014.

[28] R. S. Evans, *Un Panorama des Hallucinogènes du Nouveau Monde*, L'esprit Frappeur, Paris, France, 2000.

[29] A. Farshchi, G. Ghiasi, S. Farshchi, and M. Khatabi, "Effects of boswellia papyrifera gum extract on learning and memory in mice and rats," *Iran Journal of Biomedical Science*, vol. 22, pp. 9–15, 2010.

[30] G. Chapouthier, M. Lepicard, A. Rössler, and P. Venault, "L'anxiété, un pont entre l'épilepsie et la mémoire," *Philosophie des sciences*, vol. 6, pp. 75–91, 2002.

[31] A. Diaby, "Etude de la chimie de *Daniellia oliveri* (rolfe, hutch et dalz) dans la prise en charge de l'epilepsie au Mali," Thèse de Pharmacie, p. 139, Université des Sciences, des Techniques et Des Technologies de Bamako, Bamako, Mali, 2014.

[32] H. O. Edeoga, D. Okwu, D. E. Okwu, and B. O. Mbaebie, "Phytochemical constituents of some Nigerian medicinal plants," *African Journal of Biotechnology*, vol. 4, no. 7, pp. 685–688, 2005.

[33] C. Zhichun and Z. Chunjiu, "Oxidative stress in Alzheimer's disease," *Neuroscience Bullettin*, vol. 30, pp. 271–281, 2014.

[34] L. M. Saclay, "Le Glutathion, première défense contre les métaux lourds," *International Dental Journal*, vol. 47, pp. 2113–2123, 2017.

[35] E. N. Marieb, "Anatomie et Physiologie Humain," *De Boeck Université*, 4th édition, pp. 811–883, 1999.

[36] R. W. Williams and K. Herrup, "The control of neuron number," *The Annual Review of Neuroscience*, vol. 11, no. 1, pp. 423–453, 2001.

Research Article

Effect of Cellgevity® Supplement on Selected Rat Liver Cytochrome P450 Enzyme Activity and Pharmacokinetic Parameters of Carbamazepine

Seth Kwabena Amponsah [iD],[1] **Benoit Banga N'guessan** [iD],[1] **Martin Akandawen,**[1]
Abigail Aning,[2] **Sedem Yawa Agboli,**[1] **Eunice Ampem Danso,**[2]
Kwabena Frimpong-Manso Opuni,[3] **Isaac Julius Asiedu-Gyekye** [iD],[1]
and Regina Appiah-Opong [iD][2]

[1]*Department of Pharmacology and Toxicology, School of Pharmacy, College of Health Sciences, University of Ghana, Accra, Ghana*
[2]*Department of Clinical Pathology, Noguchi Memorial Institute for Medical Research, College of Health Sciences, University of Ghana, Accra, Ghana*
[3]*Department of Pharmaceutical Chemistry, School of Pharmacy, College of Health Sciences, University of Ghana, Accra, Ghana*

Correspondence should be addressed to Benoit Banga N'guessan; bbnguessan@ug.edu.gh

Background. There is considerable evidence that many patients concurrently administer dietary supplements with conventional drugs, creating a risk for potential drug-supplement interaction. The aim of this study was to determine the effect of Cellgevity® supplement on selected rat liver cytochrome P450 (CYP) enzymes. Also, based on our previous finding, we sought to determine the effect of Cellgevity® on the pharmacokinetics of carbamazepine, a CYP3A4 substrate. *Methods.* Male Sprague–Dawley (SD) rats were randomly put into 5 groups and administered either distilled water (negative control), Cellgevity® (3 separate doses), or phenobarbital (positive control), *per os*. Modulation of liver CYP enzyme activity was evaluated after 30 days of treatment, using probe substrates, spectroscopic, and high-performance liquid chromatographic methods. In the pharmacokinetic study, 12 SD rats were put into 2 groups and administered carbamazepine plus normal saline (group 1) or carbamazepine plus Cellgevity® (group 2), *per os*, both over a period of 14 days. Blood samples from rats in the same group were collected after treatment. Serum samples were prepared and pooled together at each specific sampling time point. Levels of carbamazepine were determined using a fluorescence polarization immunoassay. *Results.* Activities of rat liver CYP1A1/2, CYP2C9, and CYP2D6 were significantly increased by Cellgevity® after 30-day treatment. Pharmacokinetic parameters for rats administered carbamazepine with Cellgevity® vis-a-vis carbamazepine with normal saline were as follows: C_{max}; 20 μmol/L vs 11 μmol/L, $AUC_{0 \longrightarrow 24}$; 347 μmol h/L vs 170 μmol h/L, K_e; 0.28 h^{-1} vs 0.41 h^{-1}, and $t_{1/2}$; 2.3 h vs 1.7 h, respectively. *Conclusions.* Cellgevity® increased the activity of rat CYP1A1/2, CYP2C9, and CYP2D6 enzymes and was found to alter the pharmacokinetics of carbamazepine in rats.

1. Background

Dietary supplements may be vitamins, minerals, or herbal products that are known to improve the well-being of humans [1]. This clearly denotes the use of these supplements as an addition to dietary requirements that may not be met by daily meals. However, under no circumstance should dietary supplements be used as a replacement for daily meals. The United States Food and Drugs Administration also prohibits the indication of dietary supplements as a treatment for diseases or any indication that connotes dietary supplements as primary therapeutic agents [1].

With an increase in the incidence of noncommunicable diseases (NCDs) such as diabetes, cardiomyopathies, cancers, and epilepsy, which are often associated with oxidative stress, people resort to the use of dietary supplements (known antioxidants) to prevent these diseases [2]. Interestingly, some individuals who use dietary supplements have the notion that these agents may enhance the effects of conventional drugs [3]. This assertion may be false. It is noteworthy, however, that synergy between some dietary supplements and conventional drugs have been reported [4].

Currently available on the market are a number of dietary supplements known to replenish levels of reduced glutathione, a free radical scavenger, in cells of humans. One such supplement is Cellgevity®, which contains a glutathione precursor molecule, ribocene (D-ribose-L-cysteine). Riboceine is known to deliver cysteine into cells and enhance reduced glutathione levels in the body [5, 6]. The other constituents of Cellgevity® are broccoli seed extract, turmeric root extract, resveratrol, grape seed extract, quercetin, curcumin, milk thistle, vitamin C, selenomethionine, cordyceps, black pepper, and aloe extract. Some of these constituents of Cellgevity® are known inducers and/or inhibitors of cytochrome P450 (CYP) enzymes [7, 8]. Cellgevity® is marketed and distributed by Max International, which has branches in 14 countries (United States, Nigeria, Cote d'Ivoire, New Zealand, Singapore, Costa Rica, Columbia, Philippines, El Salvador, Malaysia, Guatemala, Ghana, and Hong Kong). Cellgevity® has gained popularity in these countries due to the fact that patronizers know that the supplement has a high antioxidant potential [9].

Reports suggest that there could be clinically important modulation of CYP enzyme activity by supplements and/or herbal products. This could result in adverse or subtherapeutic effects of concurrently administered conventional drugs. For example, St. John's wort was reported to decrease the serum concentration of theophylline (a bronchodilator) as a result of CYP enzyme induction [10]. This interaction between St John's wort and theophylline could lead to subtherapeutic effect of normal doses of theophylline when there is coadministration. For this reason, patients are often advised not to take theophylline concomitantly with St. John's wort. Most of the individual constituents of Cellgevity® can modulate xenobiotic metabolizing enzyme activity, and several studies have reported these. However, there is paucity of scientific data on the effect of all these constituents (extracts) combined in Cellgevity® on xenobiotic metabolizing enzymes (CYP enzymes). In our earlier study, we reported that Cellgevity® at 4 and 8 mg/kg significantly inhibited rat liver CYP2C9, CYP2B1/2B2, and CYP3A4 after a 7-day treatment period [11]. In animal models, it is relevant that doses of test agents (drugs/food supplements/herbal products) are at equivalent doses of what pertains to humans. Therefore, as a follow-up to our earlier study, we decided to use animal equivalent doses of Cellgevity® after scaling doses used in humans [12] in the current study. We also decided to administer Cellgevity® over a longer period of time, i.e., 30 days.

We have previously reported that Cellgevity® inhibited rat liver CYP3A4 after a 7-day treatment period [11]. We,

therefore, sought to elucidate the possible effect of Cellgevity® on carbamazepine, also known to be extensively metabolized by CYP3A4. This was to aid in assessing potential interaction between these two agents. Carbamazepine is one of the most commonly prescribed drugs in the management of epilepsy. Due to the chronic nature of epilepsy, and the fact that patients have to take carbamazepine for a long time (lifetime in most cases), there is the potential for clinically significant interactions between carbamazepine and coadministered agents like dietary supplements, herbal products, and food [13]. Therefore, in a parallel experiment, the effect of Cellgevity® on the pharmacokinetics of carbamazepine (a CYP3A4 substrate) was investigated.

2. Methods

2.1. Animal Care and Safety.
This research was approved by the College of Health Sciences Ethical and Protocol Review Committee (Protocol ID: CHS-Et/M.9–P1.16/2017-2018) of the University of Ghana. All animal procedures used in this study were in accordance with the National Institute of Health Guidelines for the Care and Use of Laboratory Animals [14].

Male Sprague–Dawley (SD) rats, weighing 150–200 g and 6–8 weeks old, were obtained from the Center for Plant Medicine Research, Mampong, Eastern Region, Ghana. The animals were housed in stainless steel cages. Each rat occupied a minimum space of 2 cubic feet (61 cm × 31 cm × 31 cm) with softwood shavings as bedding for their comfort. The SD rats were fed with normal pellet diet (AGRIMAT, Kumasi, Ghana), given water *ad libitum*, and maintained under standard laboratory conditions (temperature ~25°C, relative humidity 60–70%, and 12 h light-dark cycle). The animals' feeding area and water troughs were cleaned regularly to prevent contamination. Animals were acclimatized under stated conditions for 7 days before the experiment commenced.

2.2. Hepatic Enzyme Induction/Inhibition Studies

2.2.1. Animal Grouping and Treatment Administration.
In determining the effect of Cellgevity® on CYP enzymes after a 30-day treatment period, male SD rats were put into five groups (6 rats in each group). All treatments were *per os* and for 30 days. Group 1 was administered distilled water, the vehicle used in dissolving Cellgevity® (purchased from Max International, Ghana), and that served as the negative control (N-C) group. Groups 2, 3, and 4 received daily a low dose (L-D) of 38.63 mg/kg Cellgevity®, medium dose (M-D) of 77.25 mg/kg Cellgevity®, and high dose (H-D) of 154.50 mg/kg Cellgevity®, respectively, as reported elsewhere [15]. The doses of Cellgevity® administered to SD rats were animal equivalents of what pertains to humans and calculated as described by Nair AB and Jacob SA [16]. The human dose of Cellgevity® is 12.46 mg/kg *per os*. The SD rats in Group 5 received an oral dose of phenobarbital (Kinapharma, Ghana) 15 mg/kg daily, and that served as the positive control (P-C). After the 30-day treatment period, animals were sacrificed by cervical dislocation. Livers were

excised, washed in ice-cold saline solution, weighed, and stored at −80°C until use.

2.2.2. Microsomal Preparation.

Livers were thawed and homogenized in potassium phosphate buffer (pH 7.4) using a mortar and pestle on ice. Homogenized samples were first centrifuged at 4,000 rpm for 20 min. The supernatant obtained was recentrifuged (Beckman Avanti J-25, USA) at 25,000 rpm for 2 h. The pellets were obtained, and microsomes were collected and stored at −80°C until use.

2.2.3. CYP2C9 (Diclofenac Hydroxylation) and CYP2D6 (Dextromethorphan O-Demethylation) Assays.

The assays were performed as previously described [17], with some modification. A volume of 350 μL of 0.1 M potassium phosphate buffer (pH 7.4), 50 μL of 1 mM substrate (diclofenac for CYP2C9 assay and dextromethorphan for CYP2D6, both substrates purchased from Sigma-Aldrich, USA) and 50 μL of 2.5 mg/mL microsome (obtained from rat livers from respective groups) were mixed separately in Eppendorf tubes. The mixtures were preincubated at 37°C for 5 min. A volume of 50 μL of 1 mM nicotinamide adenine dinucleotide phosphate (NADPH) (Sigma-Aldrich, USA) was added, mixed, and incubated at 37°C for 45 min. A 100 μL stopping solution (ZnSO$_4$.7H$_2$O) was added, and the mixture centrifuged at 4000 rpm for 5 min. The supernatants were aliquoted into High-Performance Liquid Chromatography (HPLC, Shimadzu, Japan) vials.

Samples were analyzed using HPLC. The chromatographic system consisted of a binary solvent delivery system (LC-20AB), a degasser (DGU-20A3), an autosampler (SIL-20ACHT), a column temperature controller (CTO-10AS VP), and a photodiode array detector (SPD - M20 A) for CYP2C9 metabolites and fluorescence detector (RF-10A$_{XL}$) for CYP2D6 metabolites. The following chromatographic conditions were used for the analysis of CYP2C9; column, C18 (Shimadzu, Japan), diameter 5 μm, length x width 150 mm × 4.6 mm; flow rate, 1 mL/min; column temperature, 40°C; injection volume, 20 μL; mobile phase, 20 mM potassium phosphate buffer (pH 7.4)/methanol/acetonitrile (60 : 22.5 : 17.5, v/v/v). The same chromatographic conditions were used for the analysis of the CYP2D6, with modification to the mobile phase, where 3 solvents were used (acetonitrile/distilled water/triethylamine; 24 : 75 : 1, v/v/v).

2.2.4. CYP1A1/1A2-Ethoxyresorufin O-Deethylase (EROD), CYP2B1/2B2-Pentoxyresorufin O-Depentylase (PROD), and CYP3A4 - Benzyloxyresorufin O-Debenzylase (BROD) Assays.

The assays were performed as previously described [18, 19], with some modification. In brief, microsomes (CYP enzymes) were tested in a total volume of 100 μL. Aliquots of 70 μL potassium phosphate buffer (pH 7.4) were placed into 96-well black plates. This was followed by the addition of 10 μL of 50 μM substrate concentration (resorufin ethyl ether for CYP1A1/2, pentoresorufin for CYP2B1/2 and resorufin benzyl ether for CYP3A4; all substrates purchased from Sigma-Aldrich, USA). The final substrate concentration in 100 μL total reaction volume was 5 μM with 0.25% (v/v) dimethyl sulfoxide (DMSO). It is noteworthy that CYP activities were not expected to be affected at the DMSO concentration used in this experiment [20]. Aliquots of 10 μL enzyme (microsome from each rat liver from respective groups) corresponding to 1 mg/mL protein concentration and the vehicle were added in triplicate. The mixtures were preincubated at 37°C for 5 min. A volume of 10 μL of NADPH was then added to each well, and the setup was incubated for 10 min for CYP1A1/2, 20 min for CYP2B1/2, and 30 min for CYP3A4 assays, respectively. Aliquots of 40 μL of stopping solution (20% 0.5 M Tris: 80% acetonitrile) were added to each well and shaken gently. Fluorescence of wells was read at wavelengths of 530 nm excitation and 586 nm emission. Triplicate experiments were performed. The average absorbance of the blank was subtracted from the average absorbance of each sample.

2.3. Fourteen-Day Treatment of Cellgevity® on the Pharmacokinetics of Carbamazepine in Rats

2.3.1. Animal Grouping and Treatment Administration.

Twelve male SD rats were obtained for this aspect of the study. The animals were put into 2 groups of 6 (Group 1 and Group 2). All treatments were *per os* and for 14 days. Group 1 was administered carbamazepine plus saline and Group 2, Cellgevity® plus carbamazepine. A dose of 77.25 mg/kg/day of Cellgevity® plus 80 mg/kg of carbamazepine, both equivalent doses per serving/administration in humans scaled to SD rats [14], were administered to rats in Group 2. Rats in Group 1 received 80 mg/kg/day of carbamazepine plus normal saline (same volume as calculated per rat for the Cellgevity® dose).

2.3.2. Blood Sample Collection.

After administration of carbamazepine with or without Cellgevity® every 24 h for 14 consecutive days to Groups 1 and 2, tail vein blood samples were taken following the dose administered on the 14th day. Samples were drawn after 0.5, 1, 4, 12, and 24 h. Blood was collected into microtainer gel tubes and centrifuged at 2000 rpm for 5 min to separate serum, and this was stored at −20°C until analysis.

2.3.3. Assay for Carbamazepine in Serum.

Due to low sample volumes from tail veins of SD rats, serum samples from rats in the same group (6 animals) at each time point were pooled together. Such that, for instance, serum samples of Group 1 SD rats at time 0.5, 1, 4, 12, or 24 h, were pooled together to obtain a single sample. Usually, challenges with low sample volume can be circumvented by the approach of sample-pooling [21]. Analysis of carbamazepine in serum was by fluorescence polarization immunoassay (FPIA) (Cobas Integra® 400 Plus, Roche, Philippines). The lower limit of quantification of serum carbamazepine concentration was 0.8 μmol/L and the coefficient of variation was <5% over the entire calibration range.

2.4. Statistical Analysis. CYP activity of treatment groups was expressed as a percentage relative to the negative control group. All values were expressed as mean ± standard deviation. Differences between groups were tested for significance using a One-Way Analysis of Variance (ANOVA). This was followed by post hoc analysis using Bonferroni's Multiple Comparison Tests. p-values < 0.05 were considered statistically significant.

Noncompartmental pharmacokinetic analysis was used to estimate the various pharmacokinetic parameters of carbamazepine. The maximum serum drug concentration (C_{max}) and its corresponding time (T_{max}) were determined by visual inspection of the concentration-time curve. The linear trapezoidal rule was applied in extrapolating area under the concentration-time curves (AUCs) for the two groups. The elimination rate constant (K_e) for both groups was extrapolations (apparent slope) from the last sample time point, i.e., 24 hours. K_e for both groups was used to calculate corresponding elimination half-lives ($t_{1/2}$). Pharmacokinetic analysis was conducted using GraphPad Prism 7.0.

3. Results

3.1. Hepatic Enzyme Induction/Inhibition Studies. All CYPs enzyme activities in the treatment groups were estimated relative to the negative control (N-C) group.

3.1.1. CYP2C9 Activity in SD Rats after 30-Day Treatment. CYP2C9 enzyme activity was higher in the phenobarbital- and Cellgevity®-treated groups in comparison with the N-C group. The phenobarbital- and Cellgevity®-treated groups were significantly different from the N-C group. The increase in rat CYP2C9 enzyme activity by Cellgevity® was dose-dependent. Presentation of the effect of Cellgevity® on rat CYP2C9 enzyme activity in various groups is shown in Figure 1.

3.1.2. CYP2D6 Activity in SD Rats after 30-Day Treatment. CYP2D6 enzyme activity was about 2.5-fold higher in the phenobarbital-treated and about 2-fold higher in the Cellgevity®-treated groups in comparison with the N-C group. The positive control (P-C) and H-D Cellgevity®-treated groups differed significantly ($p < 0.01$) from the N-C group. The L-D and M-D groups also differed significantly ($p < 0.05$) in comparison to the N-C group. The increase in rat CYP2D6 enzyme activity by Cellgevity® was not dose-dependent. CYP2D6 enzyme activity of SD rats in various groups after the 30-day treatment period is shown in Figure 2.

3.1.3. CYP1A1/2 Activity in SD Rats after 30-Day Treatment. CYP1A1/2 enzyme activity was higher in the phenobarbital- and Cellgevity®-treated groups in comparison with the N-C group. The Cellgevity®-treated L-D and M-D groups showed elevated CYP activity compared to the N-C group, but these differences were not statistically significant. However, there
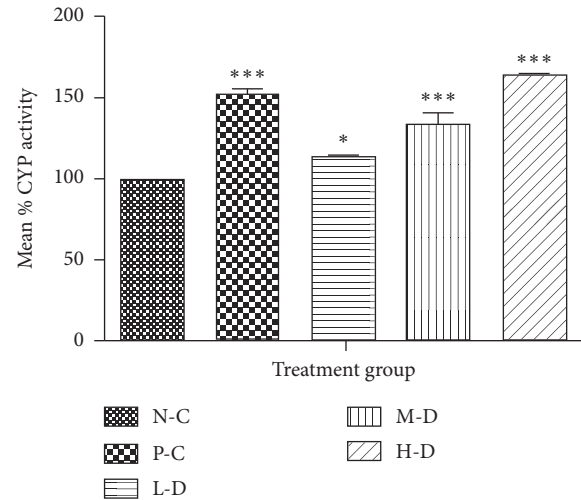

Figure 1: Rat liver CYP2C9 activity for various treatment groups after 30-day administration: N-C = Negative control; P-C = Positive control (Phenobarbital); L-D = Low dose (38.63 mg/kg) of Cellgevity®; M-D = Medium dose (77.25 mg/kg) of Cellgevity®; H-D = High dose (154.50 mg/kg) of Cellgevity®. Data represent mean ± standard deviations. * and *** represent values significantly different from the negative control as indicated by $p < 0.05$ and $p < 0.01$, respectively.
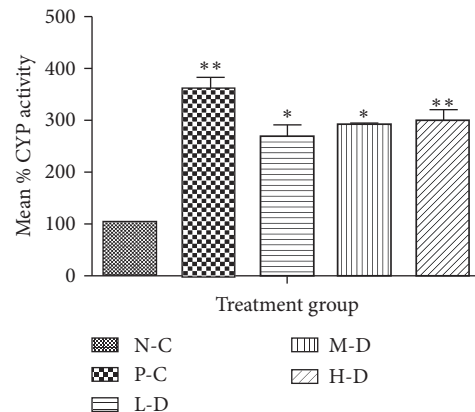

Figure 2: Rat liver CYP2D6 activity for various treatment groups after 30-day administration: N-C = Negative control; P-C = Positive control (Phenobarbital); L-D = Low dose (38.63 mg/kg) of Cellgevity®; M-D = Medium dose (77.25 mg/kg) of Cellgevity®; H-D = High dose (154.50 mg/kg) of Cellgevity®. Data represent mean ± standard deviations. * and ** represent values significantly different from the negative control as indicated by $p < 0.05$ and $p < 0.01$, respectively.

was a significant difference between the H-D Cellgevity®-treated group and the N-C group. There was somewhat a dose-dependent increase in rat CYP1A1/2 enzyme activity in the Cellgevity®-treated group. CYP1A1/2 enzyme activity of SD rats in various groups after the 30-day treatment is shown in Figure 3.

3.1.4. CYP2B1/2 and CYP3A4 Activity in SD Rats after 30-Day Treatment. There was no statistically significant
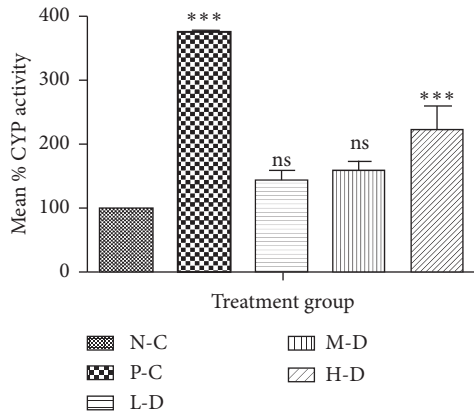
FIGURE 3: Rat liver CYP1A1/2 activity for various treatment groups after 30-day administration: N-C = Negative control; P-C = Positive control (Phenobarbital); L-D = Low dose (38.63 mg/kg) of Cellgevity®; M-D = Medium dose (77.25 mg/kg) of Cellgevity®; H-D = High dose (154.50 mg/kg) of Cellgevity®. Data represent mean ± standard deviations. *** represents values significantly different from the negative control as indicated by $p < 0.001$, and ns means not significantly different.

FIGURE 4: Rat liver CYP2B1/2 activity for various treatment groups after 30-day administration: N-C = Negative control; P-C = Positive control (Phenobarbital); L-D = Low dose (38.63 mg/kg) of Cellgevity®; M-D = Medium dose (77.25 mg/kg) of Cellgevity®; H-D = High dose (154.50 mg/kg) of Cellgevity®. Data represent mean ± standard deviations. *** represents values significantly different from the negative control group as indicated by $p < 0.001$, and ns means not significantly different.

difference between CYP2B1/2 and CYP3A4 enzyme activities in Cellgevity®-treated groups when compared with the N-C group. CYP2B1/2 and CYP3A4 enzyme activities of SD rats in various groups after 30-day treatment are shown in Figures 4 and 5.

3.1.5. Overall Effect of Cellgevity® on Rat CYP Enzyme Activity. After 30 days, when the Cellgevity®-treated groups were compared to the N-C group, the activities of CYP3A4 and CYP2B1/2 did not differ significantly. However, CYP1A1/2, CYP2C9, and CYP2D6 activities in SD rats treated with Cellgevity® were significantly increased compared to the N-C group. Additionally, the increase in CYP2C9 activity was dose-dependent. The overall effect of Cellgevity® on selected rat CYP enzymes is shown in Table 1.

3.2. Fourteen-Day Treatment of Cellgevity® on the Pharmacokinetics of Carbamazepine in Rats. Carbamazepine concentration-time curves of rats administered carbamazepine with Cellgevity® and carbamazepine with normal saline are shown in Figure 6. From the concentration-time curves, rats administered carbamazepine with Cellgevity® had a higher peak concentration at 4 h compared to the rats administered carbamazepine with normal saline.

The total carbamazepine exposure ($AUC_{0 \rightarrow 24}$) and peak carbamazepine concentration for rats administered carbamazepine with normal saline were 170 μmol h/L and 11 μmol/L, respectively, as against 347 μmol h/L and 20 μmol/L, respectively, for rats administered carbamazepine with Cellgevity®. Elimination rate constants were 0.28 h^{-1} for SD rats administered carbamazepine with Cellgevity® and 0.41 h^{-1} for SD rats administered carbamazepine with normal saline. Pharmacokinetic parameters obtained from the concentration-time curves for the two groups are shown in Table 2.
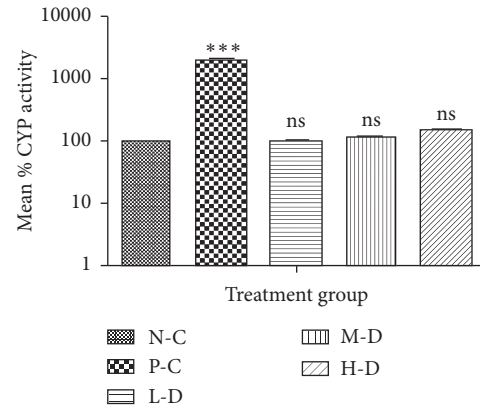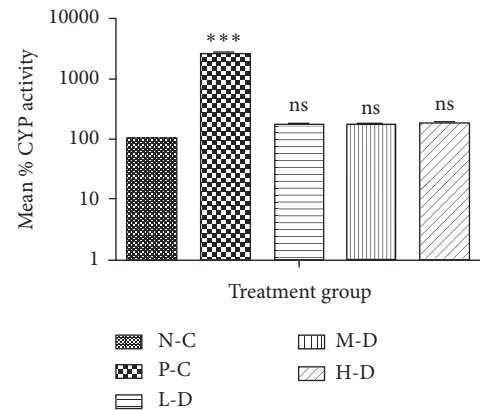

FIGURE 5: Rat liver CYP3A4 activity for various treatment groups after 30-day administration: N-C = Negative control; P-C = Positive control (Phenobarbital); L-D = Low dose (38.63 mg/kg) of Cellgevity®; M-D = Medium dose (77.25 mg/kg) of Cellgevity®; H-D = High dose (154.50 mg/kg) of Cellgevity®. Data represent mean ± standard deviations. *** represents values significantly different as indicated by $p < 0.001$, and ns means not significantly different.

4. Discussion

We earlier reported the potential of Cellgevity® to modulate CYP enzymes in rats [11]. In that study, 4 mg/kg and 8 mg/kg of Cellgevity® were admistered to SD rats over a period of 7 days. Cellgevity® inhibited rat liver CYP3A4, CYP2C9, and CYP1A2, after the 7-day treatment period [11]. In the current study, an equivalent dose of Cellgevity® per serving in humans (12.46 mg/kg) was scaled to SD rats [16], and three doses were used over a period of 30 days. Reports suggest that xenobiotics can modulate CYP enzymes depending on dose and treatment duration [12]. This study, therefore, sought to investigate the effect of Cellgevity® on

TABLE 1: Summary of the effect of Cellgevity® on selected rat CYP enzyme activity.

CYP isoform	Assay	Effect of Cellgevity® on CYP activity
CYP3A4	BROD	No significant increase in enzyme activity
CYP2B1/2	PROD	No significant increase in enzyme activity
CYP1A1/2	MROD	Significant increase in enzyme activity (H-D: $p < 0.001$)
CYP2C9	Diclofenac hydroxylation	Significant increase in enzyme activity (L-D: $p < 0.05$; M-D and H-D: $p < 0.001$)
CYP2D6	Dextromethorphan O-Demethylation	Significant increase in enzyme activity (L-D and M-D: $p < 0.05$; H-D: $p < 0.01$)

L-D = Low dose (38.63 mg/kg) of Cellgevity®; M-D = Medium dose (77.25 mg/kg) of Cellgevity®; H-D = High dose (154.50 mg/kg) of Cellgevity®.
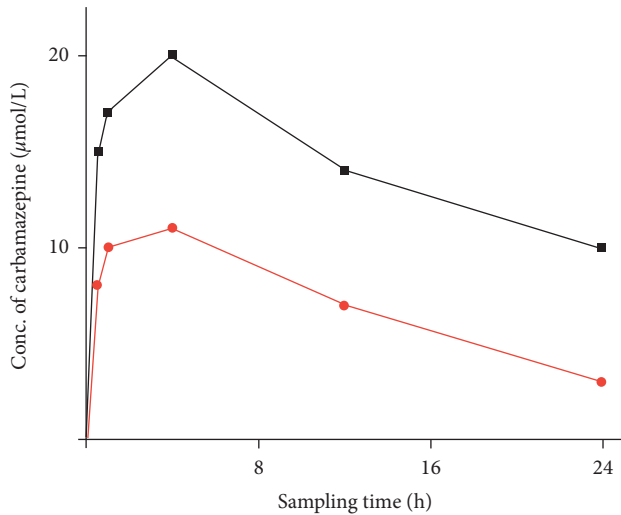

FIGURE 6: Concentration-time curves of carbamazepine with Cellgevity® (grey solid line; filled squares) and carbamazepine with normal saline (red solid line; filled circles). Serum samples from rats in the same group ($n = 6$) were pooled together at each sampling time point.

rat liver CYP enzymes using 38.63 mg/kg, 77.25 mg/kg, and 154.50 mg/kg of Cellgevity® calculated after scaling from humans and administering Cellgevity® for 30 days.

In the present study (after the 30-day treatment period), Cellgevity® significantly increased the activity of rat CYP1A1/2, CYP2C9, and CYP2D6. These results differ from what we earlier reported [11], where Cellgevity® significantly inhibited rat CYP3A4, CYP2B1/2B2, and CYP2C9 after a 7-day treatment period. Horn et al. [12] showed that CYP activity can be modulated by both dose and treatment duration. Pichard-Garcia et al. [22] reported that higher concentrations of eletriptan induced CYP3A in culture medium; however, lower concentrations did not cause CYP3A induction. Organisms after exposure to xenobiotics or foreign chemicals often develop adaptive mechanisms where they increase metabolism in an attempt to get rid of the insulting agent. This adaptive mechanism may have accounted for the increased activity of rat CYP1A1/2, CYP2C9, and CYP2D6 observed when relatively higher doses of Cellgevity® (38.63 mg/kg, 77.25 mg/kg, and 154.50 mg/kg) were used in the current study as compared to our earlier study (4 mg/kg and 8 mg/kg of Cellgevity®).

Indeed, it may not be entirely prudent to extrapolate animal studies to humans, but these data give credence to the fact that dietary supplements could modulate CYP enzymes in humans. If this increase in rat CYP1A1/2, CYP2C9, and CYP2D6 (dose-dependent in the case of CYP2C9) activity is of clinical relevance, then emphasis should be made on maximum daily doses of Cellgevity® in humans.

There are reports of potential interaction between dietary supplements/herbal products and conventional drugs. The commonest of these interactions appear to occur at the level of drug metabolism, especially with liver microsomal enzymes. We earlier reported that Cellgevity® significantly inhibited rat liver CYP3A4, CYP2C9, and CYP2B1/2B2 after a 7-day treatment period [11]. On the premise that CYP3A4 was inhibited by Cellgevity® in our earlier research, the current study also sought to determine the effect of Cellgevity® on the pharmacokinetics of carbamazepine (a CYP3A4 substrate) after a 14-day treatment period in SD rats. The peak concentration for rats administered carbamazepine with Cellgevity® was about 2-fold greater than rats administered carbamazepine with saline. Total drug exposure at the last sample time point ($AUC_{0 \longrightarrow 24}$) was also about 2-fold greater in rats administered carbamazepine with Cellgevity® compared to carbamazepine with saline. This meant that there was a relatively slower elimination of carbamazepine in rats administered carbamazepine with Cellgevity®, possibly via inhibition of rat CYP 3A activity by Cellgevity®. This ultimately led to a longer half-life (2.3 h) among rats administered carbamazepine with Cellgevity®. Although the current study using an animal model showed some level of interaction between Cellgevity® and carbamazepine, a limitation was the inadequate sample volumes at each time point, which led to the pooling of serum. Therefore, mean pharmacokinetic parameters within each group could not be obtained for statistical comparison. Notwithstanding, a comparison of pharmacokinetic parameters of traditional versus pooled samples has found no statistically significant difference between the two sets of parameter estimates [21]. It can, therefore, be inferred from the current study that Cellgevity® had some level of interaction with carbamazepine, possibly through inhibition of CYP3A, the enzyme known to metabolize carbamazepine.

In a related study, anecdotal reports suggested that epileptic patients were taking diosmin, a widely used flavonoid in the treatment of varicose veins and haemorrhoids, along with carbamazepine. This led to a study to ascertain possible interaction between these two agents in an animal model [23]. C_{max}, AUC, and $t_{1/2}$ of carbamazepine were significantly elevated in diomin-treated rats compared to control rats [23]. This, therefore, corroborates findings from

TABLE 2: Pharmacokinetic parameters of carbamazepine for the two groups of rats administered carbamazepine plus Cellgevity®, or carbamazepine plus normal saline over a period of 14 days.

Parameters (unit)	Carbamazepine + normal saline	Carbamazepine + cellgevity®
$C_{\max}$ (μmol/L)	11	20
$T_{\max}$ (h)	4	4
k_e (h^{-1})	0.41	0.28
$t_{1/2}$ (h)	1.7	2.3
$AUC_0 \longrightarrow_{24}$ (μmol h/L)	170	347
$AUC_0 \longrightarrow_{\infty}$ (μmol h/L)	178	375

the current study that there is the potential for herbal medicines, dietary supplements, and food to interact with conventional drugs *in vivo* [24], and that studies of this nature ought to be conducted to identify potential herb-drug interactions.

5. Conclusion

In the current study, Cellgevity® caused an appreciable increase in the activities of rat liver CYP1A1/2, CYP2C9, and CYP2D6 enzymes after a 30-day treatment period. Additionally, Cellgevity® altered the pharmacokinetics (elimination rate and half-life) of carbamazepine in Sprague–Dawley rats after a 14-day treatment. Although this study was conducted in an animal model, this finding is noteworthy, as this may serve as a basis for future studies, i.e., assessing the effect of Cellgevity® on protein content and/or mRNA of distinct CYP proteins in rat livers and direct effect of Cellgevity® on recombinant human CYP enzymes.

Abbreviations

ANOVA: One-way analysis of variance
AUC: Area under the concentration-time curve
$C_{\max}$: Maximum serum drug concentration
CYP: Cytochrome P450 enzymes
DMSO: Dimethyl sulfoxide
FPIA: Fluorescence polarization immunoassay
H-D: High dose
HPLC: High-performance liquid chromatography
K_e: Elimination rate constant
L-D: Low dose
M-D: Medium dose
NADPH: Nicotinamide adenine dinucleotide phosphate
N-C: Negative control
NCD: Noncommunicable disease
P-C: Positive control
rpm: Revolutions per minute
SD: Sprague–Dawley
$t_{1/2}$: Elimination half-life
$T_{\max}$: Time to reach maximum serum drug concentration.

Data Availability

Data used to support the findings of this study are available from the corresponding author upon request.

Ethical Approval

This research was approved by the College of Health Sciences Ethical and Protocol Review Committee (Protocol ID: CHS-Et/M.9–P1.16/2017-2018) of the University of Ghana.

Disclosure

Conflicts of Interest

The authors declare that they have no conflicts of interest.

Authors' Contributions

Benoit Banga N'guessan and Seth Kwabena Amponsah contributed equally to this work. BBN and SKA conceived the study and designed the methodology. MA, SYA, AA, and EAD performed experiments under the supervision of BBN, SKA, KFMO, and RAO. SKA, BBN, KFMO, IJAG, RAO, MA, SYA, AA, and EAD conducted the analysis of data. SKA, BBN, KFMO, IJAG, and RAO drafted the manuscript. All authors read and approved the final version of the manuscript.

Acknowledgments

References

[1] A. Valavanidis, "Dietary supplements: beneficial to human health or just peace of mind? a critical review on the issue of benefit/risk of dietary supplements," *Pharmakeftiki*, vol. 28, no. 2, pp. 60–83, 2016.

[2] R. Pitetti, S. Singh, D. Hornyak, S. E. Garcia, and S. Herr, "Complementary and alternative medicine use in children," *Pediatric Emergency Care*, vol. 17, no. 3, pp. 165–169, 2001.

[3] J. M. Cott, "Herb-drug interactions: theory versus practice," *Molecular Nutrition & Food Research*, vol. 52, no. 7, pp. 745-746, 2008.

[4] E. P. K. Ameade, M. Ibrahim, H.-S. Ibrahim, R. H. Habib, and S. Y. Gbedema, "Concurrent use of herbal and orthodox medicines among residents of Tamale, Northern Ghana, who patronize hospitals and herbal clinics," *Evidence-Based Complementary and Aternative Medicine*, vol. 2018, Article ID 1289125, 8 pages, 2018.

[5] H. S. Oz, T. S. Chen, and H. Nagasawa, "Comparative efficacies of 2 cysteine prodrugs and a glutathione delivery agent in a colitis model," *Translational Research*, vol. 150, no. 2, pp. 122–129, 2007.

[6] J. C. Roberts, R. L. Charyulu, R. T. Zera, and H. T. Nagasawa, "Protection against acetaminophen hepatotoxicity by ribose-cysteine (RibCys)," *Pharmacology & Toxicology*, vol. 70, no. 4, pp. 281–285, 1992.

[7] W. K. Chan and A. B. Delucchi, "Resveratrol, a red wine constituent, is a mechanism-based inactivator of cytochrome P450 3A4," *Life Sciences*, vol. 67, no. 25, pp. 3103–3112, 2000.

[8] R. P. Singh, S. Dhanalakshmi, and A. R. Rao, "Chemo-modulatory action of Aloe vera on the profiles of enzymes associated with carcinogen metabolism and antioxidant status regulation in mice," *Phytomedicine*, vol. 7, no. 3, pp. 209–219, 2000.

[9] H. T. Nagasawa, "Method to enhance delivery of glutathione and ATP levels in cells," Google Patents-US8501700B2, 2015.

[10] A. Nebel, B. J. Schneider, R. K. Baker, and D. J. Kroll, "Potential metabolic interaction between St. John's wort and theophylline," *The Annals of Pharmacotherapy*, vol. 33, no. 4, p. 502, 1999.

[11] B. B. N'guessan, S. K. Amponsah, G. J. Dugbartey et al., "In vitro antioxidant potential and effect of a glutathione-enhancer dietary supplement on selected rat liver cytochrome P450 enzyme activity," *Evidence-Based Complementary and Alternative Medicine*, vol. 2018, Article ID 7462839, 8 pages, 2018.

[12] T. L. Horn, M. A. Reichert, R. L. Bliss, and D. Malejka-Giganti, "Modulations of P450 mRNA in liver and mammary gland and P450 activities and metabolism of estrogen in liver by treatment of rats with indole-3-carbinol," *Biochemical Pharmacology*, vol. 64, no. 3, pp. 393–404, 2002.

[13] E. Spina, F. Pisani, and E. Perucca, "Clinically significant pharmacokinetic drug interactions with carbamazepine," *Clinical Pharmacokinetics*, vol. 31, no. 3, pp. 198–214, 1996.

[14] National Research Council (US), *Committee for the Update of the Guide for the Care and Use of Laboratory Animals. Guide for the Care and Use of Laboratory Animals*, National Academies Press (US), Washington, DC, USA, 8th edition, 2011.

[15] N. W. Spurling and P. F. Carey, "Dose selection for toxicity studies: a protocol for determining the maximum repeatable dose," *Human & Experimental Toxicology*, vol. 11, no. 6, pp. 449–457, 1992.

[16] A. Nair and S. Jacob, "A simple practice guide for dose conversion between animals and human," *Journal of Basic and Clinical Pharmacy*, vol. 7, no. 2, p. 27, 2016.

[17] R. Appiah-Opong, I. de Esch, J. N. M. Commandeur, M. Andarini, and N. P. E. Vermeulen, "Structure-activity relationships for the inhibition of recombinant human cytochromes P450 by curcumin analogues," *European Journal of Medicinal Chemistry*, vol. 43, no. 8, pp. 1621–1631, 2008.

[18] R. Appiah-Opong, J. N. Commandeur, B. van Vugt-Lussenburg, and N. P. Vermeulen, "Inhibition of human recombinant cytochrome P450s by curcumin and curcumin decomposition products," *Toxicology*, vol. 235, no. 1-2, pp. 83–91, 2007.

[19] K. Umegaki, K. Saito, Y. Kubota, H. Sanada, K. Yamada, and K. Shinozuka, "Ginkgo biloba extract markedly induces pentoxyresorufin O-dealkylase activity in rats," *The Japanese Journal of Pharmacology*, vol. 90, no. 4, pp. 345–351, 2002.

[20] W. F. Busby, J. M. Ackermann, and C. L. Crespi, "Effect of methanol, ethanol, dimethyl sulfoxide, and acetonitrile on in vitro activities of cDNA-expressed human cytochromes P-450," *Drug Metabolism and Disposition: The Biological Fate of Chemicals*, vol. 27, no. 2, pp. 246–249, 1999.

[21] L. E. Riad, K. K. Chan, and R. J. Sawchuk, "Determination of the relative formation and elimination clearance of two major carbamazepine metabolites in humans: a comparison between traditional and pooled sample analysis," *Pharmaceutical Research*, vol. 8, no. 4, pp. 541–543, 1991.

[22] L. Pichard-Garcia, R. Hyland, J. Baulieu, J.-M. Fabre, A. Milton, and P. Maurel, "Human hepatocytes in primary culture predict lack of cytochrome P-450 3A4 induction by eletriptan in vivo," *Drug Metabolism and Disposition*, vol. 28, no. 1, pp. 51–57, 2000.

[23] S. K. Bedada and P. Neerati, "Modulation of CYP3A enzyme activity by diosmin and its consequence on carbamazepine pharmacokinetics in rats," *Naunyn-Schmiedeberg's Archives of Pharmacology*, vol. 391, no. 2, pp. 115–121, 2018.

[24] S. Y. K. Fong, Q. Gao, and Z. Zuo, "Interaction of carbamazepine with herbs, dietary supplements, and food: a systematic review," *Evidence-Based Complementary and Alternative Medicine*, vol. 2013, Article ID 898261, 15 pages, 2013.